Dissertation
submitted to the
Combined Faculty of Natural Sciences and Mathematics
of the Ruperto Carola University Heidelberg, Germany
for the degree of
Doctor of Natural Sciences

Presented by

MSc in molecular biotechnology, Shakhawan Mustafa

born in: Sulaimani / Iraq

Oral examination: 13.06.2018

Activated pancreatic stellate cells regulate macrophage polarization and function in tumor microenvironment

Referees:

Prof. Dr. Gert Fricker

Prof. Dr. Aurelio Teleman

1. Table of contents

2. List of figures

3. List of Tables

4. Acknowledgements

I would like to thank my supervisor Dr. Jörg Hoheisel for giving me the chance to work in his group. My deepest appreciation goes to him. I'm sure, without his constructive comments, support, guidance and persistent help this thesis would not have been possible. Thanks for the wonderful atmosphere in the group and for the social communication.

I have greatly benefited from working with Dr. Alhamdani, therefore, I would like to express my gratitude. Thanks for the team work and the discussions.

I appreciate the feedback offered by the members of my thesis advisory committee, Prof. Dr. Gert Fricker and Prof. Dr. Aurelio Teleman. Thanks for the helpful suggestions, concerns and advices.

I'm deeply grateful to all the members of the B070 group. I can't find any words to tell you for creating the nice atmosphere, the Pasta club, the football and tennis playing, for the excursions, parties….so on.

Big thanks go for Janek, my roommate who brought me mineral water and Steffie for her continuous help. Laureen made enormous contribution to the big experiments, I'm really grateful for that. I also want to thank Patrick for his nice discussions.

I would like to thank Andrea, Sandra and Melanie for their support and help. I will not forget our discussions with Soroosh. I appreciate the efforts and helps of the master and bachelor students for their generous support, Kyra, Justus, Maureen, Hannah, Benedict, Jan

To my parents, my brothers and friends who have supported me from the beginning till the end through this long journey. You are the ones I share this achievement with.

I received invaluable support and love from my wife. Her persistent motivation and encouragement made me do my best.

Finally, I would also like to express my gratitude to the HCDP and DAAD for their financial support.

5. Abstract

Pancreatic ductal adenocarcinoma (PDAC) is a highly lethal malignancy remaining incurable to date. The tumor cells and the relevant oncogenic signaling have been extensively investigated, still, the exact molecular and cellular pathology of the disease is not well known due to its fibrous stroma. The tumor microenvironment of PDAC is characterized by a dense desmoplastic stroma consisting of fibroblast, pancreatic stellate cells (PSC), immune cells and the extracellular matrix components. PSCs and tumor associated macrophages (TAM) are the most abundant and important cells in the tumor microenvironment of PDAC and their cellular communication play a significant role in PDAC progression and immune escape.

The molecular mechanisms of PSCs activation and the role of their secreted proteins in macrophage polarization as well as the possibility of defining biomarkers from the secretome of pancreatic cancer cells were studied in this thesis. The secretome of tumor necrosis factor-alpha (TNF-α) activated PSCs were analyzed and validated using different techniques. Activation of PSCs resulted in regulating the secretome profile of PSCs and increased ROS production. The study also demonstrated that activated PSCs secrete numerous proteins which are associated with the cancer cell proliferation and immune cells activation.

Co-culturing PDAC cells with the secretome of activated PSCs resulted in a significant increase of cells proliferation. Moreover, the secretome of PDAC cells and activated PSCs promoted the expression of HLA-DR on monocytes and induced the polarization of macrophages into the immunosuppressive M2 phenotype. The M2 polarization was confirmed by their ability to express CD163 and CD206 surface markers, higher arginase activity and interestingly, their conditioned medium increased Panc-1 cell proliferation. Additionally, interleukin-6 (IL-6) differentially regulated the expression of M1 and M2 surface markers pre- and post-polarization.

Moreover, the secreted molecules by pancreatic cancer cells, sera of PDAC patients, chronic pancreatitis (CP) and sera from healthy donors were studied for the establishment of a set of defined biomarkers. The study indicated that eight markers which were similarly regulated in the PDAC cell secretome and serum of PDAC patients could increase the accuracy of PDAC diagnosis up to 10%.

Taken together, these results will provide insight into the complex and dynamic microenvironment of pancreatic cancer and show the critical role of tumor and stromal cell's secretome in PDAC development and cellular communications in the tumor microenvironment.

6. Zusammenfassung

Das duktale Pankreasadenokarzinom (PDAC) ist eine höchst letale maligne Erkrankung, die bis heute als unheilbar gilt. Die Tumorzellen und die relevanten onkogenen Signalwege wurden umfassend untersucht, dennoch ist die genaue molekulare und zelluläre Pathologie der Erkrankung auf Grund des fibrösen Stromas bisher nicht ausreichend bekannt. Die Tumormikroumgebung von PDAC ist durch ein dichtes desmoplastisches Stroma bestehend aus Fibroblasten, Sternzellen des Pankreas (PSC), Immunzellen sowie Komponenten der extrazellulären Matrix gekennzeichnet. PSC und Tumor-assoziierte Makrophagen (TAM) sind die am häufigsten vorkommenden und wichtigsten Zellen in der Tumormikroumgebung von PDAC und ihre zelluläre Kommunikation spielt eine bedeutende Rolle für die Tumorprogression und die Fähigkeit der Tumorzellen, den Kontrollmechanismen des Immunsystems zu entgehen („immune escape“).

In dieser Arbeit wurden die molekularen Mechanismen der PSC-Aktivierung, der Einfluss der von PSC sezernierten Proteine auf die Makrophagen-Polarisation sowie die Möglichkeit, basierend auf dem Sekretom der Pankreaskrebszellen Biomarker zu definieren, untersucht. Das Sekretom von TNF-α-aktivierten PSC wurde mittels verschiedener Techniken analysiert und validiert. Die Aktivierung resultierte in einer Regulierung des Sekretomprofils der PSC und einer vermehrten Produktion von ROS. The Untersuchung zeigte außerdem, dass aktivierte PSC zahlreiche Proteine sezernieren, die mit der Proliferation von Krebszellen und der Aktivierung von Immunzellen assoziiert sind.

Die Co-Kultivierung von PDAC-Zellen mit dem Sekretom aktivierter PSC führte zu einer signifikanten Steigerung der Zellproliferation. Darüber hinaus förderten sowohl das Sekretom von PDAC-Zellen als auch das Sekretom von aktivierten PSC die Expression von HLA-DR auf Monozyten und induzierten eine Polarisierung von Makrophagen in den immunsuppressiven M2-Phenotyp. Die M2-Polarisation der Makrophagen wurde durch ihre Fähigkeit die Oberflächenmarker CD163 und CD206 zu exprimieren, eine höhere Arginaseaktivität und, interessanterweise, die Tatsache, dass ihr konditioniertes Medium die Proliferation von Panc-1-Zellen erhöhte, festgestellt. Außerdem wurde die Expression von M1- und M2-Oberflächenmarkern sowohl vor als auch nach der Polarisation durch Interleukin-6 (IL-6) differentiell reguliert.

Des Weiteren wurden die von Pankreaskrebszellen sezernierten Moleküle sowie Seren von PDAC-Patienten, Patienten mit chronischer Pankreatitis (CP) und gesunden Spendern mit dem Ziel untersucht, eine Reihe von definierten Biomarkern festzulegen. Die Analyse ergab, dass acht Marker, welche in dem Sekretom von PDAC-Zellen und dem Serum von PDAC-Patienten in gleicher Weise reguliert waren, die Genauigkeit einer PDAC-Diagnose um bis zu 10% erhöhen konnten. Insgesamt werden diese Ergebnisse einen Einblick in die komplexe und dynamische Mikroumgebung des Pankreaskrebs geben sowie die entscheidende Rolle des Sekretoms von Tumor- und Stromazellen in der Entwicklung von PDAC und der Zellkommunikation in der Tumormikroumgebung zeigen.

7. Introduction

7.1. Pancreatic cancer

7.1.1. Epidemiology

Pancreatic cancer is a highly lethal malignancy with near 100% mortality and a dismal prognosis. Pancreatic ductal adenocarcinoma (PDAC) is the most aggressive and common type of pancreatic cancer which accounts for around 95% of cases [2]. The 5-year survival rate of PDAC is recently increased to about 8% still, it is ranked as the fourth leading cause of cancer deaths among the most common cancers in the world [3, 4]. It is assumed that the mortality of PDAC is equal to its incidence and the average survival period after diagnosis is around five months. Pancreatic cancer causes more than 331000 deaths in 2012 and the highest incidence and mortality rates are found in males in the developed countries [5]. The ratio is increasing, in 2015 for example, an estimated 367000 new cases of pancreatic cancer were diagnosed worldwide of which 359,000 were died in the same year [6].Therefore, pancreatic cancer is expected to become the second leading causes of cancer death by 2030 [7]. This is in part due to the fact that most patients are diagnosed only at the advanced stages with already metastatic so that only 20% of the patients are eligible for tumor resection [6]. The high mortality rate can also be attributed to the absence of apparent signs and symptoms during early stages, a lack of sensitive and specific tumor markers as well as inadequate therapeutic agents [8]. Finally, pancreatic cancer exhibits a very early and high rate of metastases to liver, peritoneum and lung which are the most common causes of cancer death [6, 9].

7.1.2. Etiology and risk factors

Although PDAC is the most intensively investigated type of pancreatic cancer, still it's molecular causes are not well understood [2]. The activation of oncogenes and inactivation of the tumor suppressor genes by mutations are the main genetic alteration in PDAC [10]. In a global genome analysis of human pancreas the most common signaling pathways such as, metabolism, cell cycle, cellular repair mechanism and metastasis were discovered which are affected in the genome of more than 75% of pancreatic cancer cases [11]. However, genetic factors comprise only 10% of all pancreatic cancer cases and the rest 90% is attributed to the environmental risk factors [12]. The most strongly associated risk factors to PDAC is family history, chronic pancreatitis (CP), smoking, diabetes, alcohol consumption, age and obesity. Smoking, for example, increases the risk by 75% compared to the

non-smokers and the risk remains even after 10 years of quitting [13, 14]. Further risk factors are age, still, pancreatic cancer rarely occurs before the age of 40 whereas over 80% of cases develop between the 60 and 80 years [15]. Studies have also shown that individuals with diabetes showed a twofold increased occurrence of pancreatic cancer [16] however, the risk is decreased with the duration of diabetes [17]. Pancreatic cancer has been associated with numerous risk factors such as life style, diet, infections and medical conditions all of which are well reviewed [14, 18, 19]. The studies have classified the risk factors to the high-risk groups, moderate risk and low risk, even factors which are not associated to PDAC are included [14]. Nevertheless, there is very few risk factors with relative risks greater than two which might be valuable for screening.

7.1.3. Diagnosis

Pancreatic cancer develops insidiously as the early indications are non-specific and can be easily missed due to the lack of reliable and sensitive diagnostic markers [20]. The available serum biomarkers, such as carcinoembryonic antigen (CEA) and carbohydrate antigen 19-9 (CA19-9), are of only limited utility due to a significant lack of specificity and sensitivity [21, 22]. It has been shown that around 10% of PDAC patients do not express the enzyme needed for CA19-9 synthesis, therefore they are not able to produce CA19-9. Besides, patients with small cancers show false negative [23] whereas false positive CA19-9 is also frequently observed in patients with CP, hepatocellular cancer, upper gastrointestinal tract and ovarian cancer [24]. Due to these limitations and inabilities of CA19-9, studies presented several other markers such as MIC1[25], AFP [26], SPan-1 [27] and PAM4 [28], however, only PAM4 achieved the required sensitivity and specificity in diagnostics. PAM4 is the monoclonal antibody which is highly specific for a glycoprotein MUC1 produced by pancreatic cancer. It is identified in more than 90% of pancreatic cases whereas in normal pancreas it was not detected [28, 29]. PAM4 presented a high sensitivity and specificity of 77% and 95% respectively, thereby it is recommended as a potential biomarker for early detection of PDAC [29]. Moreover, there are some genetic and epigenetic markers and microRNA markers still, they failed to be successfully implemented in PDAC detection [30]. “Therefore, the search is on for better performing biomarkers in body fluids that could be applied effectively in a non-invasive and routine manner for a timely detection of the disease. Recently, GPC1+ circulating exosomes were described as highly accurately detecting pancreatic

cancer patients [31]. With respect to protein profiles, the screening of PDAC patient sera for suitable biomarkers was recently reported using recombinant single-chain variable fragment (scFv) binders that target 57 mainly immunoregulatory biomolecules [32]. However, the definition of specific protein biomarkers in blood or other body fluids can be a challenge. One reason is the fact that the origin of the proteins are quite variable [33, 34]"

7.1.4. Pathology

Most of the pancreatic cancers are originating from exocrine pancreas. PDAC is the most common form of pancreatic cancer and accounts for around 95% of all pancreatic cancers [6]. The origin of PDAC is not known yet, however, it is postulated that PDAC originated from ductal cells of the exocrine pancreas [35]. Moreover, it has been reported that PDAC develops from the precursor lesions, pancreatic intraepithelial neoplasia (PanIN), intraductal mucinous papillary neoplasm (IMPNs) and mucinous cystic neoplasms (MCNs) [36]. PanIN is the most common precursor lesion of PDAC which is characterized by the acinar to ductal metaplasia (ADM), a key event for PDAC [37, 38]. Chronic pancreatitis is thought to promote PanIN via inducing ADM and leading to the PDAC development [39, 40]. The first change in PanINs is KRAS mutation which leads to the increased STAT, MAPK and AKT/PI3K signaling pathways [41, 42]. Of note, KRAS mutation is the most common and outstanding hallmark of PDAC which is found in more than 90% of PDAC patients [43]. Constitutive mutation of KRAS leads to the upregulation of oncogenic proteins such as cMYC and EGFR as well as subsequent changes in tumor suppressor genes, such as p21 and p53, which are associated to the epithelial transformation into carcinoma [44]. The American Joint Committee on Cancer (AJCC) and the International Union for Cancer Control (UICC) have released TNM staging system to characterize tumor stages. The system determines the stage of the disease by the size of the primary tumor and its relationship to the celiac axis (T), the presence or absence of regional lymph node involvement (N), and distant metastases (M) and provides a "stage grouping" based on T, N, and M [45].

7.2. The tumor microenvironment

7.2.1. Role of the tumor microenvironment in cancer

Tumors are not anymore considered only a homogeneous accumulation of malignant cells but rather a complex ecosystem made of tumor cells and the recruited non-

tumor cells. The interactions between these cells creates the tumor microenvironment (TME) or stroma [46]. The TME consists of different stromal cells along with the extra cellular matrix and soluble molecules. Due to the direct or indirect interactions of stromal cells with the tumor cells, they are transformed to an aberrant phenotype and play a critical role in tumorigenesis [47, 48]. These communications are primarily driven by the altered cytokines, chemokines and growth factors which were released into the extracellular space by the stromal cells [46, 49]. The direct stimulations contribute to hypoxia, increased cell proliferation and gene expression and by this means contribute to the acquirement of caner hallmarks [46, 48].

7.2.2. The tumor microenvironment of PDAC

Along with the oncogenic mutations, histologically, PDAC is characterized by a desmoplastic tumor microenvironment (TME) which comprises up to 90% of the tumor mass [50, 51]. The TME of PDAC plays a key role in tumor initiation, progression, metastasis, and response to treatment. For instance, the desmoplastic reaction is creating a high intratumoral pressure and solid stress leading to the vasculature collapse [52]. This consequently affects the access of oxygen and nutrients between the smaller compartments within tumors, causing hypoxia which plays an active role in promoting tumor progression, malignancy, and resistance to therapy [53].The TME of PDAC is not a static entity and comprised of pancreatic stellate cells (PSC) [54], fibroblast [55], immune cells [56], endothelial cells and the extra cellular matrix (ECM) components [57]. It has been shown that, the fibrotic matrix functions as a physical barrier generating stiffness, insolubility, spatial arrangement and porosity, thereby creating unique mechanical support and is giving elasticity to the tissue [58, 59]. However, studies found that this structural platform is the pool of secreted cytokine and growth factors which initiate carcinogenesis [60, 61]. In addition, the stromal cells in the TME promote tumor growth and proliferation and modify the ECM as such, they increase metastasis [62, 63]. So far, the specific interactions among stromal cells as well as the underlying molecular mechanisms are only partially known. Studies demonstrated that, the overexpression of several growth factors, such as, Vascular endothelial growth factor (VEGF), epidermal growth factor (EGF) and fibroblast growth factor (FGF) with their receptors are the result of the high proportion of stromal cells in PDAC [64]. Understanding the cellular constituents of TME and how the stromal cells interact with each other, leading to the

tumor growth, is therefore necessary to improve PDAC therapy and increase survival rate [57].

7.2.3. The extracellular matrix (ECM)

The ECM is the non-cellular components of the tissue which is composed of a complex network of several proteins secreted into the extracellular space. In normal tissues, the ECM keeps the integrity of the tissue by providing physical supports to the cells and it is also the source of crucial biochemical reactions maintaining tissue hemostasis [59]. Another important function of the ECM is to protect cells by a buffering action to maintain the water retention [65]. However, the ECM undergoes constant remodeling by the enzymes like matrix metalloproteases (MMPs) and tissue inhibitor metalloproteinases (TIMPs), an important function associated with wound healing [66]. The excessive and uncontrolled ECM remodeling is therefore increasing the tissue stiffness which is characteristics of solid tumors. It has already been found that the stiffening of the ECM in pancreatic cancer reduces the efficacy of chemotherapeutic agents and directed the cancer cells to gain tumorigenic potential [67]. Changes in the ECM can also influence pancreatic cancer invasion. For instance, expression of fibroblast activation protein (FAP-α) was shown to change the orientation of fibronectin fibers leading to increased scattering and motility of pancreatic cancer cells [68]. The tumor and stromal cells in pancreatic cancer, secret different components such as collagens, glycoproteins, growth factors and proteoglycans as well as modulators of the matrix such as, periostin, tenascin C, thrombospondin and secreted protein acidic and rich in cysteine (SPARC) [69]. SPARC is a noncellular remodeling element of the ECM which enhances intratumoral drug delivery [70]. Studies have shown that, periostin and tenascin-C are contributed to the enhanced tumor proliferation, aggressiveness and migration whereas osteopontin associated with a better survival rate [69]. Nevertheless, the stromal cells in PDAC are numerous and they have a key role in ECM degradation and tumor development. PSCs, CAFs and TAMs are the main contributors in such desmoplastic changes as they have been identified as the main source of proteins and are attributed to the deposition of the ECM [71-73] as in **Error! Not a valid bookmark self-reference.**.

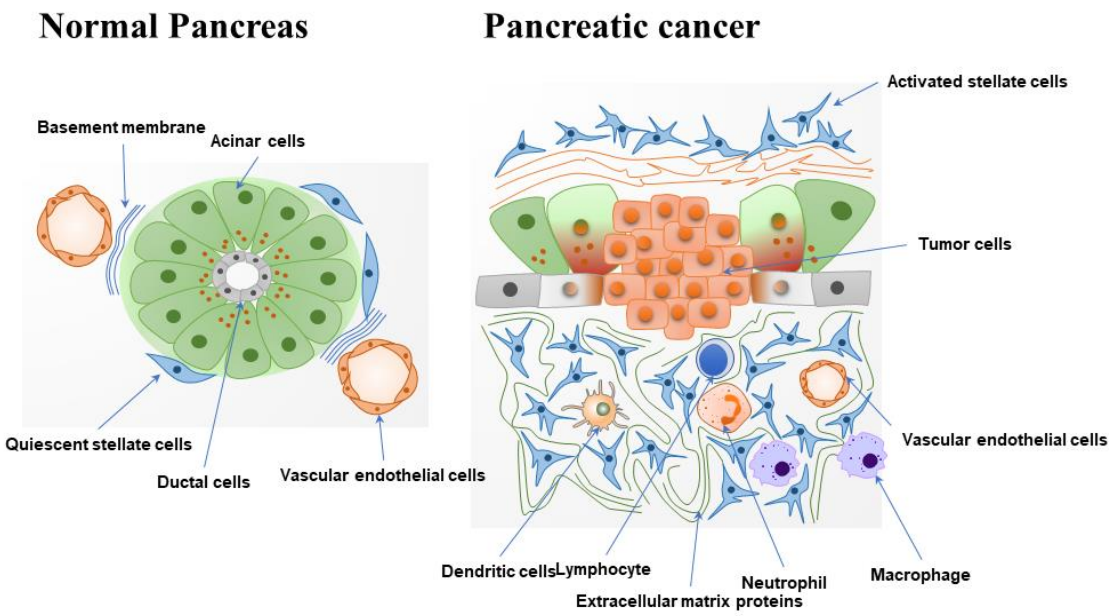

Figure 1. The tumor microenvironment of pancreatic ductal adenocarcinoma with the stromal cells*. Activation of pancreatic stellate cells and recruitment of different immune cells to the tumor site changes the basement membrane consequently leading to fibrosis.*

7.3. Pancreatic stellate cells (PSCs)

In the healthy pancreas, quiescent PSCs are located in the periacinar space in close proximity to the basolateral aspect of acinar cells. PSCs comprise around 7% of the total pancreatic cells and are characterized by expression of desmin, vimentin, nestin and glial fibrillary acidic protein (GFAP) [74]. A very typical feature of quiescent PSC is the existence of vitamin-A containing lipid droplets which is one of the differentiating markers of PSCs from fibroblasts [75]. The main functions of PSCs in normal pancreas are maintaining the structure of the basement membrane, growth of the ECM and production of MMPs and TIMPs for tissue homeostasis [76, 77].

7.3.1. Activation of PSCs

During pancreatic injury and chronic pancreatitis (CP), PSCs transform into activated myofibroblast-like cells which express alpha-smooth muscle actin (α-SMA) filaments and produce ECM components such as collagen and fibronectin [74]. PSCs are activated by different inflammatory factors, cytokines and growth factors such as transforming growth factor beta-1 (TGF-β1), fibroblast growth factor (FGF-2), tumor necrosis factor alpha (TNF-α), IL-1, activin A, IL-6, IL-8, platelet-derived growth factor (PDGF) and vascular endothelia growth factor (VEGF) [71, 78]. These factors are produced by the different cells in the TME such as macrophages, acinar cells and platelets as well as by the pancreatic cancer cells. Moreover, reactive oxygen

species (ROS), ethanol and pressure are also known to activate PSCs [79, 80]. In normal conditions, activated PSCs undergo apoptosis after wound healing [81] however, repeated injury and recurrent inflammation keep the PSCs activated, leading to produce excessive amount of ECM proteins and causing fibrosis in PDAC [82]. As it is shown in the Figure 2, the persistent activation of PSCs is in part due an autocrine loop created by the secretion of growth factors by their own [1, 82].

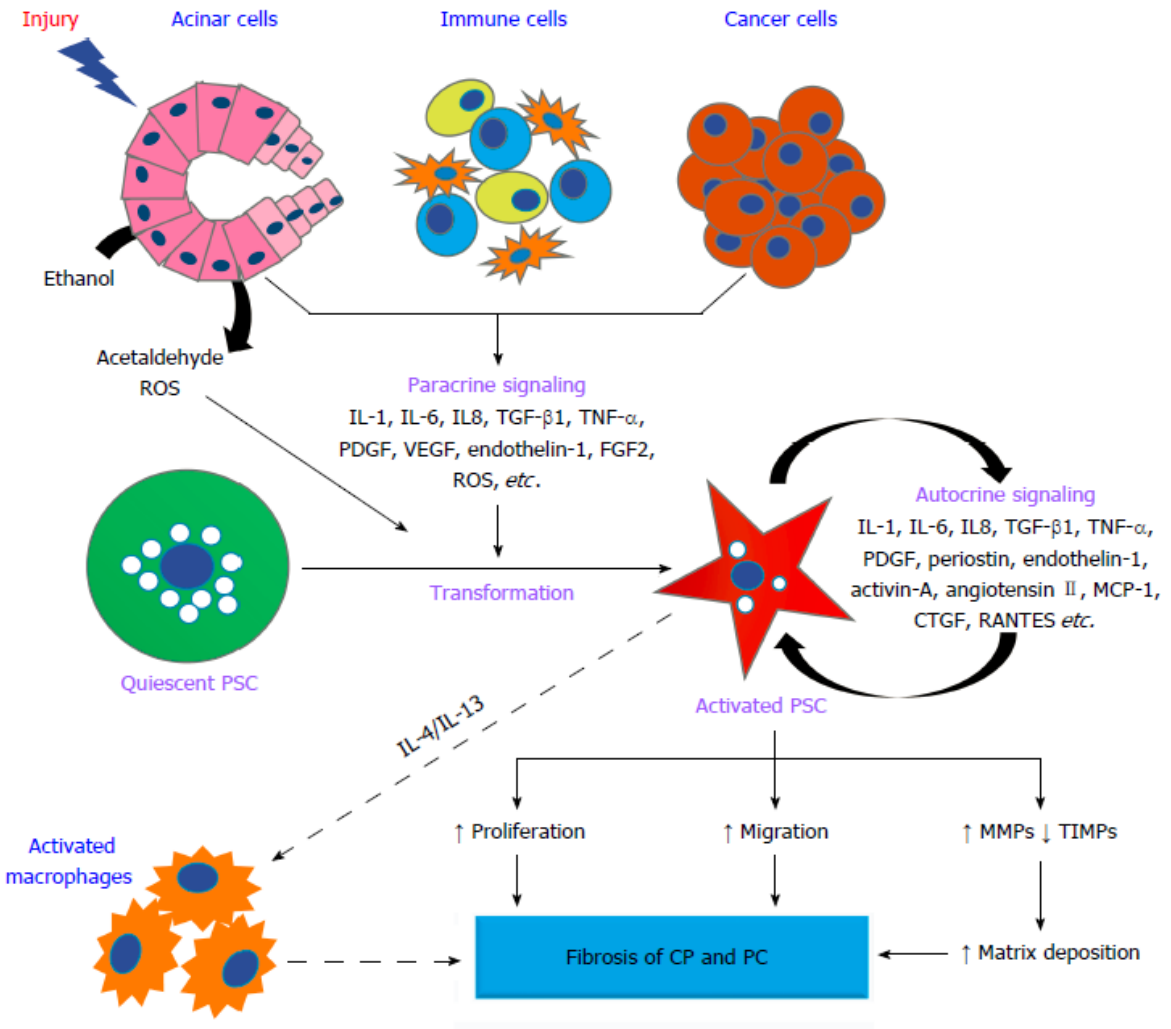

Figure 2. Autocrine and paracrine factors mediating pancreatic stellate cell activation*. Cytokines and growth factors secreted by injured acinar cells, immune cells and cancer cells activate the pancreatic stellate cells (PSCs) in a paracrine fashion and stimulate them to secrete various factors. These factors secreted by PSCs in turn acts in a paracrine fashion and sustains its activation. This autocrine and paracrine signal cycles may help PSCs to retain its activated phenotype, resulting in excess ECM deposition, culminating to pancreatic fibrosis. Illustration by the author. Bynigeri et al. 2017 [1],with permission.*

7.3.2. Interaction between PSC and PDAC

Studies have shown that the increased tumor growth of pancreatic cancer is due to the presence of important interactions between PSCs and tumor cells [78, 83]. In this reciprocal interaction, pancreatic cancer cells recruit PSCs, for example, by secreting sonic hedgehog (SHH) protein, and in turn, overexpression of MMP3, MMP13 and MMP14 by PSCs promote the proliferation and invasion of PDAC cells [84, 85]. It has been shown that conditioned medium of PSCs increases the proliferation of pancreatic cancer cells via stimulating the expression of galectin-3 [86]. Decreased occurrence of apoptosis is found in PSC rich tumors. In agreement with that, the conditioned medium of PSCs is proven to reduce the apoptotic effect of oxidative stress on pancreatic cancer cells [83]. The anti-apoptotic effect of PSCs could be attributed to the secretion of ECM proteins, fibronectin and laminin, which are shown to inhibit both mitochondrial dysfunction and caspase activity [87].

Recently, it was shown that the secreted IL-6 by activated PSCs induced PDAC cell invasion and colony formation through activating STAT-3 signaling [88]. Of note, the activation of notch signaling pathway in direct co-culture of PSCs with PDAC cells is already connected with the proliferation of PDAC cells [89]. Moreover, compelling evidences have proven the crucial contribution of activated PSCs in stimulating PDAC invasion, migration and metastasis via secreting PDGF, TGF-β, FGF2, EGF, connective tissue growth factor (CTGF), MMPs, adrenomedullin (AM) stroma cell-derived factor-1 (SDF-1), and galectin-1 proteins [90-93]. Interestingly, immunohistochemical analysis of PDAC tissues, showed that the number of PSCs which express CD10 surface marker are remarkably higher in pancreatic tumor than in normal tissue [85].

Nevertheless, the interaction between PSCs and PDAC cells are not restricted to only the paracrine signaling. For instance, by injecting PSCs with pancreatic cancer cells in mice, Xu *et al.* revealed the physical interaction between PSCs and tumor cells. They found that, the PSCs which accompanied cancer cells to the metastatic sites, stimulate angiogenesis and are able to intravasate or extravasate to and from blood vessels [94].

There are several investigations ongoing to unravel the mechanism of chemoresistance in PDAC. Hypoxia is described to affect chemotherapy via different signaling pathways such as NF-κB, hedgehog pathway, ERK1/2 signaling and reduction of produced ROS [95-97]. It has been previously found that PSCs are

activated in hypoxia [98] and also contribute to the hypoxic microenvironment of PDAC [60]. However, PSCs can also regulate tumor vasculature and hypoxia by secreting pro-angiogenic factors such as FGF and VEGF [99, 100]. The role of activated PSCs in PDAC chemoresistance could be due to the physical barrier for drug delivery or through secreting different proteins. Wang et al. have demonstrated that gemcitabine and radiotherapy were less effective in cancer cells treated with the conditioned medium of PSCs [101]. The resistance could be mediated by the secretion of cysteine-rich angiogenic inducer 61 (CYR61) by the activated PSCs which reduces the expression of nucleoside transporters hENT1 and hCNT3 [102]. Additionally, the expression of cytidine deaminase (CDA) in PSCs may also deactivate gemcitabine, reducing its effect and thus protecting tumor cells [103]. In another study by Zhang et al. indicated that PSCs promote resistance to gemcitabine through activating FAK-AKT and ERK1/2 signaling pathways through paracrine SDF-1α/CXCR4 signaling and, subsequently, the IL-6 autocrine loop in pancreatic cancer cells. Furthermore, release of NO, periostin and IL-1β by PSCs is attributed to the chemoresistance [90, 104].

7.4. Macrophages

The innate and adaptive immune responses are the two main immune reactions of human immune system. Macrophages are differentiated from monocytes of the bone marrow and are the most important cell types of the innate immune system. They destroy pathogens and phagocytose cell debris, facilitate tissue remodeling during wound healing, orchestrate inflammation and stimulate adaptive immunity [105]. Macrophages are originally heterogenous; tissue macrophages are originating from the yolk sac progenitors while those involved in pathogen clearance arise from bone marrow [105, 106]. It is known that monocytes are attracted by chemoattractant signals to migrate to the tissues in which they differentiate into macrophages [106].

7.4.1. M1 macrophages (Classically activated)

Activated macrophages are divided into two functional phenotypes based on their response to the environmental signals. The M1 or classically activated macrophages are triggered by bacterial lipopolysaccharide (LPS), IFNγ or TNF-α [107]. They are proinflammatory macrophages which are able coordinate an effective adaptive immune response against tumors and intracellular pathogens [108]. M1 macrophages secret high amounts of inflammatory cytokines such as TNF-α, IL-1β,

IL-12, IL-23, IL-6, ROS [109, 110] and show a highly active iNOS enzyme which produces nitric oxide (NO) [111]. M1 macrophages express CD80 (B7-1) and CD86 (B7-2) on their surface which are significant to initiate immune response and activate T-cells [112]. CD80/86 are critical ligands for T-cell costimulatory molecule CD28 and are one of the highly expressed markers on M1 macrophages, CD86 is also expressed but at a very low ratio in M2a subtype [113, 114]. High NO production is the main weapon of M1 macrophages against pathogens and tumors. NO is a small lipophilic molecule that can easily cross membranes and reacts chemically with ROS molecules, such as superoxide, to generate biologically active derivatives [115]. In tumors, depending on its concentration, NO has both pro- and anti-tumor effects [116].

7.4.2. M2 macrophages (alternatively activated)

On the contrary, M2 macrophages are activated by anti-inflammatory factors such as IL-4, IL-10, IL-13 and glucocorticoid hormones [117]. M2 macrophages mediate immunosuppression by secreting IL-10 and TGF-β and play a critical role in wound healing [110, 118]. In respond to the activating stimuli, M2 macrophages are divided into different subtypes which are M2a, M2b and M2c [111]. M2 macrophages are characterized by the cell surface expression of the macrophage mannose receptor (MMR) CD206 [119], scavenger receptor CD163 [118] and the synthesis of soluble factors, such as the CC chemokine ligand 17 (CCL17) , IL-10 [120], CCL-18 and TGF-β [121]. Beside the surface markers and cytokines, M2 macrophages induce arginase enzyme which metabolizes arginine and produces proline [110, 118]. To distinguish between the two activation states of macrophages, metabolism of L-arginine is thought to be a distinctive means [122]. Arginase-1 (Arg-1) is a key feature of M2 macrophages which contributes in wound healing and fibrosis by catalyzing arginine to urea and ornithine [122, 123]. Of note, ornithine is the precursor of polyamines which are critical for collagen synthesis and cell proliferation [124]. It is already known that, Arg-1 is induced by exogenous Th2 cytokines such as IL-4 and IL-13 through STAT-6 activation [125, 126].

7.4.3. Tumor associated macrophages (TAM)

Macrophages that migrate to the tumor environment are called tumor associated macrophages (TAM) which are associated with poor prognosis in pancreatic cancer [127, 128]. TAMs have a key role in tumor initiation, development and metastasis [109]. TAMs are M2-resembling macrophages which are activated by factors such as IL-4, IL-10, IL-13, colony stimulating factor-1 (CSF-1) and TGF-β [129]. However, their phenotype varies during the stages of tumor development and often reflects a mix of M1 and M2 [130].

M1 and M2 macrophages differ functionally; M1 macrophages are dominated in acute pancreatitis whereas M2 macrophages are dominant in chronic pancreatitis and in PDAC which are associated with poor prognosis [129]. It is assumed that the persistent release of cytotoxic molecules by M1 macrophages destroy infectious agents and resolve inflammation however, secreted pro-inflammatory factors may stimulate cancer cells survival [112, 131]. It has been shown that CCL2 and IL-6 in the TME attract monocytes and eventually polarize them into M2 type [132]. Moreover, recruitment and polarization of macrophage can also be initiated by the ECM components such as hyaluronic acid [133] or by hypoxia [134]. TAMs could have different functions in the TME. It has been demonstrated that TAMs inhibit anti-tumor immune response mediated by T cells followed by the promotion of tumor progression [135]. Interestingly, high numbers of TAMs are exist in the hypoxic area of the tumor where they increase VEGF expression leading to the recruitment of monocytes and induce M2 polarization via IL4 [136, 137]. It has been found that TAMs are able to enhance anti-cancer drug resistance of cancer stem cells in cooperation with IL-6 [138].

Previous studies have indicated that IL-6 which is also secreted by PSCs [88], is considered as the main regulator of immunosuppression in autoimmune diseases and cancer [139]. IL-6 induced the expression of IL-4 receptor on macrophages which activates signal transducer and activator of transcription-6 (STAT-6) after IL-4 binding. STAT-6/IL-4 axis is then promoting M2 phenotype of macrophages [140] which in turn induce the production of high amount of arginase-1 [141]. Moreover, the immunosuppression could be partly due to the expression of ligands for the inhibitor receptors PD-1 (programmed cell death protein 1) and cytotoxic T-Lymphocyte Antigen-4 (CTLA-4) [142]. Granulocyte colony-stimulating factor (G-CSF), for example, increases CD163 expression and prevents cell apoptosis [143]. Of note, G-

CSF is highly upregulated in the conditioned medium of BxPC-3, a highly metastatic human pancreatic cancer cell line, and is responsible for the suppression of dendritic cells in the pancreatic cancer [144].

7.4.4. Interaction between PSC and macrophages

Several investigations have been done to understand the role of stroma in immune escape mechanism of PDAC cells, still, the available therapies are inadequate [145]. This however, is due to the fibrous microenvironment of PDAC in which the stromal and cancer cells creating a barrier for immune- and chemotherapeutic agents [146]. As mentioned above, the interaction between PDAC and PSCs have been tremendously studied and the activated signaling pathways were elucidated [147, 148]. Moreover, the immune cells communication with the tumor cells in the stroma of PDAC has revealed the contribution of tumor cells in regulating immune response [73, 149]. Nonetheless, the cellular cross-talks between PSCs and macrophages are limited. It has been shown that macrophages are recruited to the tumor area by M-CSF and CCL-2 pathways where they gain the anti-inflammatory phenotype [150, 151]. Therefore, determining the tumor-promoting impact of macrophages represents a promising target [152]. For instance, Affara *et al.* showed that depletion of B-cells resulted in reprogramming the macrophages which leads to the inhibition of tumor [153].

Macrophages can communicate with the PSC by which they increase the cytokine production. In a study by Shi *et al.,* the co-cultured quiescent PSCs with macrophages became activated and produced high amount of IL-6, MCP-1 and KC/CXCL1. This interaction dramatically increased G-CSF/CSF3, MCP-1, MIP-1α/CCL3, MIP-1β/CCL4, MIP-2/CXCL2 and TNF in macrophages resulted in fibrogenesis [154]. Similarly, secretion of granulin by metastasis associated macrophages resulted in activating hepatic stellate cells and induced periostin production which resulted in sustaining metastatic tumor growth [155]. Collectively, understanding the molecular interactions among stromal cells and tumor cells in the tumor microenvironment can be considered as a target for therapy.

7.5. The secretome

The term secretome was first introduced by Tjalsma *et al.* and later revised by Agrawal *et al.* which stands for all proteins that are released from cells into the extracellular space [156, 157]. In the conventional protein secretion pathway,

secreted proteins contain N-terminal signal peptides which guides them to the endoplasmic reticulum (ER) then to the Golgi apparatus which subsequently fused with the plasma membrane and released them into the microenvironment [158]. However, the unconventional pathway includes Golgi-independent trafficking of integral membrane proteins [159]. Of any kind the pathways are, about 10% of the 22,000 protein-encoding human genes are estimated to encode proteins that are secreted which accounts for 13-20% of total human proteome [157, 160, 161]. They are involved in many cellular activities, such as cell interaction, signalling, proteolysis, adhesion, proliferation, migration and immune response. In addition, studies have shown that microRNA, lipids and messenger-RNA may be secreted by the cells via small membranous vesicles, the exosomes and macrovesicles [162, 163]. The secretome is very dynamic in nature and highly sensitive to changes of the overall cellular state, whether at physiological or pathological circumstances. Functional secretory pathways are necessary for the normal physiology of human body therefore, any dysfunction or malfunction may lead to a various systemic problems including cancer [164].

7.5.1. Role of secretome in cancer

Cancer cells modify their protein secretion due to the continuous growth and adaptation to the microenvironment which is the hallmark of cancer [165]. Secreted proteins into the extracellular space interact between stroma and tumor cells and represent the main molecules involved in the intercellular communication, cell adhesion and invasion [166]. Since the secreted proteins are linked to the development of cancer, therefore, several studies have compared the secretome of cancer cells to the normal tissue and have seen a differential regulation of proteins [167]. Cancer secretome can induce a resistance mechanism to chemotherapy. Eckstein et al. have shown that MCF-7 cells increased the expression of amphiregulin, a specific ligand of the EGFR (ERBB1), when treated with cisplatin and found that, amphiregulin is attributed to the resistance [168]. Nodal and activin are necessary for cancer stem cells self-renewal in PDAC. Interestingly, it has been shown that despite the stem cells, nodal and activin in the conditioned medium of PSCs promoted the sphere formation and invasiveness of PDAC [169]. IL-6, for example, is a bioactive multifunctional cytokine which promotes the accumulation of myeloid derived suppressor cells (MDSC) and increased the migration of pancreatic cancer cells via STAT-3 pathway [170, 171].

Previous studies have proven that IL-6 is secreted by PSCs [88] and regulated the immunosuppression in autoimmune diseases and cancer [139]. IL-6 induced the expression of IL-4 receptor on macrophages which after IL-4 binding, the STAT-6/IL-4 axis promoted M2 phenotype of macrophages [140] which in turn induced the production of high amount of arginase-1 [141]. Consequently, detection and quantification of secretome composition could be instrumental for deciphering the molecular architecture of disease and thus for defining specific approaches toward patient management and therapy, in particular for a disease as heterogenous as pancreatic cancer.

7.5.2. Role of secretome in biomarker identification

There have been several reports about an exploration of secretomes for the identification of potential biomarkers [172-175]. A large portion of the secreted proteins – cytokines, hormones or growth factors, for example – are present at very low levels [161]. Sarkissian *et al.* analyzed the secretome of renal cell carcinoma (RCC) aiming at finding a biomarker. By comparing the serum samples of RCC patients with the healthy ones, they found an increased concentration of pro-matrix metalloproteinase-7 (pro-MMP-7) [176]. In another study, cancer cell secretome was used to identify possible biomarkers in nasopharyngeal carcinoma. Interestingly, three candidates of the cell line secretome, fibronectin, Mac-2 binding protein (Mac-2 BP) and plasminogen activator inhibitor 1 (PAI-1) were highly expressed in patients tissues when validated [177]. Similarly, secretome of lung cancer primary cells and colorectal cell line secretome were used in biomarker identification [178, 179]. However, the sensitivity and resolution of the analysis processes were frequently limited.

In serum analyses, the problem of low abundance is magnified by the presence of large quantities of albumin and globulins, which can obscure an analysis of rare proteins or mask their presence altogether. Depletion of highly abundant proteins is not a solution, since their removal does affect the abundance and relative ratios of the other proteins, too [34]. To circumvent these problems, immunofractionation with appropriate antibodies is often applied prior to analysis. To gather enough protein in such a process, however, rather large sample volumes are required. Also, quantification is difficult to achieve since different antibody affinities lead to different yields during the purification process and normalization processes are not easily applicable. In addition, a translation into clinical practice is difficult to achieve" [180].

8. Materials

8.1. Cell lines and primary cells

Cell name	Cell type	Description	Source / Reference
A818-1	Cell line	PDAC	ATCC, Manassas, USA
AsPC-1	Cell line	PDAC	ATCC, Manassas, USA
BxPC-3	Cell line	PDAC	ATCC, Manassas, USA
CFPAC-1	Cell line	PDAC	ATCC, Manassas, USA
Colo357	Cell line	PDAC	ATCC, Manassas, USA
Fibroblast	Cell line	Human fibroblast	Promocell, Heidelberg, Germany
MIA PaCa-2	Cell line	PDAC	ATCC, Manassas, USA
MiaPaca2	Cell line	PDAC	ATCC, Manassas, USA
Monocyte	Primary monocyte	Human monocyte	Isolated from healthy blood donor
PaCa-44	Cell line	PDAC	ATCC, Manassas, USA
PacaDD119	Primary cancer cell line	PDAC	Dr. Pilarsky, technical university of Dresden, Germany
PacaDD135	Primary cancer cell line	PDAC	Dr. Pilarsky, technical university of Dresden, Germany
PacaDD137	Primary cancer cell line	PDAC	Dr. Pilarsky, technical university of Dresden, Germany
PacaDD159	Primary cancer cell line	PDAC	Dr. Pilarsky, technical university of Dresden, Germany
PacaDD161	Primary cancer cell line	PDAC	Dr. Pilarsky, technical university of Dresden, Germany
PacaDD183	Primary cancer cell line	PDAC	Dr. Pilarsky, technical university of Dresden, Germany
Panc-1	Cell line	PDAC	ATCC, Manassas, USA
PSC	Cell line	Pancreatic stellate cells	Dr. Ralf Jesnowsky (Mannheim University Hospital)
Pt45P1	Cell line	PDAC	ATCC, Manassas, USA
Raw264.7	Cell line	Mouse macrophages	ATCC, Manassas, USA
SK-PC-1	Cell line	PDAC	ATCC, Manassas, USA
THP-1	Cell line	Human monocyte	Division of Redox Regulation, DKFZ, Heidelberg, Germany

8.2. Cell culture media and solutions

Reagent	Manufacturer / provider
DMSO cell culture grade	AppliChem GmbH, Darmstadt, Germany
Dulbecco´s phosphate buffered saline (PBS)	Gibco/ Life Technologies, Carlsbad, USA
Dulbecco's Modified Eagle Medium (DMEM)	Gibco/ Life Technologies, Carlsbad, USA
Fetal Bovine Serum (FBS), heat-inactivated	Gibco/ Life Technologies, Carlsbad, USA
Fibroblast Growth Medium (Ready-to-use)	Promocell, Heidelberg, Germany
Ficoll Histopaque-1077	Sigma-Aldrich, Munich, Germany
Iscove's Modified Dulbecco's Medium (IMDM)	Gibco/ Life Technologies, Carlsbad, USA
L-Glutamine 200mM	Gibco/ Life Technologies, Carlsbad, USA
Penicillin 1,000u/ml-Streptomycin 100µg/ml	Gibco/ Life Technologies, Carlsbad, USA
Phosphate buffered saline (DPBS)+ $MgCl_2$	Gibco/ Life Technologies, Carlsbad, USA
Phosphate buffered saline (PBS)	Gibco/ Life Technologies, Carlsbad, USA
RPMI 1640 with L-glutamine and phenol red	Gibco/ Life Technologies, Carlsbad, USA
Trypsin-EDTA (0.05%) with phenol red	Gibco/ Life Technologies, Carlsbad, USA

8.3. Chemicals, enzymes and general materials

Reagent	Manufacturer / provider
2′,7′-Dichlorodihydrofluorescin diacetate	Sigma-Aldrich, Munich, Germany
6-Aminocaproic acid	Sigma-Aldrich, Munich, Germany
α-isonitrosopropiophenone	Sigma-Aldrich, Munich, Germany
Amidosulfobetaine-14 (ASB-14)	Sigma-Aldrich, Munich, Germany
Ammonium peroxydisulfate (APS)	Sigma-Aldrich, Munich, Germany
Benzonase	Millipore Novagen, Darmstadt, Germany
Bicine; N, N-Bis(2-hyrdoxyethyl)	Biomol , Hamburg, Germany
Blotting filter paper sheet	Neolab, Heidelberg, Germany
Blotting-Grade Blocker (non-fat dry milk)	BioRad, München, Germany
Buffy Coats	Deutsches Rotes Kreuz, Mannheim, Germany
Chloroform	VWR BDH Prolabo, Bruchsal, Germany
Cholic acid sodium salt	Thermo Fisher Scientific, Bonn, Germany
Dimethylsulfoxide (DMSO)	Sigma-Aldrich, Munich, Germany
Disodium hydrogen phosphate (Na2HPO4)	Merck, Darmstadt, Germany
DY-549 NHS-ester fluorescent dye	Dyomics, Jena, Germany
DY-649 NHS-ester fluorescent dye	Dyomics, Jena, Germany
EDTA	Sigma-Aldrich, Munich, Germany
Ethanol	Sigma-Aldrich, Munich, Germany
Glycerol	Sigma-Aldrich, Munich, Germany
Glycine	Sigma Aldrich, Munich, Germany
Glycogen, RNA grade	Thermo Fisher Scientific, Bonn, Germany
GM-CSF	Miltenyi Biotec, Bergisch Gladbach, Germany
Griess reagent modified	Sigma-Aldrich, Munich, Germany
Halt Protease & Phosphatase Inhibitor Cocktail	Fisher Scientific, Schwerte, Germany

Reagent	Manufacturer / provider
HEPES	Carl Roth GmbH, Karlsruhe, Germany
Hydrochloric acid (HCl)	Merck, Darmstadt, Germany
Interferon 13 (IL-13)	Miltenyi Biotec, Bergisch Gladbach, Germany
Interferon 4 (IL-4)	Miltenyi Biotec, Bergisch Gladbach, Germany
Interferon 6 (IL-6)	PeproTech Inc., Rocky Hill, NJ, USA
Interferon gamma (IFN-γ)	Miltenyi Biotec, Bergisch Gladbach, Germany
Isopropanol	J.T.Backer, Darmstadt, Germany
Lipopolysaccharides (LPS)	Sigma-Aldrich, Munich, Germany
MACS Running Buffer	Miltenyi Biotec, Bergisch Gladbach, Germany
M-CSF	Miltenyi Biotec, Bergisch Gladbach, Germany
Methanol	Merck, Darmstadt, Germany
N-1-naphthylethylenediamine dihydrochloride	Sigma-Aldrich, Munich, Germany
n-Dodecyl-ß-D-maltoside	GenaXXon Bioscience, Ulm, Germany
Nitrocellulose membrane (Protran 0.45)	GE Healthcare Europe, Freiburg, Germany
NP-40 substitute	Sigma-Aldrich, Munich, Germany
Nuclease-free water	Ambion, Austin, USA
Phenylmethanesulfonylfluoride (PMSF)	Sigma-Aldrich, Munich, Germany
Phorbol 12-myristate-13 acetate (PMA)	Sigma-Aldrich, Munich, Germany
Ponceau S	Serva Electrophoresis, Heidelberg, Germany
Potassium chloride (KCl)	Sigma-Aldrich, Munich, Germany
Potassium dihydrogenphosphate (KH_2PO4)	Carl Roth GmbH, Karlsruhe, Germany
Protein Standard (200 mg/mL BSA)	Sigma-Aldrich, Munich, Germany
Resazurin, sodium salt	Acros Organics, Geel, Belgium
Roti-Load 1	Carl Roth GmbH, Karlsruhe, Germany
Sodium acetate	Thermo Fisher Scientific, Bonn, Germany
Sodium azide (NaN3)	Applichem, Darmstadt, Germany
Sodium chloride (NaCl)	VWR International, Darmstadt, Germany
Sodium dodecyl sulfate (SDS)	Sigma-Aldrich, Munich, Germany
Sodium hydroxide (NaOH)	VWR International, Darmstadt, Germany
Spectra multicolor broad range protein ladder	Thermo Fisher Scientific, Bonn, Germany
Sulphanilamide	Sigma-Aldrich, Munich, Germany
Tetramethylenediamine (TEMED)	Bio-Rad Laboratories, Munich, Germany
Tris-HCl	Sigma-Aldrich, Munich, Germany
Triton-X100	Sigma-Aldrich, Munich, Germany
Trizol	Gibco/ Life Technologies, Carlsbad, USA
Tween-20	Sigma-Aldrich, Munich, Germany

8.4. Lab equipment and disposables

Name	Manufacturer
12-channel-pipette Biohit proline	Biohit, Helsinki, Finland
384-well Lightcycler plates	Sarstedt AG & Co., Nümbrecht, Germany
96F Microwell plates	Thermo Fisher Scientific, Bonn, Germany
Amicon Ultra-0.5 ml Filters (MWCO 3,000 Da)	Merck Millipore, Darmstadt, Germany
Analytical balance scale 434-33	Kern, Balingen-Frommern, Germany
Brunswick Galaxy 170S incubator	New Brunswick Scientific, Steinheim, Germany
Cell culture flasks Cell Star (T75, T175)	Greiner Bio-One, Frickenhausen, Germany
Cell culture multiwell plates (6 well, 96 well)	Greiner Bio-One, Frickenhausen, Germany
Cell Scrapper	Techno Plastic, Trasadingen, Switzerland
Centrifuge Eppendorf 5810 R	Eppendorf, Hamburg, Germany
Centrifuge Megafuge 1.0 R	Heraeus Sepatech, Hanau, Germany
Centrifuge Sigma 2K15	Sigma, Osterode am Harz, Germany
Centrifuge Varifuge 3.0R	Heraeus Sepatech, Hanau, Germany
Cryotubes 1.0 ml	Thermo Fisher Scientific, Bonn, Germany
Electrophoresis power supply E835	Consort, Turnhout, Belgium
Epoxysilane-coated slides	SCHOTT, Jena, Germany
FACS Canto II	BD Biosciences, Heidelberg, Germany
Falcon tubes (15 ml, 50 ml)	Greiner Bio-One, Frickenhausen, Germany
Innova CO-170 Incubator	New Brunswick Scientific, Steinheim, Germany
Leucosep tubes	Greiner Bio-One, Kremsmünster, Austria
Leica DM IRBE microscope	Leica Mikrosystem, Wetzlar, Germany
LifeECO Thermal Cycler	Bioer Technology, Hangzhou, China
Light Cycler LC480	Roche, Mannheim, Germany
LS columns	Miltenyi Biotec, Bergisch Gladbach, Germany
MicroGrid-2 contact spotter	BioRobotics, Cambridge, UK
Millex-GS filters (0,22 µm)	Millipore, Darmstadt, Germany
Mini-Trans-Blot electrophoresis chamber	Bio-Rad, Munich, Germany
MP 230 ph-meter	Mettler Toledo, Gießen Germany
Nanodrop ND-1000	Thermo Fisher Scientific, Bonn, Germany
Nunc Maxisorp flat-bottom 96-Well plates	Thermo Fisher Scientific, Bonn, Germany
Orbital shaker Rotamax 120	Heidolph, Schwabach, Germany
Pasteur pipettes (230 mm)	WU Mainz, Mainz, Germany
QuadriPERM chambers	Vivascience, Hannover, Germany
Quadro MACS separator and rack	Miltenyi Biotec, Bergisch Gladbach, Germany
Roll mixer RS-TR5	Phoenix Instrument, Garbsen, Germany
Safe lock Tubes 1.5 and 2.0 ml	Eppendorf, Hamburg, Germany
Serological pipettes (5 ml, 10 ml, 25 ml)	Greiner Bio-One, Frickenhausen, Germany
SMP3B stealth pins	Telechem, CA, USA
Syringes (2ml, 5ml, 50 ml)	Terumo, Leuven, Belgium
Tecan Infinite M200 plate reader	Tecan Group, Männedorf, Switzerland
Tecan Power Scanner	Tecan Group, Männedorf, Switzerland
Trans-Blot Turbo Transfer System	Bio-rad, München, Germany
Vi-CELL Sample Vials, 4 ml	Beckman Coulter, Krefeld, Germany
Vi-CELL XR cell viability analyzer	Beckman Coulter, Krefeld, Germany
Vivaspin 20 ultrafiltration columns (MWCO 3.000)	Sartorius Biotech, Göttingen, Germany

Vortex-Genie 2	Scientific Industries, New York, USA
Water bath	Grant Instruments, Shepreth, UK
Wilovert S Light Microscope	Helmut Hund, Wetzlar, Germany

8.5. Flow cytometry antibodies

Name	Manufacturer / provider
Alexa Fluor 647 mouse anti-human CD163 (GHI/61)	BD Biosciences, Heidelberg, Germany
Alexa Fluor 647 mouse IgG1k isotype control (MOPC-21)	BD Biosciences, Heidelberg, Germany
Anti-HLA-DR-PE human (AC122)	Miltenyi Biotec, Bergisch Gladbach, Germany
CD206-FITC human (DCN228)	Miltenyi Biotec, Bergisch Gladbach, Germany
CD80-PE human (2D10)	Miltenyi Biotec, Bergisch Gladbach, Germany
CD86-PE human (FM95)	Miltenyi Biotec, Bergisch Gladbach, Germany
FITC mouse anti-human CD14 (M5E2)	Miltenyi Biotec, Bergisch Gladbach, Germany
FITC mouse IgG1 k isotype control (MOPC-21)	BD Biosciences, Heidelberg, Germany
PE mouse IgG1 k isotype control (MOPC-21)	BD Biosciences, Heidelberg, Germany

8.6. ELISA and western blotting antibodies

Antibody	Dilution	Catalog No.	Manufacturer / provider
Anti-Collagen (COL1A1)	1:1000	sc-8784	Santa Cruz, Texas, USA
Anti-FGF-1	1:500	sc-55520	Santa Cruz, Texas, USA
Anti-IL-1β	1:500	sc-1251	Santa Cruz, Texas, USA
Anti-IL-4	1:1000	ab9622	abcam, Cambridge, UK
Anti-SERPINE	1:1000	ab154591	abcam, Cambridge, UK
Anti-FN1	1:1000	15613-1-AP	Proteintech group, Chicago, USA
Anti-GAPDH	1:1000	CB1001	Merck Millipore, Darmstadt, Germany
Anti-α-Actinin	1:1000	A7811-100UL	Sigma-Aldrich, Munich, Germany
Anti-α-Enolase	1:1000	AP6526c	Abgent, San Diego, Ca, USA
Anti-α-SMA	1:500	H00000059-M02	Abnova, Taipei City, Taiwan
HRP-conjugated anti-mouse secondary antibody	1:10000	PI-2000	Vector, Burlingame, USA
HRP-conjugated anti-rabbit secondary antibody	1:10000	PI-1000	Vector, Burlingame, USA

8.7. Kits

Kit name	Manufacturer / provider
Anti-human CD14 MicroBeads	Miltenyi Biotec, Bergisch Gladbach, Germany
BCA Protein Assay Kit	Thermo Fisher Scientific, Bonn, Germany
ECL Prime Western Blotting Detection Reagent	GE Healthcare Europe, Freiburg, Germany
Fast SYBR Green Master Mix	Applied Biosystems, Foster City, USA
Human IL-2 ELISA kit	Abcam, Cambridge, UK
Human IL-6 ELISA set	Acris Antibodies, Herford, Germany
Human IL-10 ELISA Kit	Abcam, Cambridge, UK
ID-1 ELISA kit	Antibodies-online, Aachen, Germany
ProtoScript First Strand cDNA Synthesis Kit	New England Biolabs, Höchst, Germany

8.8. Primers

Gene	Sequence (5'- 3')	Company	Reference
CCL17	F- CGGGACTACCTGGGACCTC R- CCTCACTGTGGCTCTTCTTCG	Biomers.net, Ulm, Germany	Littlefield et al., 2014
GAPDH	F- GAAGATGGTGATGGGATTTCCA R- GATTCCACCCATGGCAAATT	Biomers.net, Ulm, Germany	
IL-1β	F-TGGCAATGAGGATGACTTGTTC R-TAGTGGTGGTCGGAGATTCGTA	Biomers.net, Ulm, Germany	Chanput et al., 2010
MR (CD206)	F- ACCTCACAAGTATCCACACCATC R- CTTTCATCACCACACAATCCTC	Biomers.net, Ulm, Germany	Littlefield et al., 2014
TNF-α	F-CTGCTGC ACTTTGGAGTGAT R-AGATGATCTGACTGCCTGGG	Biomers.net, Ulm, Germany	Chanput et al., 2010

8.9. Buffers and Solutions

Buffers and Solutions	Components
PBS	137 mM NaCl 27 mM KCl 100 mM NaH2PO4 17 mM KH2PO2 dissolved in ddH2O
PBST	10X PBS with 0.05% (w/v) Tween 20
10X TBS	200 mM Tris HCl 1500 mM NaCl 0.1 % (w/v) NaN3 Adjusted to pH 7.6
TBST	TBS with 0.05% (w/v) Tween 20
Stacking gel buffer	1.5 M Tris.HCl Adjusted to pH 6.6
Resolving gel buffer	1.5 M Tris.HCl Adjusted to pH 8.8
SDS-PAGE running buffer	25 mM Tris-Base 190 mM Glycine 0.1 % (w/v) SDS
Lysis buffer	1% (w/v) NP-40 1% (w/v) Cholic acid sodium salt 0.5% (w/v) ASB-14 0.25% (w/v) n-Dodecyl-ß-D-maltoside 20% (v/v) glycerol (99%) 50 mM Bicine (pH 8.5) 2mM EDTA.2Na 150 mM NaCl 1mM PMSF Halt protease and phosphatase inhibitor cocktail 1 U/µl Benzonase
Western blot anode buffer I	300 mM Tris-Base 20% (v/v) methanol
Western blot anode buffer II	25 mM Tris-Base 20% (v/v) methanol
Western blot cathode buffer	40 mM 6-aminocaproic acid 20% (v/v) methanol
Spotting buffer	0.1 M NaHCO3 0.15 M NaCl 0.01 % (w/v) NaN3 0.0001 % (w/v) Igepal 0.005 (w/v) Tween 20 0.25 % (w/v) Dextran Adjusted to pH 8.5

9. Methods

Excerpts of the following text paragraphs were taken from my publications listed below:

- **Mustafa S**. *et al.* Comparison of the tumor cell secretome and patient sera for an accurate serum-based diagnosis of pancreatic ductal adenocarcinoma. *Oncotarget*. 2017; 8:11963-11976.
- **Mustafa S**. *et al.*, Secretome of pancreatic stellate cells promote M2 polarization of macrophages in pancreatic tumor microenvironment. ***Manuscript***.

Texts taken from these publications are enclosed in quotation marks and contribution of other authors are explained.

9.1. Cell culture:

9.1.1. Regular cell maintenance

Pancreatic stellate cells (PSC) and all pancreatic ductal adenocarcinoma cell lines (See the material part; Cell lines and primary cells) were cultured in IMDM medium supplemented with 10% FBS and 1% Pen/Strep antibiotics. The cells were detached using Trypsin-EDTA and passaged at least twice a week depending on the growth rate. Raw264.7 macrophages were grown in complete DMEM medium including 10% FBS and 1% Pen/Strep antibiotics. Raw264.7 cells were detached every three days by cell scrapers and seeded in new flasks. THP-1, human monocyte cells were grown in RPMI1640 medium containing 10% FBS and 1% Pen/Strep. Since THP-1 cells are suspension, 2-3ml of the cells were taken from the suspension and re-cultured in new media every three days. Similarly, isolated primary human monocytes from blood were cultured in RPMI1640 medium. All cell types were incubated in standard humidified condition at 37°C with 5% CO_2 in the dark. All cell lines were previously authenticated and checked for mycoplasma contamination.

9.1.2. Collection of conditioned media and activation of PSCs

PSCs were activated as defined before [181]. Briefly, PSCs were grown in complete IMDM medium until they reached a sub-confluent state of 75-80%. The sub-confluent cells were then washed twice with pre-warmed PBS to remove remaining serum. The cells were afterwards starved for 12 h in IMDM serum-free medium (IMDM-SFM) to synchronize cell growth followed by treating with 10 ng/ml TNF-α for 24 h. Subsequently, PSCs (treated and non-treated) were washed twice with pre-warmed PBS and once with SFM to remove traces of TNF-α. After that, the cells were incubated in fresh IMDM-SFM for 48 h. PDAC

cell lines and fibroblast cells were not activated, therefore, when the cells reached 85-90% confluence, were washed twice with PBS and once with SFM. The cells were subsequently cultured for further 48 h in SFM, then the condition media (CM) were collected and centrifuged at 3,000 g for 10 min at 4˚C to remove cell debris. Three different methods were used to concentrate the conditioned media which were trichloroacetic acid (TCA) precipitation, dialysis with lyophilization and ultrafiltration using Vivaspin-20 centrifugal tubes. However, ultrafiltration with centrifugal tubes found to be the best method for obtaining proteins in high quality with respect to reproducibility, concentration and integrity. Therefore, Vivaspin-20 tubes with a molecular weight cut-off value of 3 kDa were used according to the manufacturer's protocol. In brief, the Vivaspin-20 tubes were filled with 20 ml CM and centrifuged at 5,000 g at 4°C for 2 h in a swing-bucket centrifuge. Following twice buffer exchange with 0.1M Bicine (pH 8.5), the concentrated CM, which is now called secretome, was either used directly in cellular experiments or stored at (-80°C) until use. The protein concentration was determined using Bicinchoninic Acid (BCA) protein assay reagent kit. PSC activation was checked with the western blot depending on the expression of alpha smooth muscle actin (α-SMA) and fibronectin (FN-1).

9.1.3. Collection and handling of serum samples

Excerpts of this paragraph were taken from my publication. "For all serum samples analyzed, written informed consent was given by the patients and healthy donors. Ethical approval was obtained from the local ethics committee at the University of Heidelberg; ethics vote 159/2002 of 28 December 2007". For the serum-based diagnosis two different serum groups were selected and analyzed separately as training and test sets. "The training set serum samples were composed of 47 patients with pancreatic ductal adenocarcinoma (PDAC), 18 people with chronic pancreatitis (CP) and 27 age and sex-matched healthy individuals. Whereas the test set was composed of 25, 25 and 22 serum samples, respectively. Patient diagnosis was based on histological analyses and the disease stage was determined by classification of tumor, node and metastasis (TNM). Exclusion criteria had been applied to patients, who had secondary conditions such as autoimmune, inflammatory or infectious diseases. The serum samples were stored immediately at -80°C until use" [180].

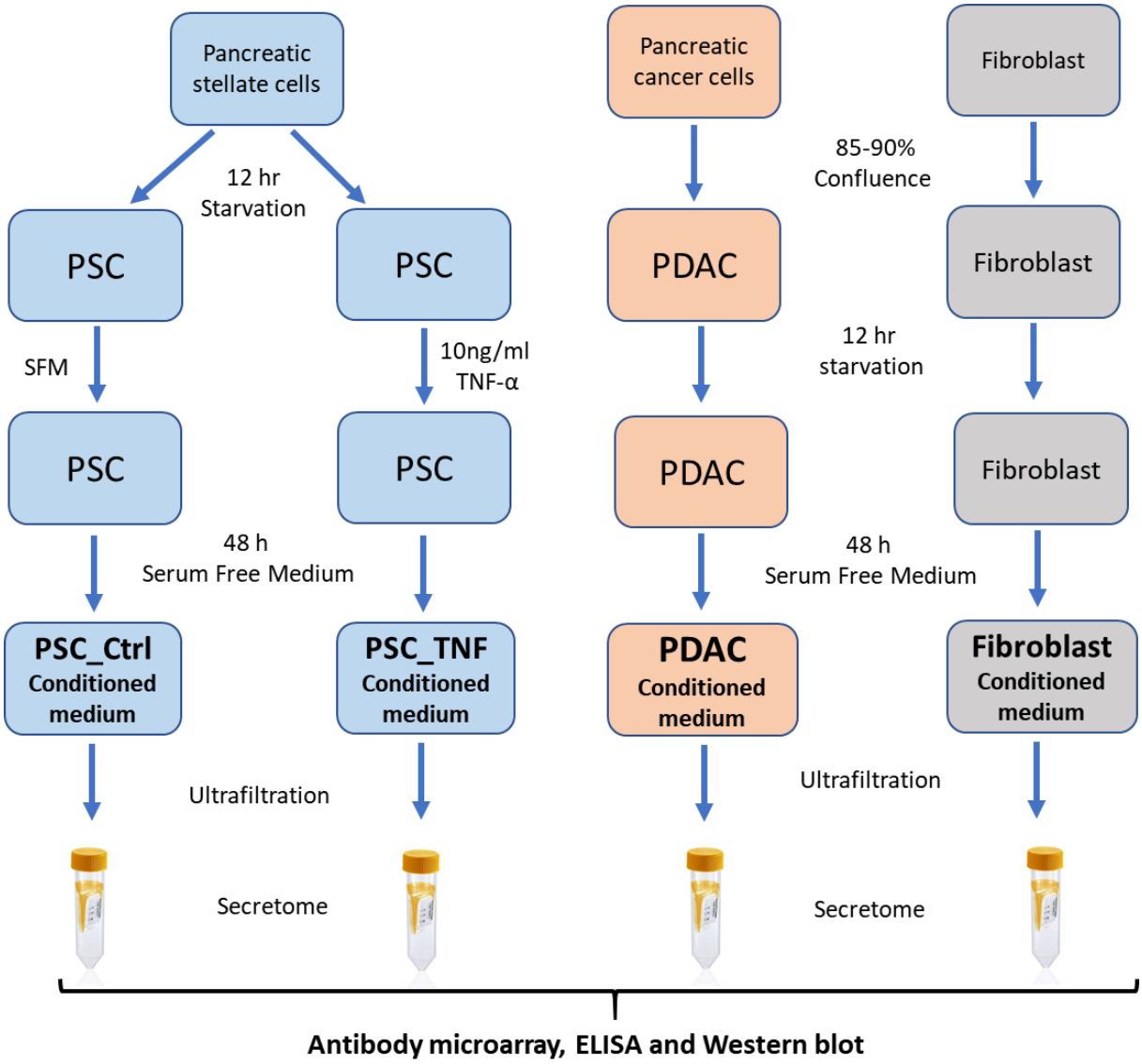

Figure 3. Workflow of PSC activation, collection of conditioned media of PDAC and fibroblast cell line and secretome extraction.

9.1.4. Monocyte isolation

Human monocytes were isolated by density gradient centrifugation. Accordingly, blood samples from healthy donors were diluted with PBS (1:4) and applied onto 50ml Leucosep tubes containing 15ml pre-warmed Ficoll Histopaque. Blood samples with the ficoll were centrifuged at 1,000g for 20 min at room temperature without break. After that, human peripheral blood mononuclear cells (PBMC) were collected and washed twice with PBS and resuspended in MACS buffer. Subsequently, total cell number was counted, and monocytes were isolated using $CD14^+$ magnetic beads according to the manufacturer's instructions. Briefly, PBMCs in MACS buffer were mixed gently with anti-$CD14^+$ magnetic beads for 15 min at 4°C. Afterwards, the labeled cells were applied onto the calibrated MACS LS columns in the magnet separator. The cells were washed three times and were

eluted with 5ml MACS buffer. The purified monocytes were counted and cultured overnight in serum free RPMI-1640 medium to improve cell attachment.

9.1.5. Monocyte differentiation to macrophages

The isolated human monocytes were cultured in RPMI-1640 complete medium with 100 ng/ml GM-CSF, 20 ng/ml M-CSF or treated with the secretome of PSC and PDAC cells to differentiate to macrophages. The differentiation of THP-1 monocytic cell line is described before [182]. Briefly, THP-1 monocytes at a concentration of 0.5 x 10^6 Cell/ml were differentiated to macrophages using 100 ng/ml PMA for 48 h followed by washing twice with RPMI and 24 h resting stage in PMA-free RPMI1640 medium. Thus, monocytes were differentiated to macrophages and the differentiation were later confirmed based on microscopic cell phenotype observation and HLA-DR expression. Hereafter, the macrophages were polarized with 100 ng/ml LPS plus 20 ng/ml IFNγ or with 20 ng/ml IL4/13 to classically activated (M1) or alternatively activated (M2) macrophages, respectively. For the cellular interactions, the macrophages were treated with the secretome of different stromal cells in later experiments.

9.1.6. Treatment of macrophages with PSC and PDAC secretome

The freshly isolated human monocytes (1x10^6 cells/ml) were cultured in RPMI 1640 for seven days with the secretome of activated or non-activated PSCs and PDAC cell lines. Meanwhile, the macrophages were polarized with 100 ng/ml LPS and 20 ng/ml IFNγ or with 20 ng/ml IL-4/13 to M1 and M2 types respectively as positive controls. The stimuli, including the secretome, and the media were changed every two days. The differentiated macrophages from the THP-1 cells were treated for 48 h with the standard stimuli or with the secretome of activated and non-activated PSCs. Macrophage polarization was determined depending on the cell surface markers expression, cytokine secretion, arginase activation and nitric oxide production. Furthermore, effect of IL-6 was evaluated in macrophage polarization targeting surface marker expression.

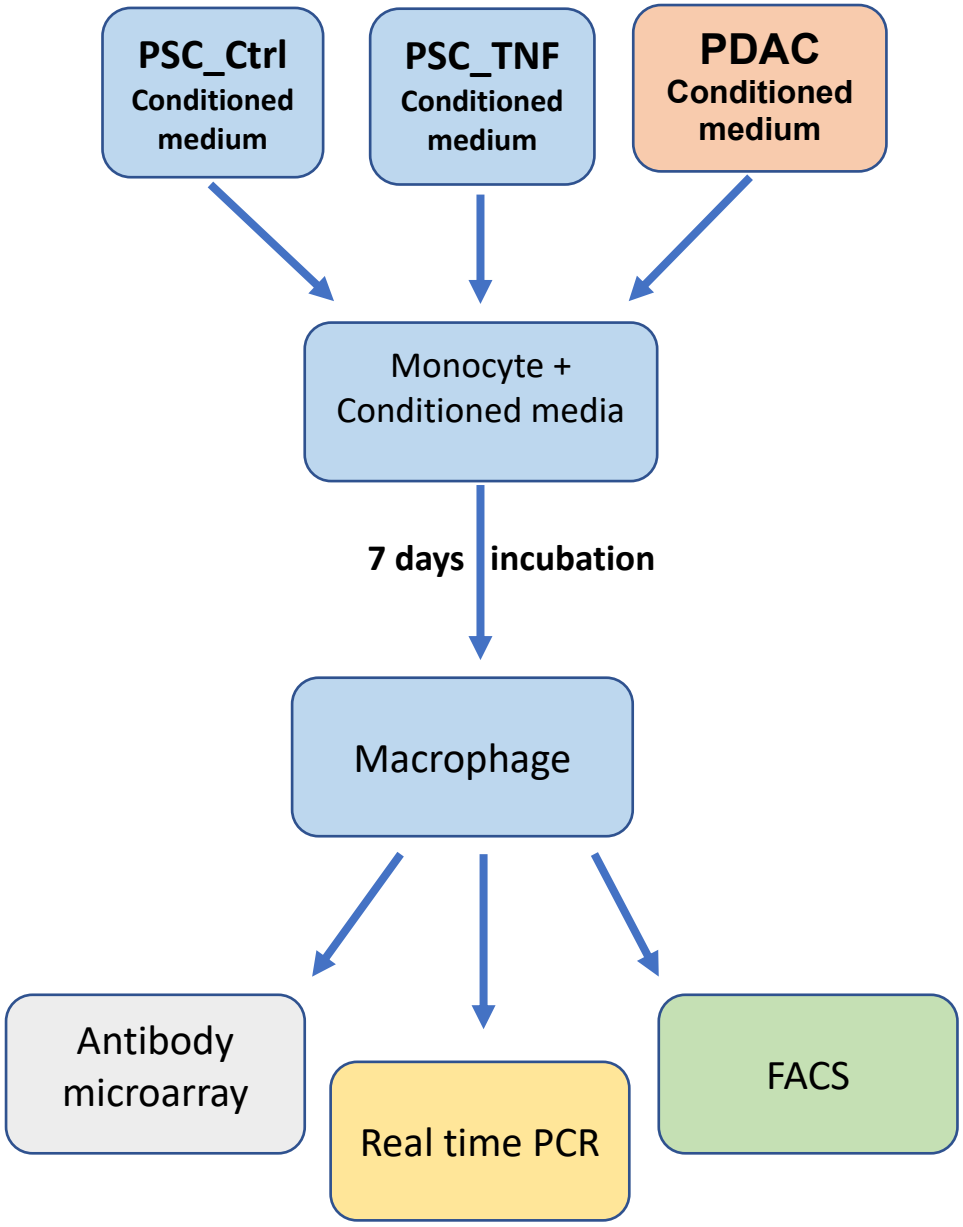

Figure 4. Workflow of macrophage incubation with the secretome of PSCs and PDAC

9.2. Protein analysis with antibody microarray

9.2.1. Antibody microarray production

Two different sets of antibody microarrays were used in protein analysis which have been used previously [180, 181]. The first set consisted of 735 antibodies whereas the second one composed of 1439 antibodies including positive and negative controls as well as positional marker molecules. The arrays were produced as described previously in detail [183]. Briefly, 5µg of each antibody was added to the spotting buffer which composed of 100 mM Bicine buffer (pH 8.5) containing 0.005% Tween-20, 0.05% sodium azide, 5%

trehalose, 5 mM magnesium chloride and 137 mM sodium chloride. The antibodies were spotted in quadruplicates on epoxysilane-coated glass slides using the contact printer MicroGrid-2 and SMP3B pins at 55-65% humidity. After the spotting, the slides were kept at room temperature at the same humidity level for 24 h before they were stored in a dry place at 4°C.

9.2.2. Protein extraction

Cellular proteome was extracted using lysis buffer as reported previously [184]. The lysis buffer composed of 50 mM Bicine buffer (pH 8.5) containing 20% glycerol, 1.0 mM magnesium chloride, 5.0 mM EDTA, 1.0 mM phenylmethanesulfonyl fluoride, 1.0 IU/ml benzonase, Halt Protease and Phosphatase Inhibitor Cocktail, 0.5% Nonidet P-40 substitute, 1.0% Cholic acid, 0.25% n-dodecyl-β-maltoside and 0.5% amidosulfobetaine-14. Briefly, cells were washed with cold PBS then minimal volume of lysis buffer was added to each flask and incubated on ice for 30 min. The cells were subsequently collected with cell scraper and pipetted up and down with a syringe through a 23G needle followed by centrifugation at 18,000g for 20 min at 4°C. Subsequently, supernatants were transferred to fresh microcentrifuge tubes and total protein concentration was determined using Bicinchoninic Acid (BCA) protein assay reagent kit according to manufacturer's instructions.

9.2.3. Protein labeling

For protein labeling, cellular proteome, secretome and serum samples were adjusted with 0.1M Bicine buffer to the same concentrations. The samples were labelled with the fluorescent NHS-ester dye DY-649P1 (Cy-5) in a molar ratio of 7.5 (dye/protein) in dark eppendorf tubes and were shaken at 4°C for 2 h. Afterwards, the unlabeled fluorescent dye was quenched by adding 10% glycine with a constant shaking for 20 min. For the reference background, cellular proteome were pooled and labeled with DY-549P1 (Cy-3) as described previously [185]. For serum analyses, a pool reference was prepared from all samples using the same concentration of each sample.

9.2.4. Microarray incubation, scanning and image processing

The procedure of antibody microarray incubation is previously described [183]. Before the incubation with the labeled samples, the arrays were equilibrated at room temperature for 30 min followed by washing twice with TBST. The arrays were then blocked with 5ml of 10% non-fat dry milk, prepared in TBST, in quadriPERM chambers and left on a shaker at

room temperature for 3 h. The arrays were subsequently washed with TBST and incubated overnight with 50 µg of the labelled samples and pool reference in 1% milk at 4°C with constant shaking. The arrays were washed four times with TBST and once with distilled water followed by drying in a ventilated oven at 25°C. Consequently, arrays were scanned using a Tecan power scanner at constant laser power and the resulting images were analyzed with GenePix Pro 6.0 software.

9.3. Flow Cytometry

Flow cytometry was performed on live macrophages. Briefly, cells were detached from the culture flask with trypsin-EDTA solution and were washed in PBS. Subsequently, the cells were labeled with the fluorochrome-conjugated antibodies CD86-PE, CD206-FITC, CD163-Alexa Fluor647 and their corresponding isotype in FACS buffer (500ml PBS pH 7.4 containing 5% FBS, 250mg sodium azide and 2ml of 0.5M EDTA) for 30 minutes at 4°C. The labeled cells were washed twice in PBS afterwards and FACS analysis was performed with a FACS Canto II. At least 10,000 events were collected per sample and the data were analyzed using flowJo software V.10. Mean fluorescence intensity (MFI) of seven different experiments were calculated by dividing the Geometric mean of each marker relative to their isotype negative controls.

9.4. Immunoblotting

Depending on the molecular weight of the examined proteins, SDS gels (1.0 mm thick) were prepared with 5% acrylamide / bisarcylamide in the stacking gel and 10-12% of the resolving part. Protein concentration of the cellular proteome, secretome and serum samples were adjusted and mixed with an appropriate amount of reducing loading buffer (Roti-Load) followed by boiling at 96°C for 5 min. The reduced samples and the protein ladder (multicolor broad range protein ladder) were loaded onto the gel. Electrophoresis was performed initially at 60 V until the dye reached the resolving gel then, the power was changed to 150 v until the dye reached the end of the gel. The proteins were transferred from SDS-PAGE onto nitrocellulose membranes using Trans-Blot Turbo transfer system using standard semi-dry protocol. Briefly, the Whatman filter papers were soaked in anode I, anode II and cathode buffer and the membrane was activated in anode II buffer. The sandwich was assembled, and the transfer carried out at 25V, 1.0 A for 30min. The protein transfer was confirmed using Ponceau stain (0.1% (w/v) Ponceau in 5 % (v/v) acetic acid) followed by washing with TBST till the stain disappeared. Afterwards, the membranes were blocked with 5% milk, prepared in TBST, for one hour and washed again twice with

TBST. Subsequently, the membranes were incubated with the diluted primary antibodies in 5% milk overnight with gentle shaking. The blots were then washed twice with TBST and incubated with HRP conjugated secondary antibody for 60 min at room temperature. Later, the blots were washed twice, and the proteins were detected by enhanced chemiluminescence (ECL) detection solution and visualized using Luminescent Image Analyzer LAS 4000 mini machine coupled with a CCD camera. Densitometry of the images were assessed by ImageJ (NIH) software, whereby the expression of each target protein was normalized to the house keeping protein.

9.5. RNA isolation

Total RNA was extracted from the non-treated macrophages, M1 and M2 positive controls as well as from macrophages which were treated with the secretome of PSCs using TRIzol LS reagent according to the manufacturer's instructions. Briefly, 106 cells were resuspended in 1 ml Trizol and vortexed. The lysate was mixed with 200 µl chloroform and were shaken vigorously then incubated at room temperature for 2-3 min. The tubes were afterwards centrifuged at 12,000 g for 15 min at 4 °C, leading to phase separation. The aqueous phase (colorless) was carefully pipetted into a new tube containing 500 µl ice-cold isopropanol and 2µl glycogen. The tubes were carefully mixed and incubated at -20 °C for 60 min followed by centrifugation at 12,000 g for 10 min at 4 °C. The RNA pellets were then washed with 1ml of 70 % (v/v) ethanol and dried at room temperature for 15 min. The pellets were finally resuspended in 50µl pre-warmed nuclease-free water and incubated at 60 °C for 10 min and RNA concentration was measured with the NanoDrop ND-100 spectrophotometer.

9.6. cDNA synthesis and Real-Time PCR

cDNA was synthesized from 700ng of total RNA of macrophages using ProtoScript First Strand cDNA Synthesis Kit according to the manufacturer's instructions. The subsequent qRT-PCR reaction (20µl) containing 2µl of each cDNA template, 2µl of both forward and reverse primers, 10µl fast Syber Green master mix and 6µl nuclease free water was performed on LightCycler 480. The reaction was performed as follows: enzyme activation at 95 °C for 1 min, followed by 40 cycles of amplification (95 °C for 10 s and 60 °C for 35 s). All samples were run in triplicate and relative expression of TNF-α, IL-1β, Mannose receptor (CD206) and CCL17 were calculated by ΔΔCt method using GAPDH as an internal control reference.

9.7. ELISA

The serum samples and secretome and proteome of the activated and non-activated PSCs were analyzed with ELISA. IL-2, IL-6, IL-10 and ID-1 were analyzed using commercial ELISA kits according to the manufacturer's instructions (see the kits in the materials part). However, fibronectin and collagen in the secretome of PSCs were analyzed using primary antibodies in a standard ELISA protocol. Briefly, five technical replicates of 20µg cell secretome were coated in Nunc-MaxiSorp 96-well plates overnight. After immobilization, the residual samples were discarded, and the plates were blocked with 5% milk in PBST for 3 h. After subsequent washing, the plates were incubated overnight with the diluted primary antibodies at 4°C. After that, the plates were washed and incubated with the HRP-conjugated secondary antibody at room temperature for 1 h. Eventually, the plates were washed followed by the addition of TMB substrate and then the absorbance was read at 540nm.

9.8. Proliferation assay

For the proliferation assay, $1x10^4$ cells/well (Panc-1 and BxPc-3) were seeded in the cell culture 96 well plates in IMDM. The medium was removed, and the cells were starved overnight. Afterwards, the cells were treated with the conditioned media (CM) of the activated and non-activated PSCs, the CM of treated macrophages with the PSCs secretome and the positive and negative controls, containing 20µg/ml Resazurin reagent a final concentration. The cells were then incubated for 1 h at 37°C and subsequently relative fluorescence was measured at 544nm excitation / 590 nm Emission, using Infinite M200 plate reader.

9.9. Nitric oxide (NO) production assay

The presence of nitrite, a stable oxidized product of nitric oxide (NO), was determined in the cell supernatant of activated and non-activated PSCs as well as in the supernatant of macrophages which were treated with the conditioned media of activated and non-activated PSCs using Griess reagent modified [186]. Briefly, equal volumes of the cell supernatant and Griess reagent were mixed in 96-well plates and incubated for 15 min at room temperature protected from light. Afterwards, the absorbance was measured at 540nm and the results were calculated based on a standard curve produced by the serial dilution of $NaNO_2$.

9.10. Reactive Oxygen Species (ROS) measurement

Reactive Oxygen Species (ROS) was measured in the PSCs activated with TNF-α and in the macrophages which were treated with the conditioned media of PSCs. The cells were cultured in 96 well plates until 80-85% confluency. The medium was removed, and the cells were washed with PBS. Afterwards, the cells were treated with the stimuli or with the conditioned media of PSCs as stated above. The stimulus and conditioned media were removed from the plates and the cells were washed carefully with PBS. Consequently, the cells were incubated with serum and phenol red free medium containing 50µM DCFH-DA (prepared in DMSO) for 30min at 37°C in the dark. After incubation, the cells were washed twice with PBS and fluorescence was measured with excitation at 488nm and emission at 530nm using fluorescence plate reader.

9.11. Arginase activity measurement

Arginase activity was measured in macrophages as described previously [187]. In short, treated macrophages lysed with Arginase lysis buffer (0.1% (v/v) Triton X-100 in 25 mM Tris–HCl pH 8.0) and protein concentration was measured using BCA kit. To measure total arginase,100 µl of lysis buffer containing the cell lysates were mixed with 10 µl $MnCl_2$ (100mM) and incubated at 55 °C for 10 min. After that, 100 µl of 0.5 M arginine was added to each microfuge tube and the samples were incubated at 37°C for 1 hr. Subsequently, the reaction was stopped by adding 800 µl acid mixture (1:3:7 (v/v/v) H_3PO_4: H_2SO_4: ddH_2O) then 40µl of 6% α-isonitrosopropiophenone (α-ISPP) were added to each reaction to generate urea. Thereafter, the samples and the standards were incubated at 95°C for 40min then cooled down at RT. Eventually, 200µl of each sample was added to 96-well plates (five technical replicates each) and absorbance was measured at 550nm.

9.12. Statistical analysis

Statistical analysis was performed using GraphPad prism 6.0. Data were represented as mean values with the respective standard deviations of at least three independent experiments or biological replicates. Differences between treatments were calculated (as indicated in the figure legends) where P-Values <0.05 considered significant. The statistical analysis of microarray data is taken from Mustafa *et al.*

“The statistical analysis of microarray data was conducted with the Chipster software package (v1.4.6, CSC, Finland). The data were presented as the median of the signal intensities in the red (DY-649) and green (DY-549) channels, respectively. The coefficient of variance for the pool reference was less than 10% across all tested microarrays. Signal-

to-noise ratio (SNR) was calculated as (median foreground vs. median background) / (standard deviation of background) for both the red and green channels. The Loess approach was used for data normalization with background correction offset (0, 50) of the normexp [188]. Two-group test between normal and cancer cells was done using the empirical Bayes test with Bonferroni-Hochberg adjustment for multiple testing [189]. A p-value of 0.05 or less was considered significant. Array quality was assessed using the ordinate method Detrended Correspondence Analysis [190]. In addition, array results were clustered using their Pearson correlations and a dendrogram was constructed using the Average Linkage method".

"For a prediction of the functional aspects of the differentially expressed proteins, the Ingenuity Pathways Analysis (IPA) software package (version 6.3; Ingenuity Systems, Redwood City, USA) was applied. Prediction of function activation of inhibition was calculated within IPA using z-score method. Component annotation was mapped using the web-based Gene Ontology tool of UniProt (www.uniprot.org). The Ingenuity software also permitted a literature analysis with respect to the biomarker status of particular proteins.

The sensitivity and specificity of discriminating patient groups were calculated with support vector machine (SVM) algorithms in R programming [191] with a threshold level of zero. The samples were divided into a training set and a test set. Using the SVM decision values, a receiver operating characteristics (ROC) curve and the respective area under the curve (AUC) value were calculated. To define biomarker signatures, a leave-one-out cross-validation procedure was applied. A linear kernel was used, and all the other parameters were set as default to avoid overfitting. Each time one sample is removed from the training set, the remained samples were analyzed as follows: each protein in the remained samples was removed in turn, the remaining protein groups were analyzed with Wilcoxon test. The most significant group was chosen and used for calculating a SVM decision value with the left-out sample. The same strategy was used with the chosen group until only one protein is left. By this approach, a candidate biomarker list was found, which was then evaluated with the test set" [180].

10. Results

The results which were obtained from my publications were clearly referenced and contributions of others were clarified in all figures which were not created by myself.

- Mustafa S. *et al.* Comparison of the tumor cell secretome and patient sera for an accurate serum-based diagnosis of pancreatic ductal adenocarcinoma. **Oncotarget**. 2017; 8:11963-11976.
- Mustafa S. *et al.*, Secretome of pancreatic stellate cells promote M2 polarization of macrophages in pancreatic tumor microenvironment. **Manuscript**.

The first part of the results is dealing the activation of pancreatic stellate cells by the pro-inflammatory factor TNF-α and characterizing the secretome with antibody microarrays. Afterwards, the secretome is validated and applied in different experimental setups to investigate cellular interactions. In the second part, the PSCs and PDAC secretome were used as cell stimuli on human monocytes to study changes in macrophage's polarization and function as well as to define the changes in macrophages cellular proteome and secretome. Moreover, the impact of the conditioned media of the treated macrophages were then explored in pancreatic cancer cell proliferation. The third part shows the significance of PDAC cell secretome in biomarker discovery which was validated with serum samples of healthy donors and patients with pancreatic cancer.

10.1. PSC activation, validation and secretome functional characterization

The aim of the project was to investigate the role of secretome in cellular communications in the pancreatic tumor microenvironment. Therefore, to imitate the tumor environment, PSCs were activated and the secretome of PSCs and PDAC were collected and used as the cellular stimulant. We have previously investigated the influence of pro-inflammatory factors such as TNF-α, CCL-4, IL-6 and FGF-2 on biological functions of PSC and shown that TNF-α is the most potent factor that activates the PSCs and changes the secretome profile [181]. Hence, throughout the thesis, PSC_TNF stands for the activated PSCs with TNF-α whereas the PSC_Ctrl represent the non-activated PSCs which were only incubated in serum free medium.

10.1.1. Activation of PSC with TNF-α

To synchronize cell growth, PSCs were first starved for 12 h in serum free medium then incubated with TNF-α for 24 h. It has been shown that PSCs highly express alpha-smooth muscle actin (α-SMA), fibronectin (FN-1), collagen, vimentin and desmin when activated [192]. Analyzing the cellular proteome of activated and non-activated PSCs, using western blot, showed a higher expression of FN-1 and α-SMA in activated PSCs compared to the non-activated control (Figure 5A & B). It has been shown that PSCs remain activated after chemotherapy [193] and for PDAC patients, gemcitabine is the main chemotherapeutic agent. Correspondingly, PSCs treated with the gemcitabine highly expressed α-SMA and FN-1 suggesting the possibility of PSC activation by therapeutic agents (Figure 6A & B). Different therapeutic agents might be used in PDAC treatment, either alone or with other factors therefore, the secreted molecules by PSCs could not be similar. Additionally, because chronic inflammation is thought to be the onset of PDAC so, activation of PSCs by the proinflammatory factors is investigated in this thesis.

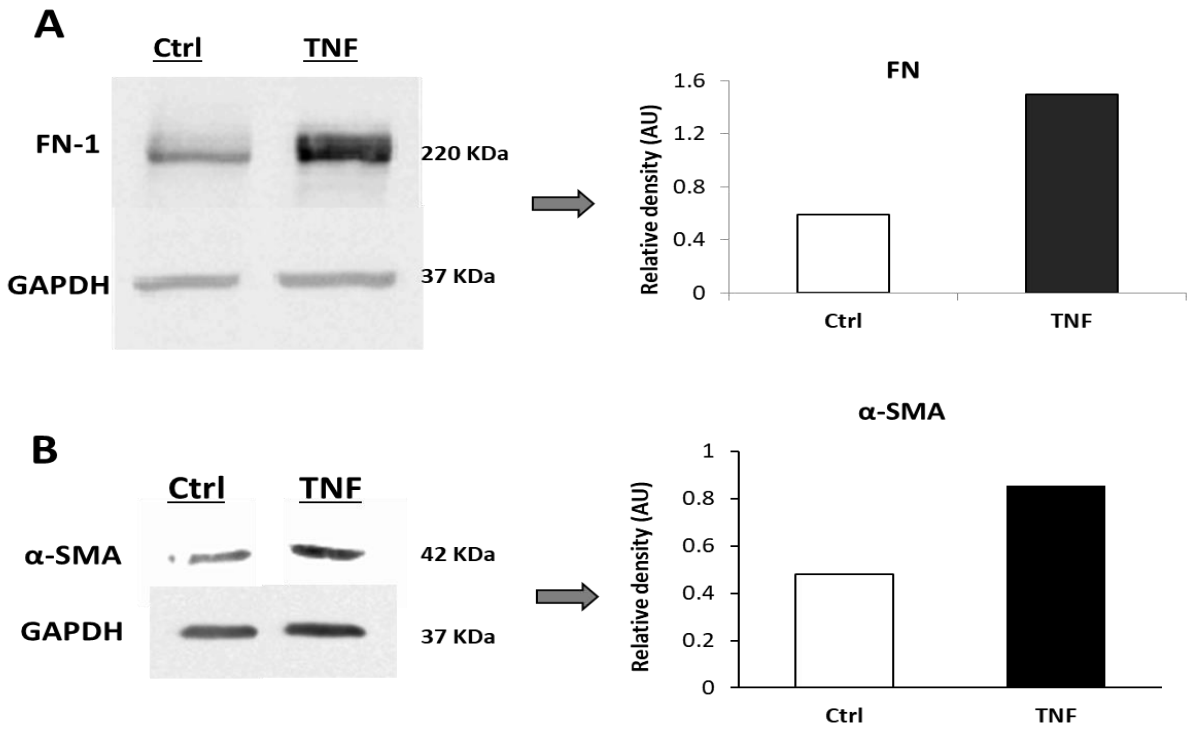

Figure 5. The expression of FN-1 and α-SMA after activation of pancreatic stellate cells (PSC) with TNF-α. *Immunoblots with the respective densitometry showed the expression of fibronectin-1 (A) and alpha-smooth muscle actin (α-SMA) (B) as activation marker of PSCs after stimulation with TNF-α (10ng/ml) compared to the untreated control cells (Ctrl). The expression level of target proteins was normalized to the level of internal control, GAPDH. Expression of α-SMA was analyzed by Maureen Buschman.*

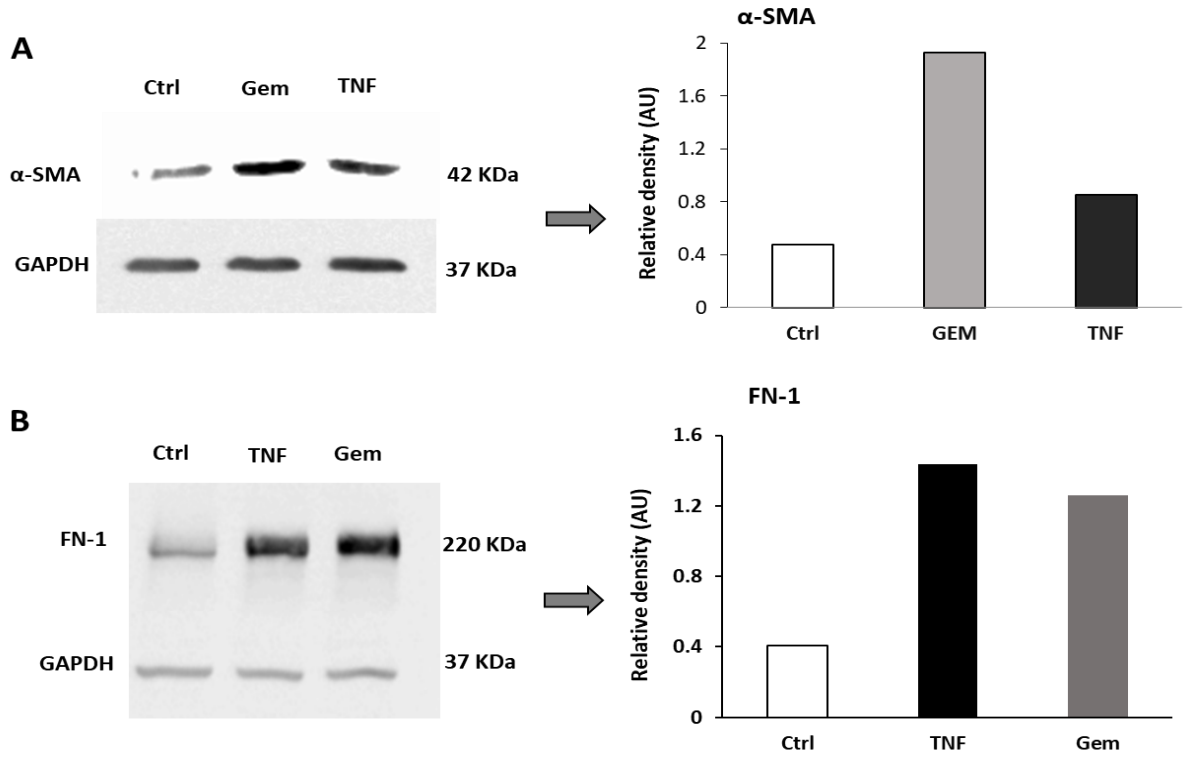

Figure 6. Effect of gemcitabine on PSC activation*. Immunoblots with the respective densitometry showing the expression of α-SMA (A) and fibronectin (B) by PSCs treated with 2μg/ml gemcitabine and TNF-α for 24 h. The experiments were done with Maureen Buschman and Hannah Kempf.*

10.1.2. Characterization and validation of PSC secretome

The secretome of five biological replicates of the activated and non-activated PSCs were analyzed by antibody microarrays. This analysis indicated more than 300 differentially regulated proteins which are reported previously with the detailed activation conditions and p-values [181]. The regulated proteins had different cellular locations when analyzed by IPA (Figure 7). The IPA analysis showed that 18% of the markers were secreted into extracellular space while 17% were originated from the plasma membrane. The other proteins were from cytoplasm and nucleus. Moreover, the antibody microarray data of the PSC secretome was validated by ELISA and immunoblotting (Figure 8). In agreement with the microarray data, immunoblot results confirmed the upregulation of IL-4, IL-1β, FGF-1, SERPINE, FN-1 and Collagen in the secretome of activated PSCs (Figure 8A, B and C). Similarly, ELISA results have shown that IL-6, collagen and fibronectin were significantly upregulated in the secretome of activated PSCs compared to the non-activated one (Figure 8D, E and F respectively).

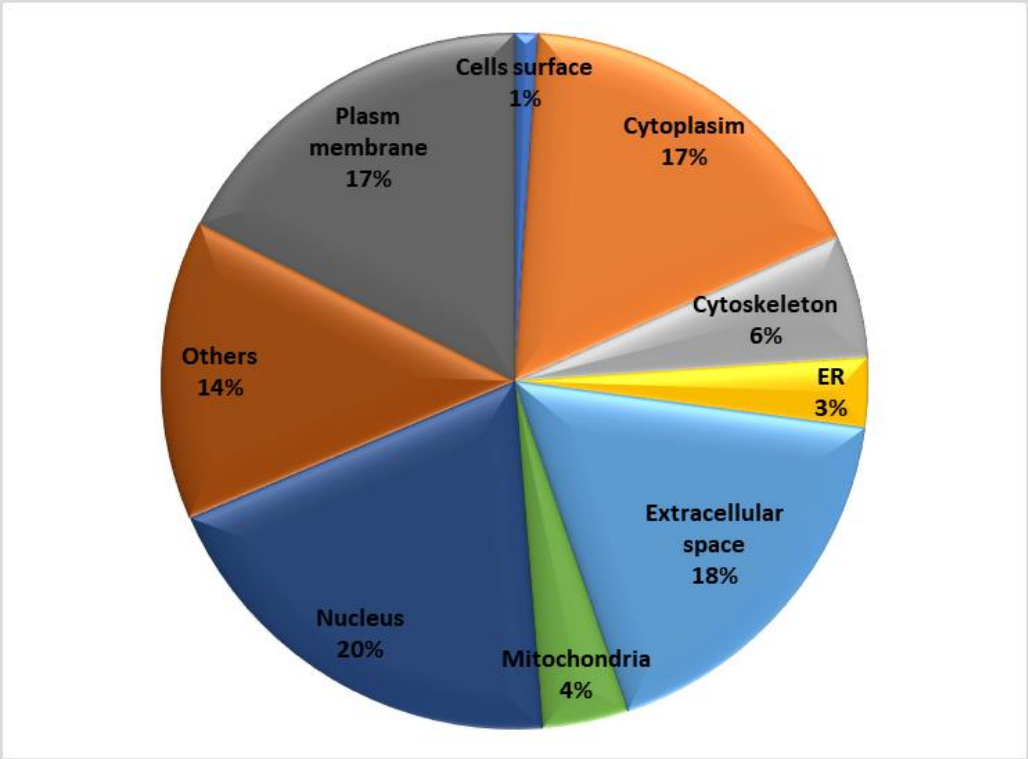

Figure 7. Percentage and cellular location of the secreted proteins by activated PSCs*. The profiled secretome data by antibody microarrays was analyzed by Ingenuity pathway analysis which was performed by Aseel Marzoq and the figure was created by myself.*

Interestingly, the disease and functional annotation analysis performed by IPA predicted increased activation of immune cells by the PSC secretome (Table 1). In such analysis the top diseased and functions with the top activation z-scores were associated to immune response of cells and phagocytes, lymphocyte homeostasis, recruitment and differentiation of mononuclear leukocytes and cell viability of leukocytes. Moreover, the functional analysis indicated that some of the molecules such as CSF-2, FN-1, IL-2RG, IL-6 and TNF were associated with macrophages activation, induction and migration (Table 2). The analysis predicted the potential influence of PSC secretome on the function of immune cells, the interaction which is particularly investigated in detail. The predicted functional analysis of the activated PSC secretome on cell death and proliferation by IPA showed that 136 proteins are involved in increasing tumor cell line proliferation and 122 others are involved in cell viability (Table 3). In contrast, the molecules related to apoptosis, necrosis and cell death had a negative z-score indicating the down regulation of those markers in the secretome of PSC.

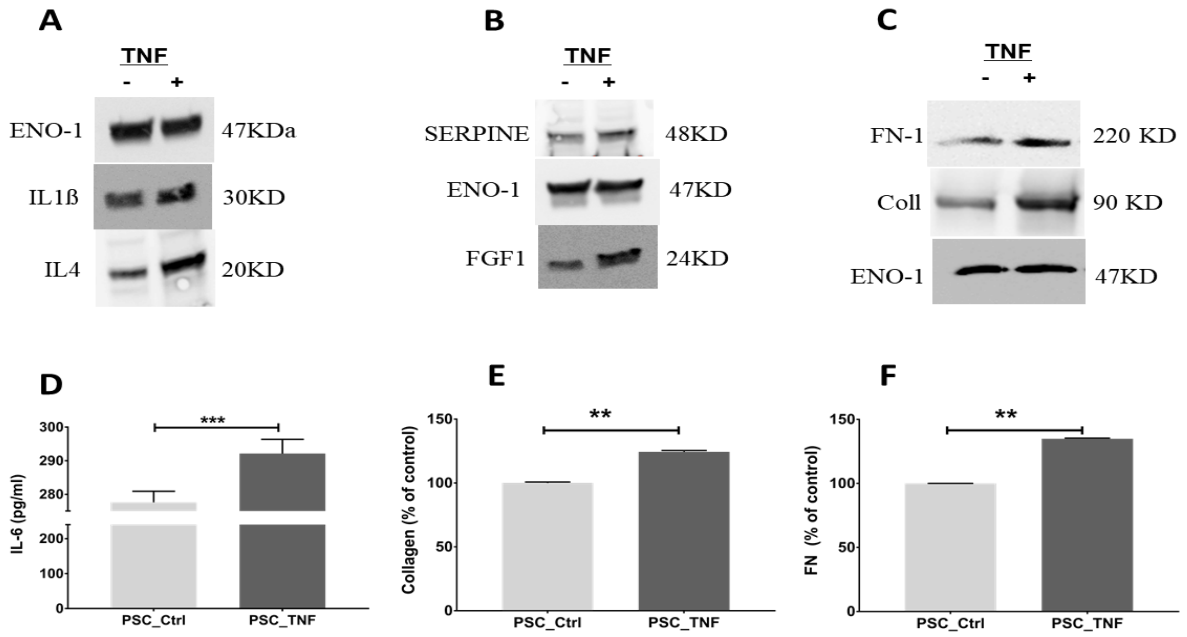

Figure 8. Validation of secreted proteins by PSCs after stimulation with TNF-α*. (A, B and C) Immunoblots show the differential regulation of different proteins in the PSCs secretome. ENO-1 was used as an internal control. IL-6 (D), collagen (E) and fibronectin (F) were validated by ELISA. Data were analyzed using an unpaired, non-parametric Mann-Whitney test. **P<0.005, ***P<0.0005. IL-6 validation was performed by myself whereas the other experiments were conducted by Aseel Marzoq.*

Table 1. Downstream effects analysis of activated PSC secretome*. List of the most relevant diseases and functions, their p-values, the predicted activation states with activation z-scores higher than 2 and the number (#) of involved molecules that are associated with each disease or function and were regulated in the PSC secretome.*

Diseases or Functions Annotation	p-Value	Predicted Activation State	Activation z-score	# Molecules
Immune response of cells	1.73E-27	Increased	3.045	59
Immune response of leukocytes	4.32E-20	Increased	2.989	37
Lymphocyte homeostasis	2.11E-22	Increased	2.892	53
Immune response of phagocytes	1.74E-18	Increased	2.879	29
T cell development	9.03E-21	Increased	2.851	49
Transmigration of cells	3.02E-18	Increased	2.694	26
Hematopoiesis of mononuclear leukocytes	2.46E-25	Increased	2.691	63
Homeostasis of leukocytes	8.32E-23	Increased	2.578	54
Response of myeloid cells	1.72E-17	Increased	2.573	29
Differentiation of mononuclear leukocytes	5.22E-26	Increased	2.558	64
Quantity of lymphatic system cells	6.15E-33	Increased	2.517	75
Migration of myeloid cells	5.17E-25	Increased	2.506	33
Quantity of lymphoid cells	1.54E-27	Increased	2.394	66
Cellular homeostasis	1.71E-34	Increased	2.332	111
Chemotaxis of myeloid cells	3.39E-21	Increased	2.303	37
Quantity of lymphocytes	8.33E-27	Increased	2.274	65
Recruitment of mononuclear leukocytes	8.65E-23	Increased	2.199	27
Activation of antigen presenting cells	1.99E-17	Increased	2.094	34
Cell viability of leukocytes	1.5E-24	Increased	2.055	38

Table 2. Functional annotation of some molecules upregulated by the TNF-α stimulation based on ingenuity pathway analysis (IPA). *The listed markers are the relevant proteins with their p-Values and predicted functional effects on macrophages.*

Protein symbol	P. Value	Functions
CSF2	2.50E-05	Activation of macrophages
FN1	0.000166	Activation of macrophages and cell movement of monocytes
VEGFC	8.80E-05	Angiogenesis
IL2RG	0.000874	Induction of macrophage
CXCL10	0.002139	Activation and cell movement of macrophages
IL2	0.000281	Activation of macrophages, cell movement of monocytes and angiogenesis
IFNg	0.000223	Migration of macrophages
IL6	0.000166	Activation of macrophages and cell movement of monocytes
MMP10	0.002299	Migration of macrophages
TNF	0.000179	Activation, cell movement of macrophages and infiltration by macrophages
IGF2	0.010064	Angiogenesis
MMP12	0.001377	Migration and cell movement of macrophages
CXCR5	0.004296	Activation of macrophages

Table 3. Predicted functional effect of activated PSC secretome on cell death and proliferation*. List of the relevant functions and the predicted activation state with the number of molecules involved.*

Function Annotation	p-value	Activation z-score	# Molecules
Apoptosis	2.24E-60	-0.797	177
Necrosis	3.1E-59	-0.28	176
Cell death	3.71E-59	-0.046	197
Cell proliferation of tumor cell lines	5.31E-54	1.604	136
Cell viability	1.03E-51	1.886	122
Cell survival	1.5E-50	1.916	124
Migration of cells	8.58E-50	1.114	143
Invasion of cells	1.93E-37	1.666	87

10.1.3. Reactive oxygen species (ROS) measurement in the PSC

The intracellular ROS was measured in the activated and non-activated PSCs using the non-fluorescent substrate dichlorofluorescein (H2DCF). The intracellular level of ROS was significantly increased in the PSCs treated with TNF-α after 24 h (but not after 6 h) compared to the non-treated cells (Figure 9). This confirmed the activation

of PSCs with TNF-α as it is known that TNF-α is inducing reactive oxygen species [194] which is a known PSC activating agent [80].

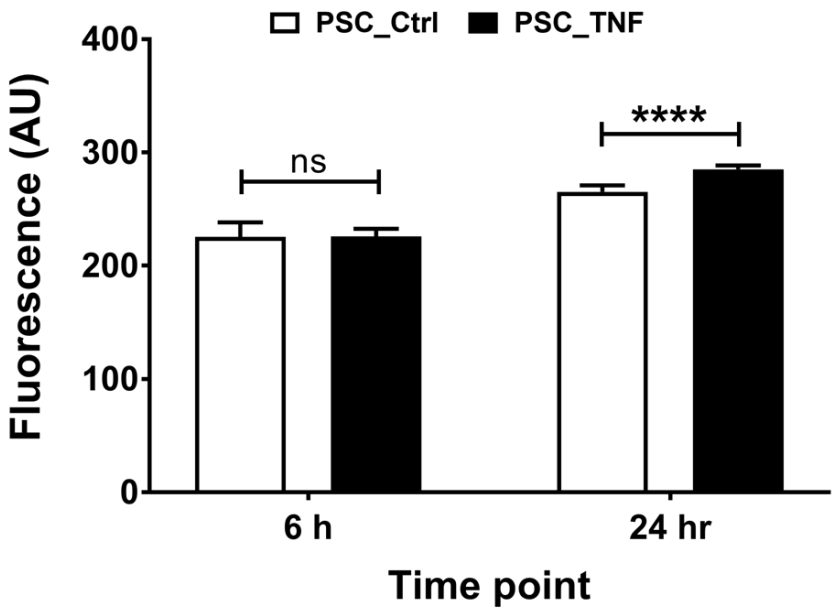

***Figure 9. Reactive oxygen species (ROS) production by PSCs**. ROS was measured in the PSCs treated with TNF-α (10 ng/ml) for 6 and 24 h and the non-treated controls. Compared to the non-treated PSCs, stimulation with TNF-α significantly increased ROS production after 24 h. Data were analyzed using two-tailed, unpaired t-test and results were expressed as mean values with the standard deviation. ****P<0.0001, ns=not significant*

10.1.4. Secretome of activated PSC increased cancer cell proliferation

We investigated the paracrine effect of stromal cells secretome on tumor cells, to see whether the secretome of PSCs have a role in cancer cell proliferation. The pancreatic cancer cell line BxPC-3 was treated with the secretome of activated and non-activated PSCs for 24 and 48 h then cell proliferation was determined using the resazurin fluorescent dye. The secretome of activated PSC, in comparison to the non-activated PSC, significantly increased BxPC-3 cell proliferation in both 24 h and 48 h time points (Figure 10). However, the secretome of non-activated PSCs increased the BxPC-3 cell proliferation only after 24 h in comparison to the untreated control but, its effect has come to an end at the 48 h time point. The significant impact of activated PSCs secretome on cell proliferation is probably due to the availability of different types of growth factors that promote survival and proliferation of cancer cells as indicated in the IPA analysis (Table 3).

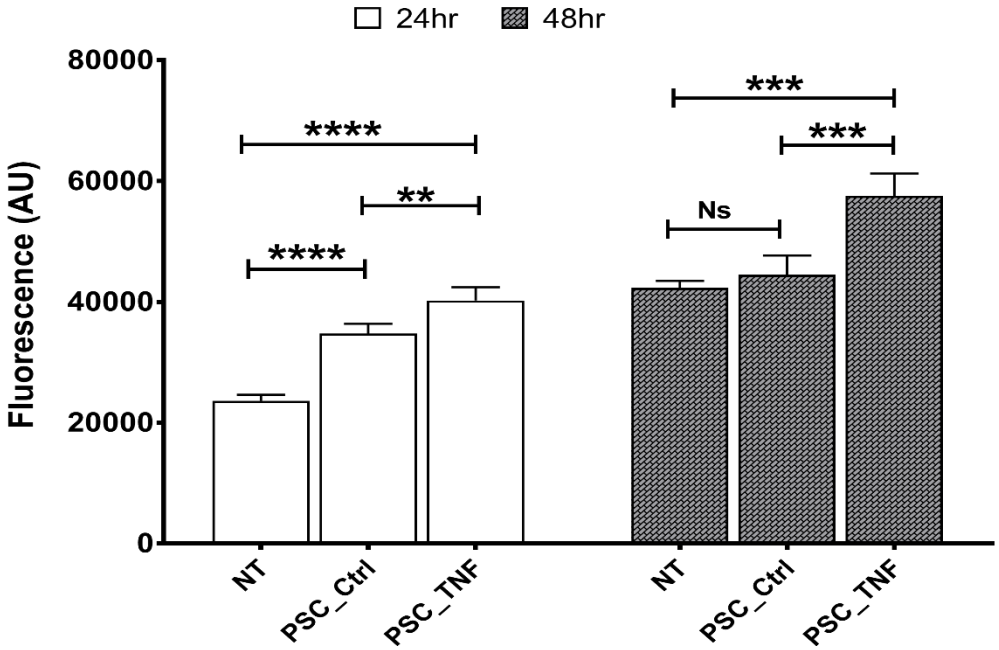

Figure 10. Regulation of pancreatic ductal adenocarcinoma cell proliferation by the secretome of PSCs. *BxPC-3 cells were treated with the secretome of activated (PSC_TNF), non-activated PSCs (PSC_Ctrl) and no treatment (NT) for 24 and 48 h in quadruplicates. Relative cellular proliferation was determined using fluorescent resazurin dye after one-hour incubation. Data were analyzed using one-way ANOVA, Bonferroni's multiple comparisons test. **P<0.005, ***P<0.0005, ****P<0.0001, ns=not significant*

Effect of IL-6 on PDAC proliferation

The secretome of activated PSCs increased PDAC proliferation (Figure 10) compared to the non-activated PSCs. Since IL-6 was significantly upregulated in the PSC secretome, the effect of different concentrations of IL-6 on Panc-1 cells proliferation was evaluated. Cell proliferation was measured with the resazurin fluorescent dye and compared to the negative and positive controls (Figure 11). However, cell proliferation significantly increased only when 10% FBS was used whereas IL-6 didn't show significant effect on cell proliferation. Thus, the results indicating that IL-6 in the secretome of PSCs is not the molecule that have increased PDAC cell proliferation.

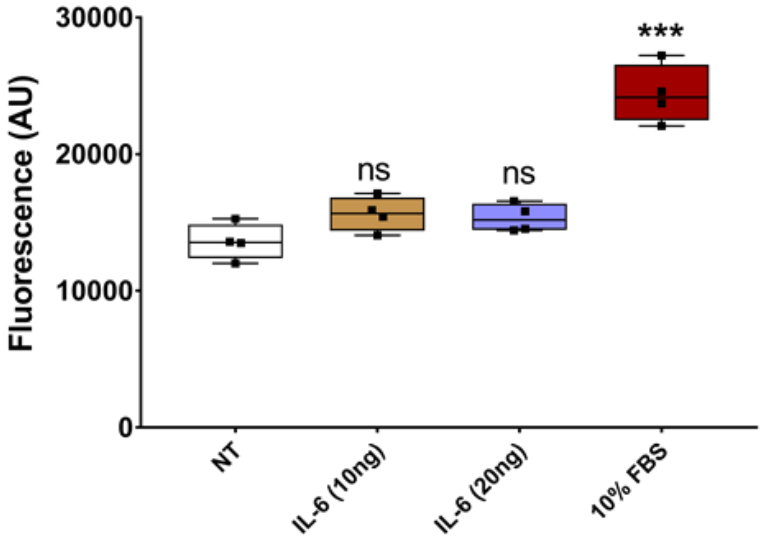

Figure 11. Box plots showing the proliferation of pancreatic ductal adenocarcinoma cells by IL-6. *Panc-1 cells were treated with IL-6 for 24 h in quadruplicates. Relative cellular proliferation was determined using fluorescent resazurin dye after one-hour incubation. Data were analyzed using a two tailed, unpaired t-test. ***P<0.0005, ns=not significant.*

10.2. PSC and macrophage cellular interaction at the secretome level

The impact of the PSCs and PDAC secretome on the function and polarization state of macrophages were investigated. Monocytes were isolated from healthy human blood by density gradient centrifugation yielding a purity of monocytes of 93% of total PBMC expressing 100% CD14 marker (Figure 12) which was analyzed by flow cytometry. Monocyte-derived human macrophages were then treated with the secretome of activated and non-activated PSCs and PDAC secretome for seven days with two days interval changing the media and the stimuli. Because of the genetic variations among different donors, monocytes stimulation may differ among different blood donor, therefore, positive controls were always included in all experiments. This was necessary to see the functional response of isolated monocytes to the stimuli and to overcome false-positive results. Monocytes were treated with LPS and IFNγ for the M1 positive control whereas IL4, IL-10 and IL-13 were used to stimulate M2 polarization.

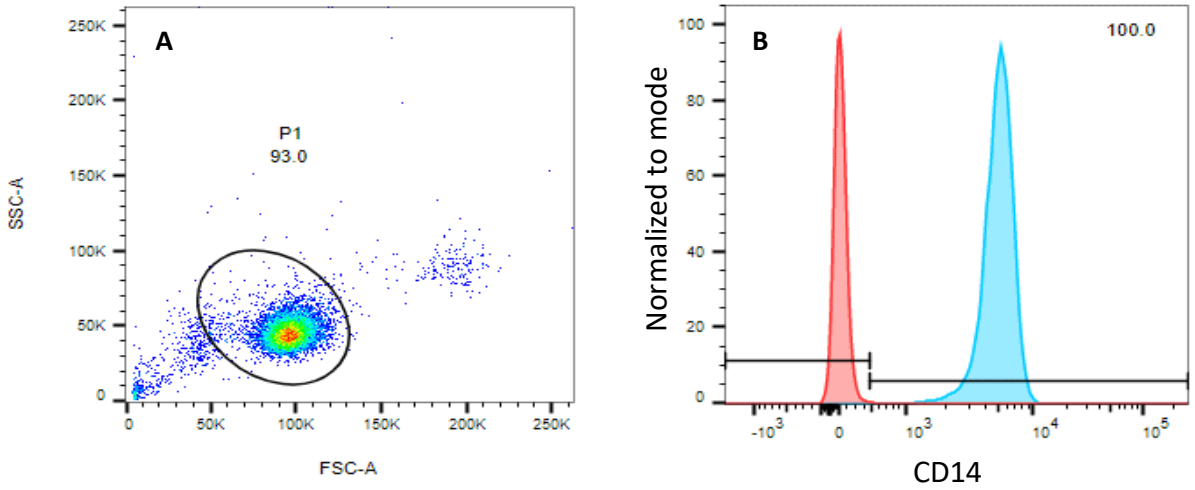

Figure 12. Representative dot plot and FACS histogram show the purity of isolated CD14⁺ monocytes. *At least 1x10⁴ events were collected and analyzed by flow cytometry using CD14-isotype as negative control (B, in red). Monocytes composed 93% of total isolated cells (A) as determined by CD14 staining (B).*

10.2.1. Differentiation of monocytes to macrophages

The differentiation of monocytes to macrophages was first confirmed either phenotypically, by observing cell structure changes or based on the expression of HLA-DR antigen (Human Leukocyte Antigen – antigen D Related). Monocytes treated with different stimuli or the PSC secretome, were checked for differentiation before the final detachment for analysis. Microscopic observation of the monocytes treated with M-CSF, GM-CSF and the PSC secretome indicated the differentiation of monocytes to different types of macrophages (Figure 13.) Microscopic images of the standard macrophage types showed spindle-shaped M1 macrophages and round or oval shaped M2 macrophages, where cells treated with the secretome of PSCs showed both phenotypes. To further inspect monocyte differentiation, HLA-DR expression was measured on the cell surface of the macrophages and found that HLA-DR is expressed significantly higher on the cells treated with the PSC secretome than those primed with M-CSF and GM-CSF (Figure 14) where no significant difference between primed cells with M-CSF and GM-CSF have been seen.

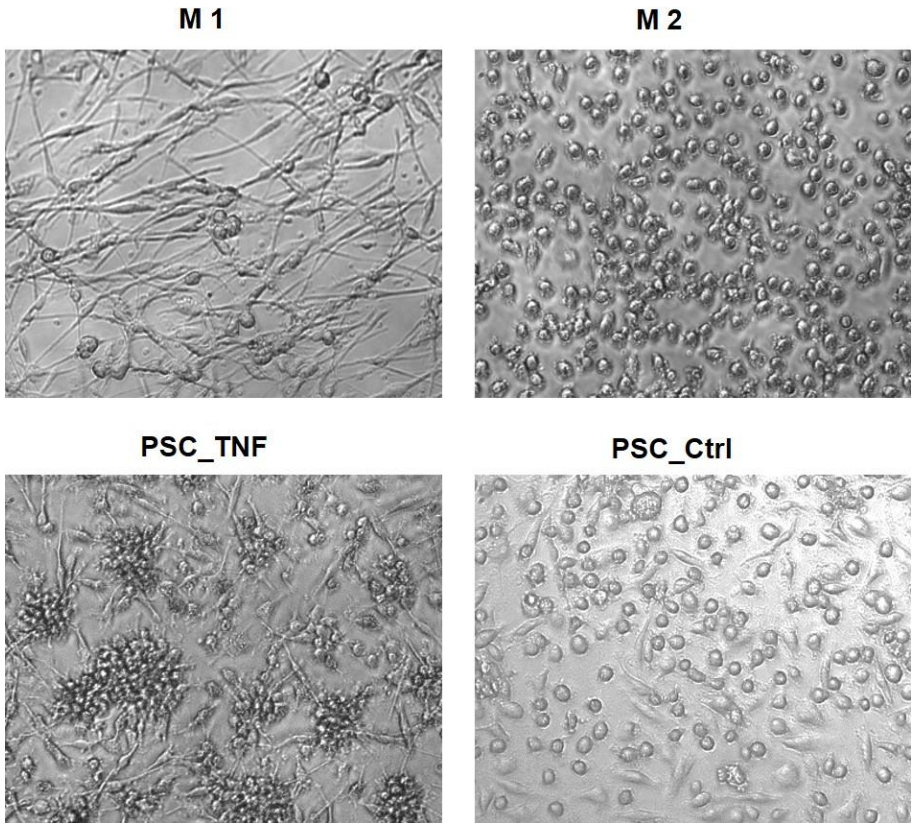

Figure 13. Characterization of monocyte differentiation to macrophages. *Microscopic images of M1 macrophages (LPS+IFNγ stimulated) exhibiting typical spindle shaped morphology whereas M2 cells (IL4/10/13 stimulated) have round-shaped cells. Monocytes treated with secretome of activated/non-activated PSCs have both M1 and M2 characteristics. All images were taken with 10x objective lens.*

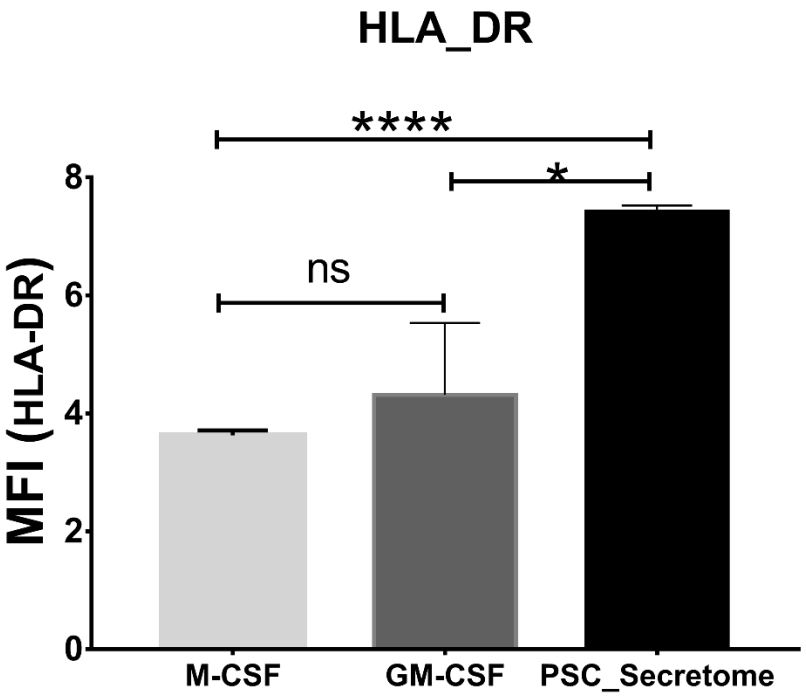

Figure 14. Expression of HLA-DR on the surface of treated macrophages*. Monocytes treated with M-CSF, GM-CSF and PSC secretome. The secretome significantly increased HLA-DR expression on macrophages confirming monocytes differentiation. Data expressed as mean values with the standard deviations of three biological replicates, * P<0.05, ****P<0.0001, ns = not significant.*

10.2.2. Analysis of macrophage polarization surface markers by FACS

After treating macrophages with the secretome of PSC and PDAC cell lines, the cells were harvested, and macrophage polarization markers were analyzed on the surface of the cells. Flow cytometry was performed for seven independent experiments whereby the analysis revealed the polarization of the macrophages based on the expression of M2 surface markers such as scavenger receptor (CD163) and mannose receptor (CD206) as well as M1 surface marker, CD86 (Figure 15). The histograms are showing the expression of cell surface markers of each treatment including the positive control groups; M1 and M2. Moreover, to show the influence of different treatments, the mean fluorescence intensity (MFI) of each marker was calculated by dividing the geometric mean of the antibody to its isotype control (Figure 16).

The M2 markers (CD163 and CD206) were highly expressed on M2 positive control and on macrophages which were treated with the secretome of activated PSC and PDAC. As it is assumed, the M1 marker CD86 was expressed higher on the surface of M1 positive control as well as on the macrophages which were treated with the secretome of non-activated PSC. From the FACS histograms, it could be concluded that the secretome of PDAC and the activated PSCs promote macrophages towards the M2 phenotype while the non-activated PSCs secretome induced M1 type of macrophages which are the physiological proinflammatory phagocytes. Nevertheless, to see the differential effect of different PSC secretome on macrophage polarization, the data of each experiment was analyzed separately by comparing the data of activated PSCs (PSC-TNF) to the non-activated PSC control (PSC_Ctrl). The secretome of activated PSCs had significantly enhanced the expression of CD163 and CD206 on the macrophages whereas the increased expression of CD86 by the secretome of non-activated PSCs was not significant (Figure 17).

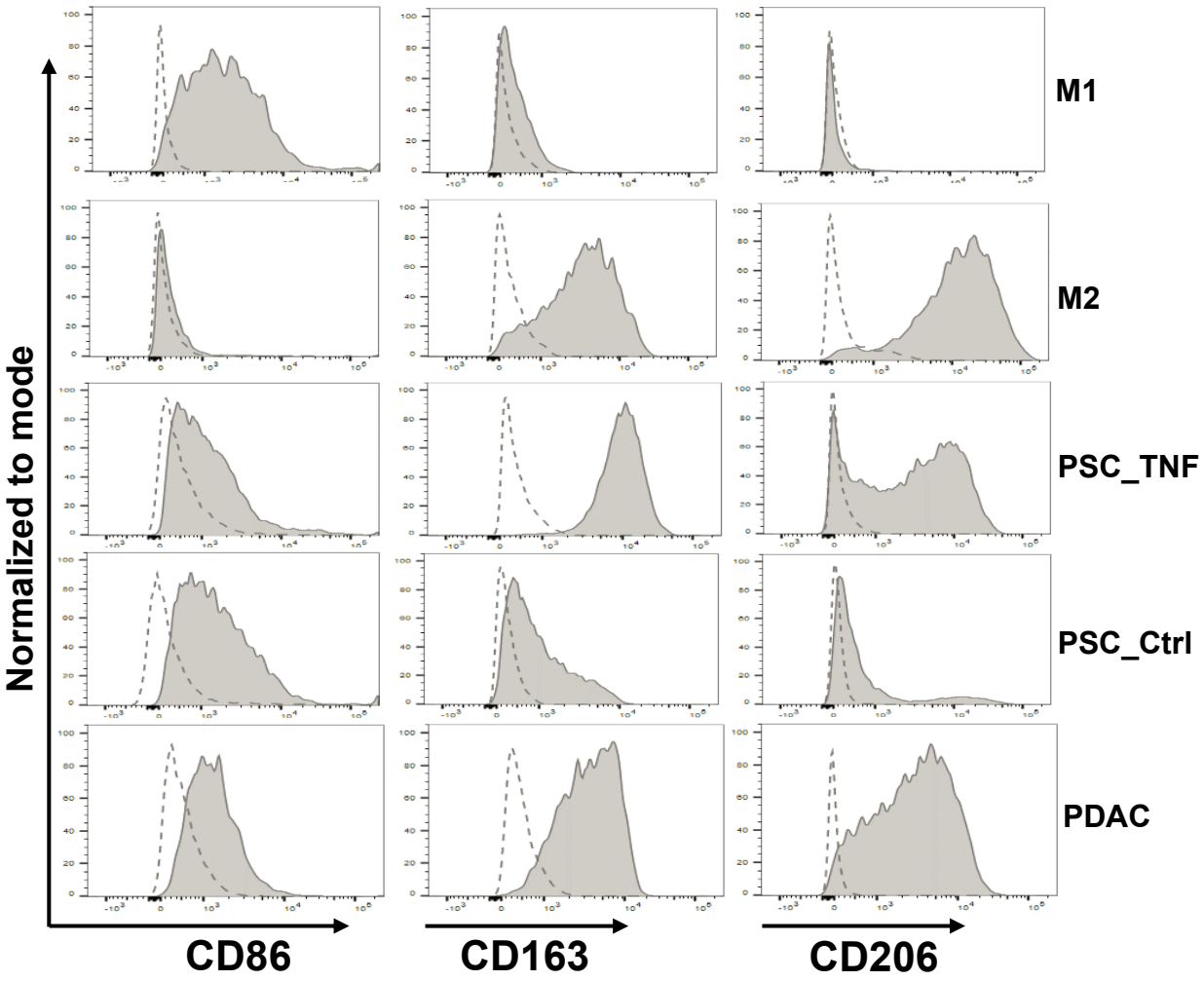

***Figure 16. FACS histograms showing the expression of M1 (CD86) and M2 (CD163 and CD206) cell surface markers**. Macrophages were treated with the secretome of activated PSC (PSC_TNF), non-activated PSC (PSC_Ctrl) and PDAC. M1 and M2, the positive controls, were treated with LPS+IFNγ and IL-4/10/13 respectively. Isotype control of each antibody was used as a negative control (dashed line). The data were analyzed using the FlowJo software.*

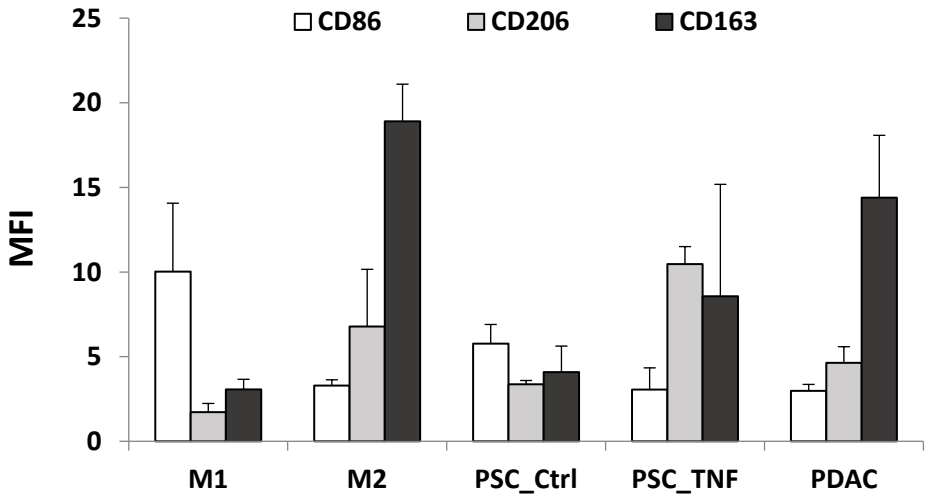

***Figure 15. Mean Fluorescence Intensity (MFI) of CD86, CD163 and CD206 markers expressed on macrophages.** MFI values were calculated relative to the isotype control of the corresponding antibodies. Data of seven independent experiments were shown as mean values with respective standard deviations.*

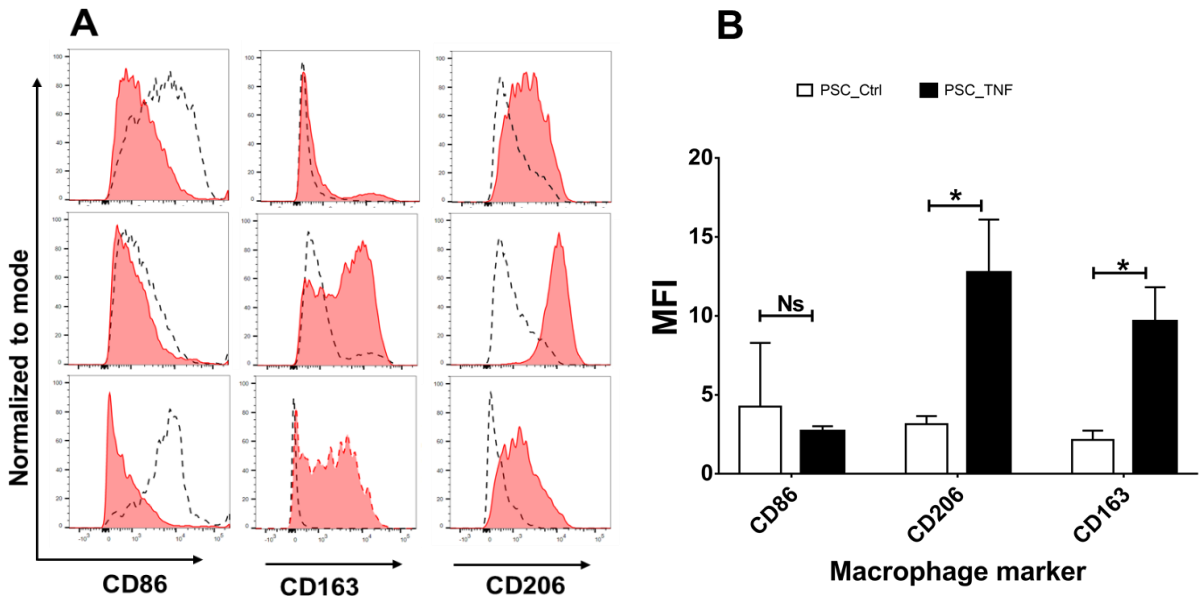

Figure 17. Changes in cell surface marker expression and median fluorescence intensity (MFI) values of macrophage markers after treatment with the secretome of activated and non-activated PSC*. A, FACS Histogram of three independent experiments showing the expression of CD86, CD163 and CD206 markers on macrophages treated with activated PSC secretome (Red area) and non-activated PSC (dashed line). B, MFI values of CD86, CD163 and CD206 markers expressed on macrophages were calculated relative to the isotype negative control. The secretome of activated PSC has significantly increased M2 (CD163 and CD206) markers whereas the expression of the M1 marker (CD86) does not change significantly. Data of seven independent experiments were analyzed and presented as median values with the respective standard deviations. * P<0.05, ns=not significant*

10.2.3. Analysis of cytokine and chemokines in macrophage at the RNA level

The effect of the PSCs secretome on macrophage polarization was evaluated at the RNA level using quantitative real time PCR (qRT-PCR). Cytokines and chemokines such as TNF-α, IL-1β, CCL17 and mannose receptor (CD206) were measured in the treated macrophages with the secretome of activated PSCs and non-activated PSCs (Figure 18). Of note, CD206 was measured again to validate the flow cytometry result. It has previously been shown that M1 macrophages express higher TNF-α, IL-1β whereas CCL17 and CD206 are highly expressed by M2 macrophages [195]. The macrophages treated with the secretome of activated PSCs expressed significantly higher levels of CD206 and CCL17 (Figure 18 A & B) but lower levels of IL-1β and TNF-α (Figure 18 C& D) compared to the macrophages treated with non-activated PSC secretome. In accordance with the flow cytometry data, the secretome of non-activated PSCs significantly increased the levels of M1 markers, IL-1β and TNF-α.

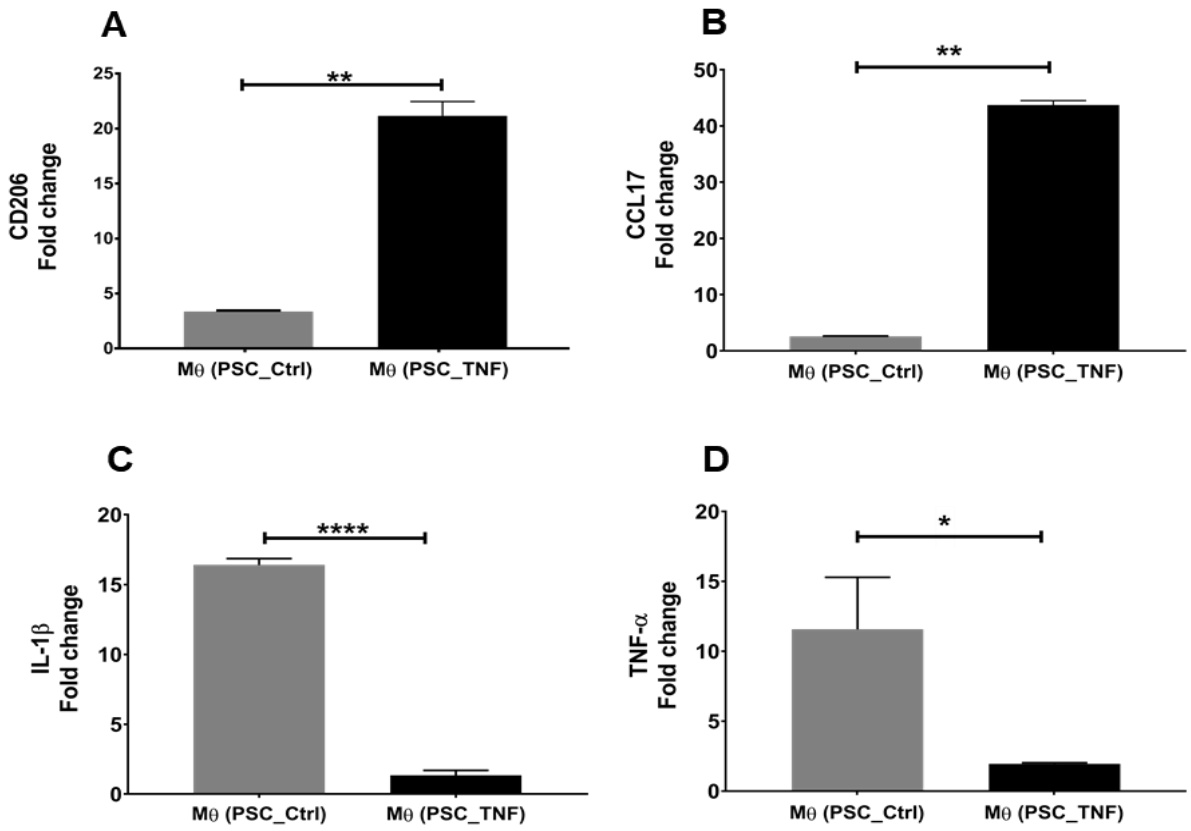

Figure 18. Real-time PCR analysis of macrophage cytokine and chemokine expression in primary macrophages treated with PSCs secretome. *RT-PCR was carried out on representative cDNA of each sample. M2 markers CD206 (A), CCL17 (B) and M1 markers, IL-1β (C), TNF-α (D), were quantified relative to the non-treated control and normalized to the internal control (GAPDH). Data were analyzed using an unpaired t-test. * P<0.05, ** P<0.005, **** P<0.0001.*

10.2.4. Arginase expression and NO production by the treated macrophages

To further characterize functional changes in macrophages after incubation with the conditioned media of PSCs, type-1 arginase (Arg-1) expression and activity as well as nitric oxide (NO) production were measured. Arginase expression is associated to the M2 type macrophages and it is involved in L-arginine metabolism in the process of tissue repairing. In contrast, nitric oxide which is also produced from L-arginine metabolism by iNOS enzyme, is associated to the M1 phenotype [123]. Arginase and NO were assessed in Raw264.7 mouse macrophages which were treated with activated and non-activated PSCs secretome for 48 hours. Arginase activity was measured based on urea production whereas arginase expression was measured in the cell lysates by western blotting (Figure 19). Arginase activity was significantly increased in macrophages which were treated with IL4/13 (positive control) and with

the secretome of activated PSCs in comparison to the treated macrophages with non-activated PSC secretome and non-treated control (NT) as in Figure 19 A. Of note, the effect of non-activated PSC secretome was not significant. The western blot data confirmed that, macrophages treated with the secretome of activated PSC promoted the expression of arginase in comparison to the macrophages treated with the secretome of non-activated PSC (Figure 19B).

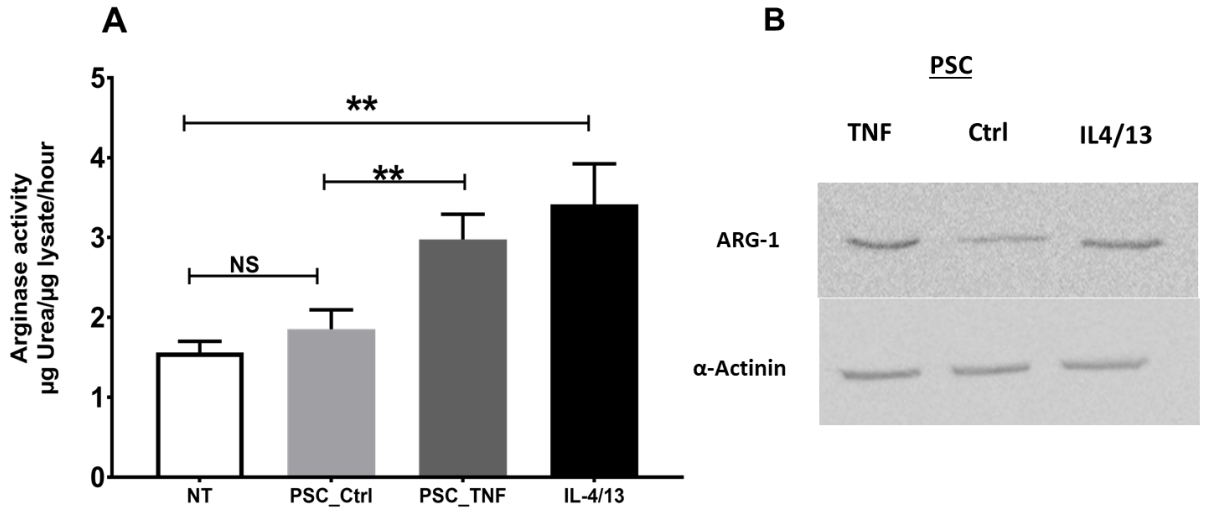

Figure 19. Effect of the PSCs secretome on arginase activity and expression by macrophages. *Macrophages were treated for 48 h with the secretome of activated PSCs (Mθ-PSC_TNF), non-activated PSC (Mθ-PSC_Ctrl), IL-4/13 as positive control and no treatment (NT) as negative control. A, arginase activity was measured in cell lysates (n=4) and compared to the non-treated control (NT). Data were analyzed using two-tailed, unpaired t-test and results were expressed as mean values with the standard deviations. B, Western blot indicated the arginase-1 expression in macrophage lysates. The relative intensity of each sample was normalized to α-Actinin which serves as the internal control. NS= not significant, ** P-value<0.005.*

On the other hand, expression of iNOS, the enzyme responsible for NO production from arginine, couldn't be detected by western blot although various parameters were changed such as concentrations of the antibody, incubation times, washing and developing time. (data not shown). Alternatively, NO was measured in the conditioned media (CM) of the PSCs and macrophages, as a byproduct of arginine metabolism by iNOS. Because CM of PSCs were used in the treatment of macrophage, therefore, NO was first measured in the PSC's CM to be subtracted from the NO values of the macrophages afterwards. However, NO production didn't change significantly between the CM of activated and non-activated PSCs (Figure 20A). But the CM of non-activated PSCs significantly increased the NO production in macrophages (Mθ-PSC_Ctrl) when compared to the macrophages which were

treated with the activated PSCs CM (Mθ-PSC_TNF) in both time points (Figure 20B). Additionally, a significant difference in NO production could be seen in the macrophages which were treated with the CM of non-activated PSCs comparing the 48 h treatment to the 24 h.

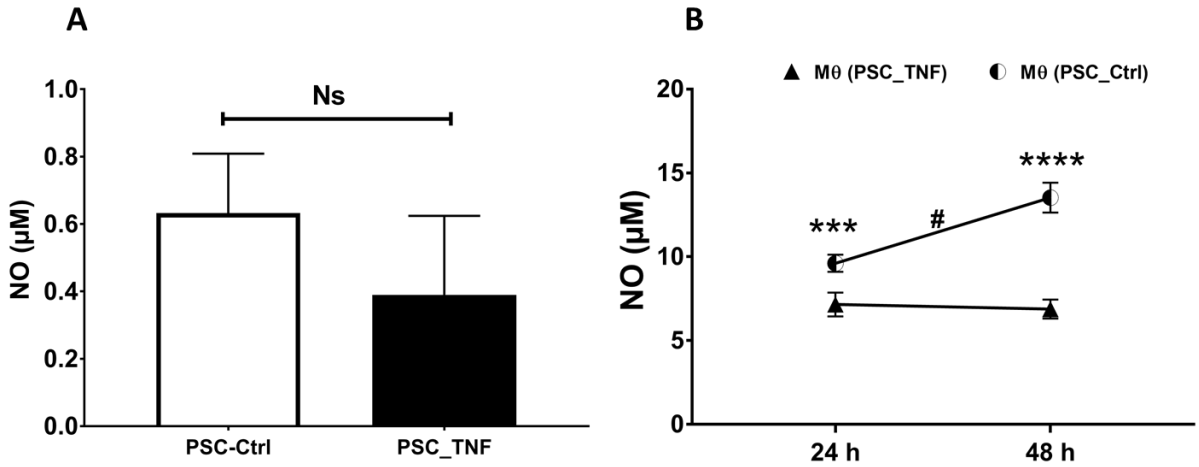

Figure 20. Nitric oxide (NO) production by macrophages and PSCs*. A, NO was measured in the CM of PSCs before they were used in macrophage treatment using Griess method. NO production was not changing significantly between the stimulated PSCs and the control. B, macrophages treated with the non-activated PSCs CM (Mθ PSC_Ctrl) produce significantly higher NO after 24 and 48 h treatment when compared to the macrophages treated with the conditioned medium of activated PSC (Mθ PSC_TNF). Data were analyzed using a two-tailed, unpaired t-test and results were expressed as mean value and respective standard deviations. ***P<0.005, ****P<0.0001, # significant comparing 24h to 48 h, ns=not significant*

10.2.5. ROS synthesis in macrophages up on treatment

ROS are known as PSC activating agents which are contributed to the polarization of macrophages into M2 type [80, 196]. Therefore, ROS was measured in the treated macrophages with the PSCs secretome. As it is shown in Figure 21, macrophages treated with the secretome of activated PSCs (Mθ-PSC_TNF) produce significantly lower ROS in both 24 h and 48 h treatments compared to the macrophages treated with the secretome of non-activated PSCs (Mθ-PSC_TNF). Remarkably, ROS production decreased in the 48 h treatment compared to the 24 h of both treatments. This suggests the possibility of M1 polarization by the secretome of non-activated PSCs because it is already known that NO and ROS are highly produced by the pro-inflammatory macrophages [110].

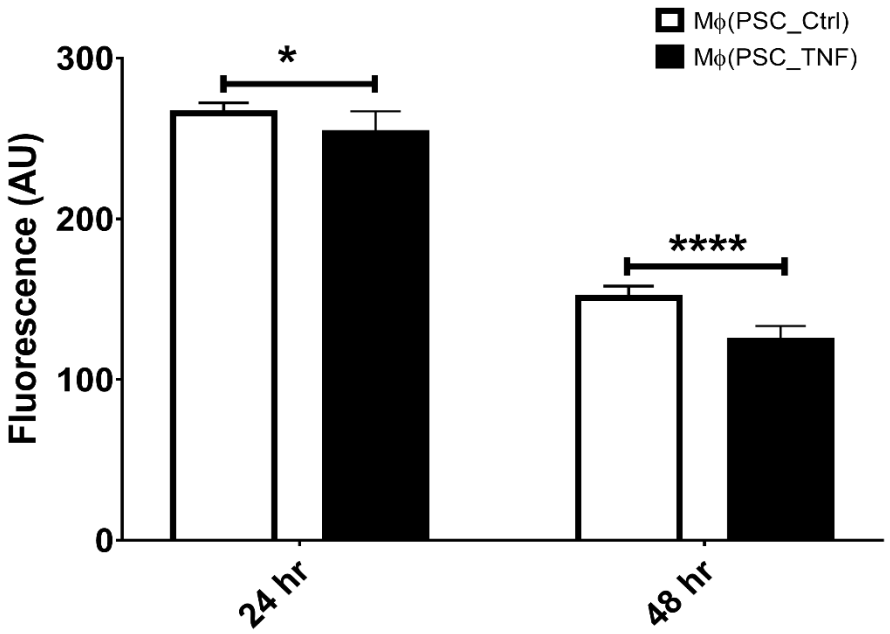

***Figure 21. Reactive oxygen species (ROS) production by macrophages**. ROS were measured in the macrophages treated with the secretome of PSCs after 24 and 48 h using 2´,7´-dichlorofluorescein diacetate (DCFH-DA). Macrophages treated with activated PSC's secretome (Mθ PSC_TNF) produce significantly lower ROS compared to the those treated with non-activated PSC (Mθ PSC_Ctrl). Data were analyzed using a two-tailed, unpaired t-test and results were expressed as mean values with the standard deviation. *P<0.05, ****P<0.0005.*

10.2.6. Role of PSC-educated macrophages in PDAC cell proliferation

The influence of macrophage CM has been studied in different tumors [197, 198], however, to our knowledge, role of macrophages which have been incubated with the PSC's secretome on the proliferation of cancer cells is not studied yet. We aimed to investigate the paracrine signaling between incubated macrophages with PSC's secretome and pancreatic cancer cells. Accordingly, Panc-1 cells were treated with the secretome of the pre-treated macrophages with PSC secretome for 24 and 48 h. Macrophages which were incubated with the secretome of activated PSCs have significantly increased Panc-1 proliferation at both time points compared to those treated with the secretome of non-activated PSCs (Figure 22 A&B). There is a significant difference between the non-treated control which is incubated in serum free medium (SFM) and the positive control (10% FBS) treatment.

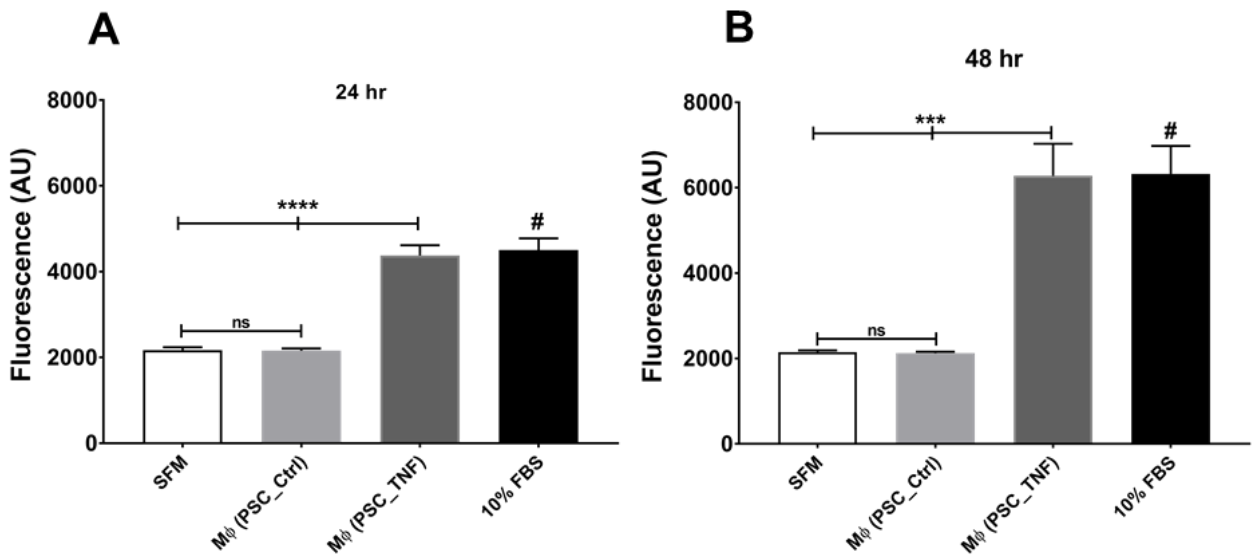

Figure 22. Regulation of pancreatic ductal adenocarcinoma cell (Panc-1) proliferation by the secretome of pre-treated macrophages with the PSCs secretome*. Panc-1 cells were treated for 24 h (A) and 48 h (B) with the secretome of macrophages which were incubated with the PSCs secretome. Relative cellular proliferation was determined using the fluorescent resazurin dye. Data were analyzed using a two tailed, unpaired t-test and results of five biological replicates were expressed as mean values with the standard deviations. ***P<0.0005, ****P<0.0001, # significant compared to SFM, ns=not significant.*

10.3. Influence of IL-6 on macrophage polarization

IL-6 is a proinflammatory factor which is significantly upregulated in the secretome of activated PSCs (Figure 8D and Table 2). It has been also shown that IL-6 is changing the differentiation of monocytes from dendritic cells to macrophages [199]. However, influence of IL-6 on the expression of surface markers during macrophage polarization, and after polarization is not known yet.

10.3.1. Pre-polarization effect of IL-6

First, IL-6 was used with the standard stimuli of macrophage polarization, so that monocytes were stimulated with LPS/IFNγ and IL-6 to polarize into M1 macrophages whereas IL4 and IL-6 were used to induce M2 polarization. After three days incubation, macrophage surface markers (CD80 and CD206) were analyzed by flow cytometry and overlaid as histograms to see the differences (Figure 23). Surprisingly, IL-6 didn't show a remarkable effect on the M1 markers CD80 (Figure 23 A) whereas the expression of M2 marker, CD206 was decreased by IL-6 compared to the controls, (Figure 23 B).

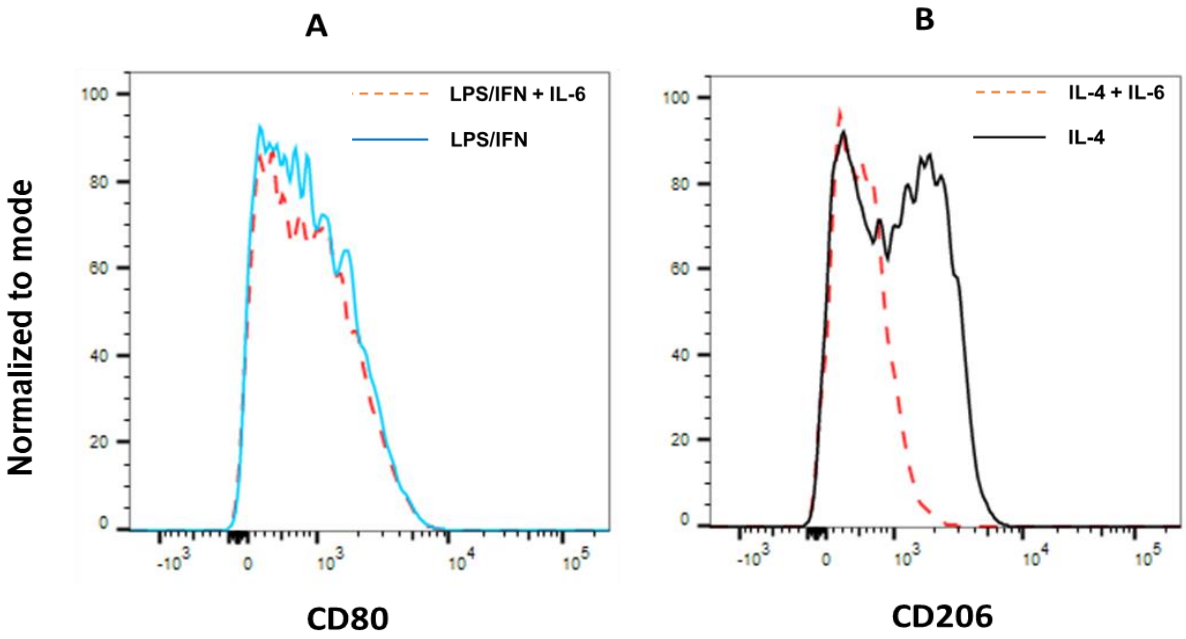

Figure 23. Effect of IL-6 in stimulating macrophage's surface marker expression*. FACS histograms are showing the difference in surface marker expression between macrophages stimulated with IL-6 (orange dashed line) and the controls of both M1 (blue line-A) and M2 (black line-B). IL-6 was used with the standard polarization stimuli of M1 (LPS/IFN) and M2 (IL-4) compared to the controls.*

10.3.2. Effect of IL-6 post-polarization

The second strategy was to evaluate the impact of IL-6 particularly on polarized macrophages. Accordingly, macrophages were polarized to M1 and M2 phenotypes using a standard procedure of LPS/IFNγ and IL4/13 stimulation respectively. After four days of polarization, M1 and M2 macrophages were subsequently, either treated only with recombinant IL-6 or kept non-treated as controls for 48 h. The expression of surface markers on both macrophage types were analyzed with FACS. The FACS histograms (Figure 24) demonstrate that, in comparison to the controls, IL-6 increased the expression of CD206 on both M1 and M2 polarized macrophages (Figure 24 C & D). Of note, IL-6 didn't show any visible effect on the expression of CD80 on M1 and M2 macrophages (Figure 24 A & B). The effect of IL-6 on macrophages at two different stages of polarization are contradictory where IL-6 decreased the M2 marker CD206 when used during polarization but in contrast, it increases CD206 expression on both M1 and M2 polarized macrophages.

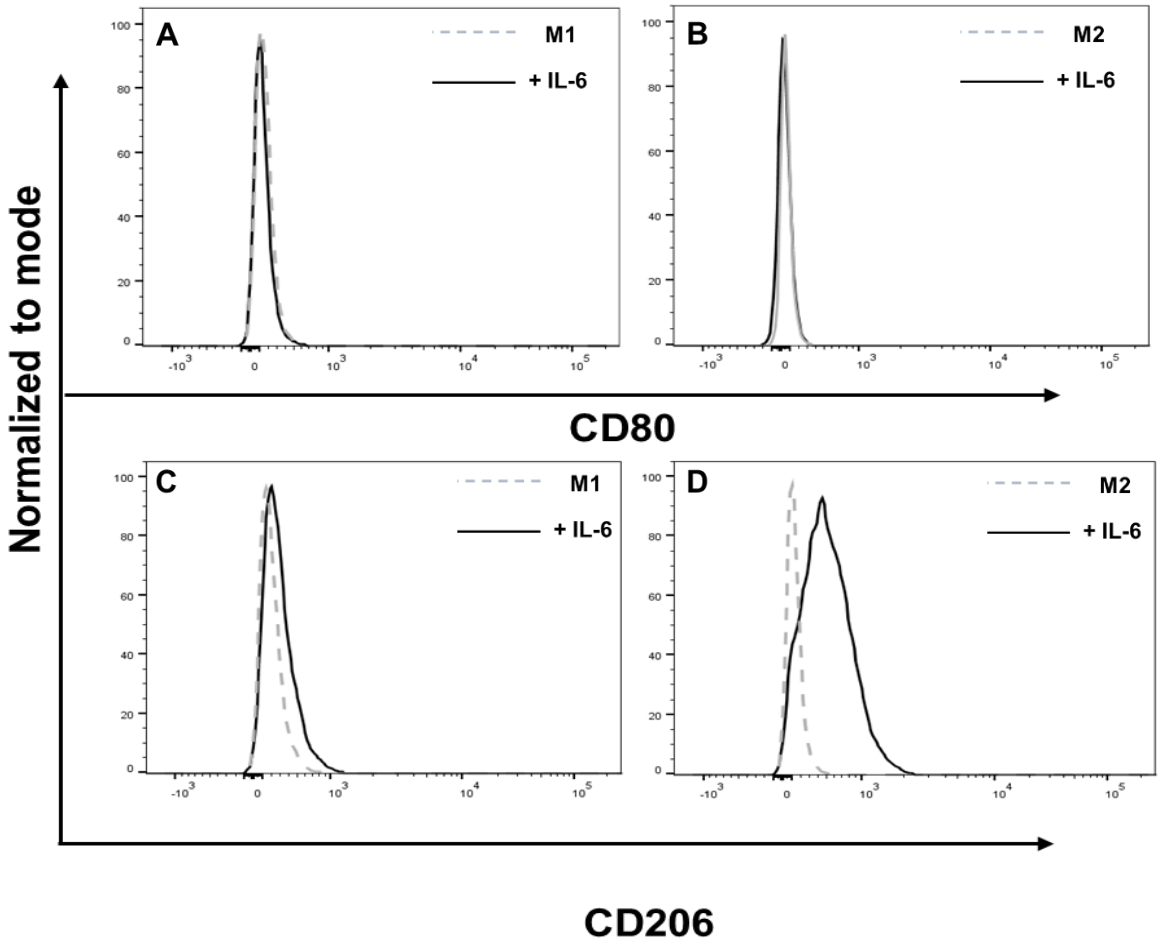

Figure 24. Effect of IL-6 on the expression of macrophage's surface markers after polarization. *Macrophages which were previously polarized to M1 (A & C) and M2 (B & D) phenotypes were exposed to recombinant IL-6. Histograms showing the change in the expression of M1 (CD80) and M2 (CD206) surface markers where the controls (dashed line) were compared to the IL-6 treated macrophages (normal line). FACS data were analyzed and histograms were made with FlowJo. This experiment was performed together with Justus Weber.*

Functional effects of IL-6 on macrophages

We have shown that PSC's secretome increases arginase activity and decreases NO production in macrophages. In the secretome of activated PSCs IL-6 is upregulated and predicted to activate macrophages (Figure 8 D, Table 2). Therefore, we have further evaluated the influence of IL-6 on arginase activity and NO production in macrophages. Arginase activity and NO were measured in M1, M2 as well as in the macrophages which were treated with IL-6 and analyzed in comparison to the control (M0). IL-6 had no significant effect neither on arginase activity (Figure 25 A) nor on NO synthesis (Figure 25 B) compared to the non-treated macrophages (M0). As it was expected, the NO synthesis and arginase enzyme activity were significantly increased by the positive controls, M1 and M2, respectively. Also, M2 macrophages

produced significantly lower NO compared to the non-treated control. Thus, IL-6 in the secretome of activated PSCs, for example, couldn't be attributed to the increase of arginase expression and decrease of NO synthesis.

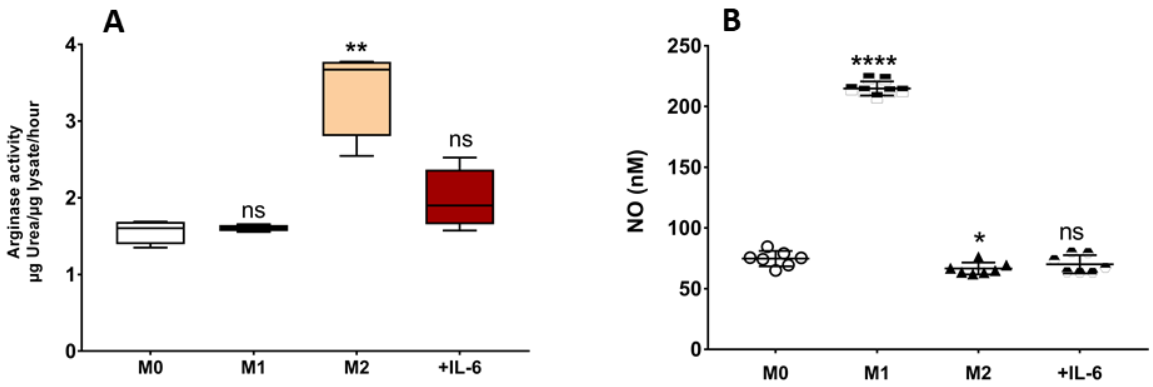

***Figure 25. Influence of IL-6 on arginase activity and nitric oxide synthesis in macrophages**. Arginase activity (A) and nitric oxide production (B) were measured in non-treated macrophages (M0), M1 and M2 polarized macrophages as well as in macrophages treated with IL-6 (+IL-6). No significant changes in arginase activity and NO are noticeable. Data were analyzed using a two tailed, unpaired t-test and represented as mean values with the standard deviations. * P<0.5, ** P 0.005, **** P<0.0001, ns – not significant. Compared to M0.*

10.3.3. Expression profiling of macrophages treated with PSC secretome

In order to investigate the impact of secreted proteins by PSCs on macrophages function, macrophages were treated with the secretome of PSCs for four days. The proteome and secretome changes of treated macrophages were analyzed by antibody microarray and ingenuity pathway analysis (IPA).

Macrophage's secretome characterization

The secretome of treated macrophages with activated and non-activated PSCs was collected and analyzed by antibody microarrays. The antibody microarray data was analyzed by Chipster to see the clustering of the samples. The dendrogram shows a clear separation of the groups indicating that the PSC secretome affects the macrophages secretome profiles (Figure 26 A). However, 689 proteins were differentially regulated between the treated macrophages (data not shown). The IPA analysis was performed and predicted that functions associated with cellular movement, development, cellular growth and proliferation, cell to cell signaling and inflammatory response were affected (Figure 26 B). Remarkably, a clear difference

can be seen in cellular movement and cell to cell signaling and interaction between the treatments. Furthermore, the IPA downstream analysis of top functions resulted in the increase and decrease of functions that are associated to immune cells, for example (Table 4.). Interestingly, activation and migration of immune cells were predicted to increase whereas phagocytosis is predicted to decrease. Taken together the predicted data by IPA indicated that, the secretome of activated PSCs mainly affect the proteins that are involved in inflammation and cell signaling. This supports the experimental data which showed that the PSCs secretome changed the polarization of macrophages and increased cancer cell proliferation.

Table 4. Downstream effect analysis for the secretome expression profiling data of macrophages after treatment with PSC secretome*. Listed are the most relevant diseases and functions, their overlap p-values, the predicted activation states with activation z-scores higher than 2 and the number (#) of molecules that are associated with each disease or function.*

Diseases or Functions Annotation	p-Value	Predicted Activation State	Activation z-score	# of Molecules
Morbidity or mortality	5.29E-66	Increased	4.297	239
Organismal death	5.7E-65	Increased	4.084	236
Function of leukocytes	1.9E-43	Increased	2.971	86
Activation of phagocytes	4.86E-37	Increased	2.559	70
Non-traumatic arthropathy	1.59E-44	Increased	2.535	118
Migration of phagocytes	8.66E-46	Increased	2.508	69
Function of blood cells	2.56E-51	Increased	2.442	99
T cell migration	1.74E-40	Increased	2.441	63
Activation of myeloid cells	1.03E-36	Increased	2.385	67
Proliferation of prostate cancer cell lines	7.63E-27	Increased	2.322	55
Rheumatic Disease	1.31E-56	Increased	2.239	155
Activation of leukocytes	1.51E-62	Increased	2.203	125
Cell movement of T lymphocytes	4.36E-34	Increased	2.154	54
Activation of blood cells	3.42E-66	Increased	2.053	133
Migration of lymphatic system cells	1.92E-53	Increased	2.013	87
Migration of antigen presenting cells	9.61E-28	Increased	2.008	41
Activation of T lymphocytes	2.18E-53	Increased	2.001	84
Diseases or Functions Annotation	**p-Value**	**Predicted Activation State**	**Activation z-score**	**# of Molecules**
Differentiation of epithelial tissue	1.4E-27	Decreased	-2.012	62
Apoptosis of fibroblast cell lines	1.03E-30	Decreased	-2.049	59
Progression of tumor	3.4E-38	Decreased	-2.137	61
Viral Infection	4.64E-57	Decreased	-2.174	180
Infection by RNA virus	1.36E-28	Decreased	-2.261	98
Phagocytosis of cells	1.11E-30	Decreased	-2.27	56
Survival of organism	4.68E-56	Decreased	-2.282	123
Phagocytosis	5.8E-30	Decreased	-2.356	58
Progression of malignant tumor	1.51E-30	Decreased	-2.384	45
Transport of molecule	8.68E-28	Decreased	-2.396	136

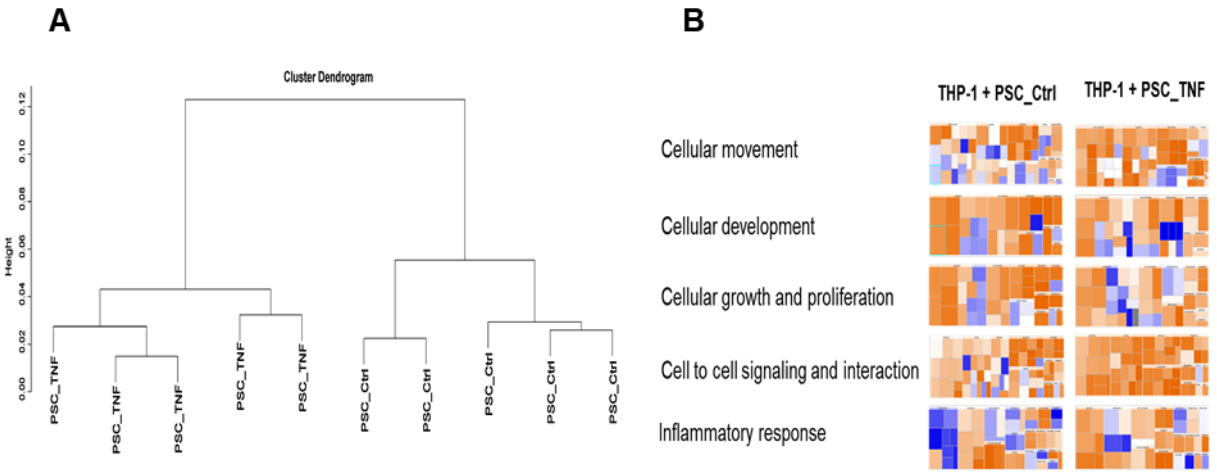

***Figure 26. Effect of PSC secretome on macrophage (THP-1) secretome profile and function**. **A,** the dendrogram shows the clustering of the macrophages treated with activated PSC secretome (PSC_TNF) and non-activated (PSC_Ctrl). **B**, Heatmaps of predicted phenotypes with the molecular and cellular functions. Each rectangle represents one function whereas the size associates with the number of involved genes. The color indicates the predicted activation state (Orange = activation, Blue = attenuation).*

Macrophage's proteome characterization

The cellular proteome of treated macrophages was analyzed by antibody microarrays as reported before. However, the downstream effect analysis by IPA resulted in a list of interesting diseases and functions (Table 5) in which invasion and movement of tumor cells were predicted to increase. This however, supports the increased PDAC proliferation by pre-exposed macrophages to PSCs secretome (Figure 22) and is consistent with the fact that tumor educated macrophages promote pancreatic cancer [200]. Similar to the secretome analysis, phagocytosis is predicted to decrease in the cellular proteome analysis under the effect of PSC secretome. Most interestingly, most of the predicted functions are associated with the functional changes in immune cells which alternatively promote cancer progression [130].

A comparison analysis by IPA has shown that cell cycle regulation is highly upregulated by macrophages upon treatment (Figure 27 A). The cell cycle progression is highly upregulated in macrophages under the effect of non-activated PSCs secretome (Figure 27 B). Still, there is no clear difference in the upstream regulators between the two groups (Figure 27 C). Nevertheless, analyzing the significantly regulated molecules which were involved in invasion of tumor cells showed that most of the molecules are upregulated in the proteome of treated macrophages and predicted to increase tumor invasion (Figure 28). Taken together, these data suggest that PSCs secretome enhance macrophages polarization into M2

type and suppress immune cells functions leading to a decreased immune response and consequently increased tumor progression.

Table 5. Downstream effect analysis for the proteome expression profiling data of macrophages after treatment with PSC secretome. *Listed are the most relevant diseases and functions, their overlap p-values, the predicted activation states with activation z-scores and the number (#) of molecules that are associated with each disease or function and were regulated in the analysis.*

Diseases or Functions Annotation	p-Value	Predicted Activation State	Activation z-score	# Molecules
Invasion of tumor cells	2.22E-27	Increased	2.648	44
Invasion of tumor	1.27E-35	Increased	2.64	59
Cell movement of carcinoma cell lines	5.31E-38	Increased	2.167	62
Transactivation	2.73E-31	Increased	2.042	88
Fibrosis	3.01E-40	Increased	2.006	100

Diseases or Functions Annotation	p-Value	Predicted Activation State	Activation z-score	# Molecules
Response of phagocytes	3.54E-31	Decreased	-2.009	55
Phagocytosis	5.07E-33	Decreased	-2.079	67
Response of myeloid cells	2.02E-31	Decreased	-2.119	55
Adhesion of granulocytes	2.98E-31	Decreased	-2.141	40
Binding of myeloid cells	5.41E-39	Decreased	-2.15	60
Binding of granulocytes	2.78E-32	Decreased	-2.195	44
Immune response of cells	1.34E-54	Decreased	-2.227	118
Interaction of leukocytes	1.34E-53	Decreased	-2.229	96
Immune response of phagocytes	2.27E-29	Decreased	-2.256	51
Adhesion of myeloid cells	3.79E-32	Decreased	-2.288	47
Binding of leukocytes	3.71E-53	Decreased	-2.31	95
Interaction of blood cells	1.42E-55	Decreased	-2.324	103
Immune response of leukocytes	6.97E-36	Decreased	-2.352	70
Binding of blood cells	4.79E-55	Decreased	-2.411	102
Phagocytosis of cells	2.4E-32	Decreased	-2.57	63
Adhesion of immune cells	1.02E-46	Decreased	-2.602	85
Adhesion of blood cells	1.53E-48	Decreased	-2.865	90

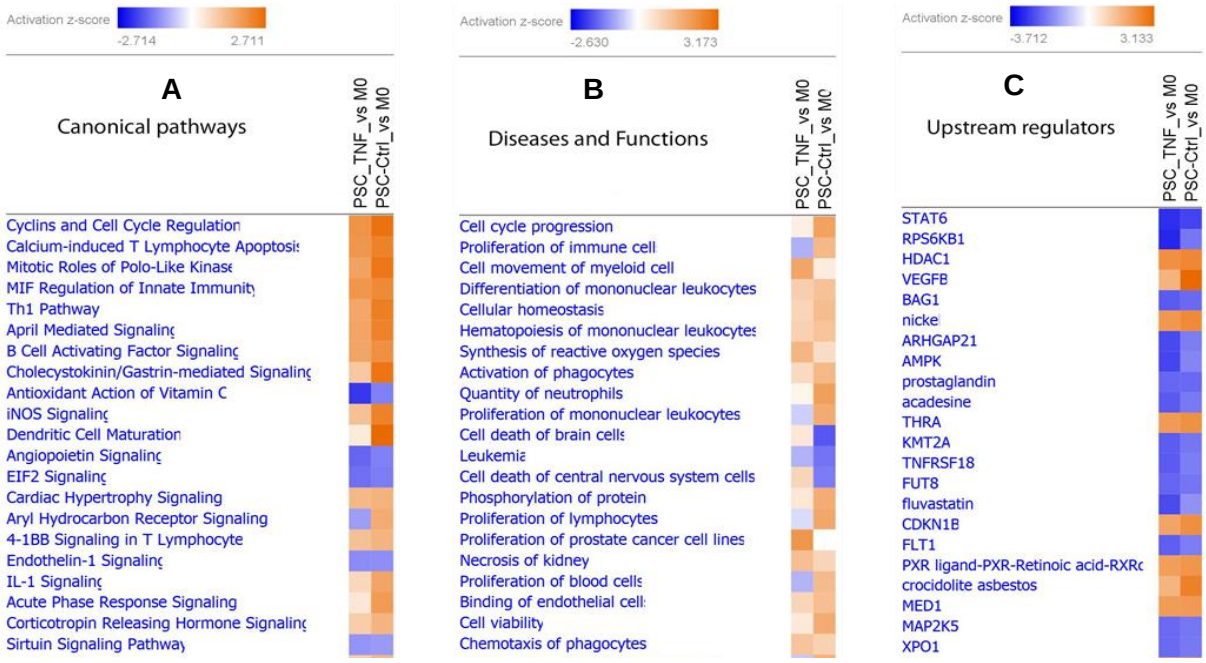

Figure 27. Ingenuity Pathway Analysis for the effects of PSC secretome on THP-1 macrophages at the proteome level. *A comparison analysis was performed for the cellular proteome of macrophages treated with the activated (PSC_TNF) and non-activated (PSC_Ctrl) PSC secretome. The color grades indicate the predicted activation state (Orange = Activation, Blue = Attenuation). Comparison analysis was performed for the proteome and canonical pathways (A), diseases and functions (B) and upstream regulators (C) are showing the differences.*

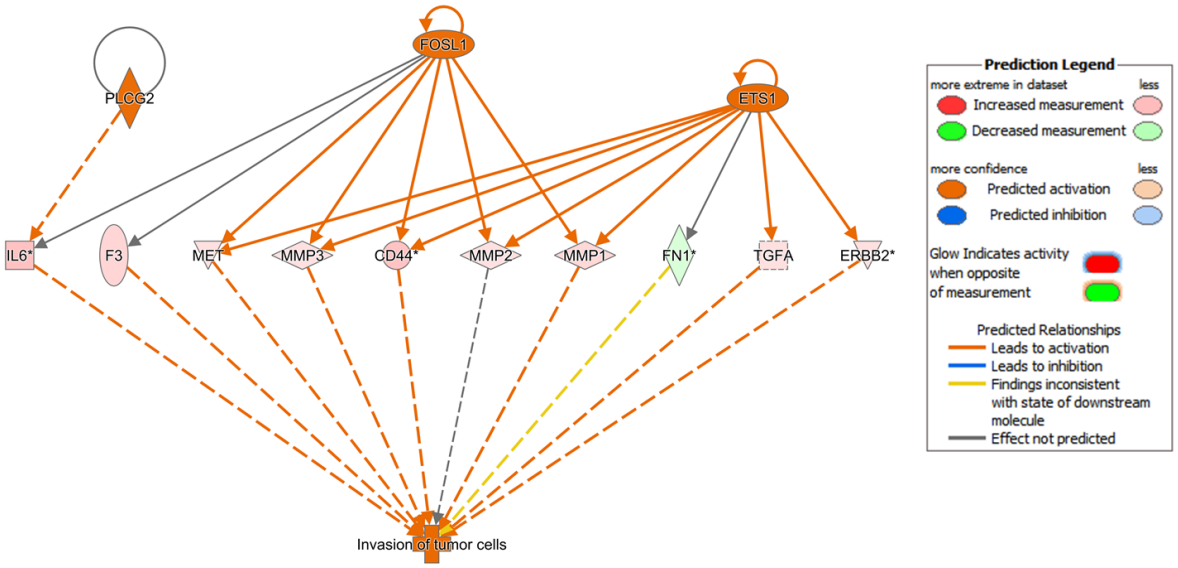

Figure 28. Molecules in the macrophages affecting the invasion of tumor cells. *Network was generated by IPA representing proteins that are related to invasion of tumor cells and whose levels were significantly different between the proteome of treated macrophages. Lines between the proteins show the known interactions. The orange arrows mean activation, blue arrows inhibition; yellow arrows indicate that the regulation observed is inconsistent with predictions; grey arrows indicate lack of existing data to formulate any prediction.*

10.4. Application of cancer cell secretome in diagnosis of pancreatic ductal adenocarcinoma

Since the PSCs secretome had shown interesting roles in cell to cell communication as explained in the previous parts, it was interesting to see which proteins could act as biomarkers for disease diagnosis. Hence, we have collected and analyzed the secretome of a panel of pancreatic tumor and non-tumorous cell lines using antibody microarrays. Based on the secretome results, we studied sera of PDAC patients, chronic pancreatitis (CP) and sera from healthy donors for the establishment of a set of defined biomarkers. The serum samples of two independent training and test sets of patients were analyzed and studied on two distinct formats of antibody microarrays, respectively. The potential of translating the identified marker signature into a clinical format was demonstrated by subsequent validation with commercial ELISA kits.

10.4.1. Secretome and array quality analysis

The cellular proteome of the pancreatic cancer cell lines which were used in the secretome analysis have been studied before using the same antibody microarray setup [185]. However, secretome of six primary pancreatic cancer cell lines and human fibroblasts were added to the study (Table 6). The established pancreatic cancer cell lines were isolated from different tumor origins of male and female patients such as, primary tumor, liver or lymph node metastasis and ascites that had different grades of differentiation. To analyze the secretome of each cell line, secretome samples were concentrated and labeled with fluorescent dye then incubated with the common proteome reference which were prepared from the pool of cellular proteome as reported previously [185]. The secretome samples were then analyzed using antibody arrays targeting 735 proteins as described in the methods. “The results without normalization had similar data quality in a way that the signal to noise ratio (SNR) larger than two times the standard deviation of the average background signal at this location was higher than 93% for the common reference but varied around 80% for the incubations of the secretome (Figure 29 A). For individual proteins, signal-to-noise ratios as high as 100 were observed; the mean across all proteins with signals above background was 4.38 (±7.68). Data normalization yielded highly comparable results (Figure 29 B). The intra- and inter-array coefficients of variation across a large number of microarray production batches ranged between 13% and 20%.”[180]

Table 6. Characteristic and clinical features of cell lines used in secretome collection.

Description of established pancreatic cancer cell lines.					
Cell line	**Patient gender**	**Cell source**	**Histology**	**Grade**	**Age (years)**
A818-1	Female	Ascites	Moderately differentiated, ductal adenocarcinoma	G2	75
AsPC-1	Female	Ascites	Well-moderately differentiated, ductal adenocarcinoma	G2	62
BxPC-3	Female	Primary tumor	Moderately differentiated, ductal adenocarcinoma	G2	61
CFPAC-1	Male	Liver metastasis	Well differentiated, ductal adenocarcinoma; cystic fibrosis	-	26
Colo357	-	Lymph node metastasis	Well differentiated, ductal adenocarcinoma	G2	-
MIA PaCa-2	Male	Primary tumor	Post-moderately differentiated, ductal carcinoma	G3	65
PaCa-44	Female	Primary tumor	Moderately differentiated, ductal adenocarcinoma	G2	44
PANC-1	Male	Primary tumor	Poorly differentiated, ductal epithelioid carcinoma	G3	56
Pt45P1	-	Primary tumor	Moderately differentiated, ductal adenocarcinoma	G3	-
SK-PC-1	Male	Primary tumor	Well differentiated, ductal carcinoma	-	-

Clinical features of the primary pancreatic cancer cell lines.									
Cell line	**Patient gender**	**Tumor localization**	**Histology**	**Classification**				**Postoperative survival (days)**	**Patient status**
				T	**N**	**M**	**G**		
PacaDD119	Male	Pancreas head	Poorly differentiated, ductal adenocarcinoma	3	1	0	3	445	Dead
PacaDD137	Female	Pancreas head	Moderately differentiated, ductal adenocarcinoma	2	0	0	2	478	Alive
PacaDD159	Male	Pancreas tail	Moderately differentiated, ductal adenocarcinoma	3	0	0	2	169	Dead
PacaDD135	Female	Liver metastasis	Moderate-poorly differentiated, ductal adenocarcinoma (partially mucinous)	-	-	Hep	2	66	Dead
PacaDD161	Female	Liver metastasis	Poorly differentiated, adenocarcinoma	-	-	Hep	3	x	Dead
PacaDD183	Female	Pancreas head	Moderate differentiated, ductal adenocarcinoma	-	-	-	2	55	Dead

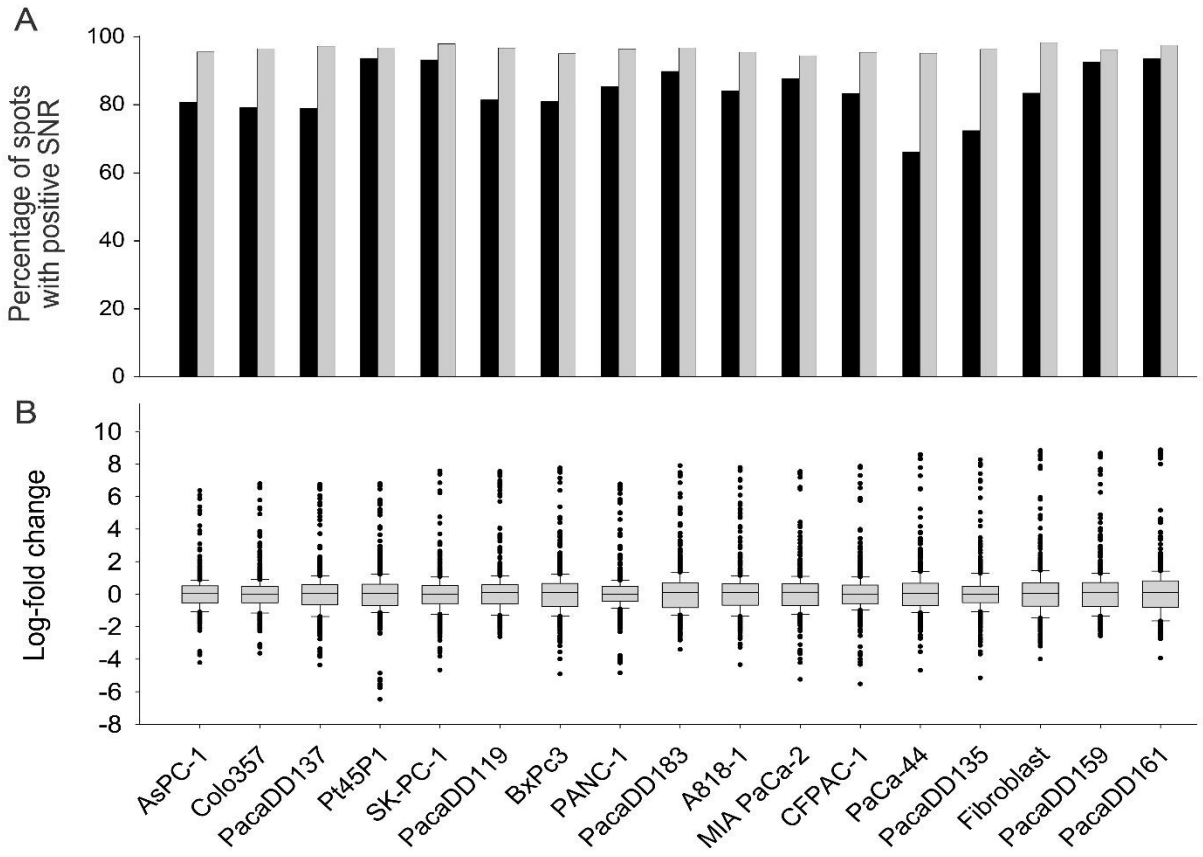

***Figure 29. Quality assessment of microarray analyses**. (A) The median percentage of microarray antibodies is shown that exhibited a signal that was significantly above background. The black bars represent the results with the intracellular proteins used as common reference; the grey bars stand for the secretome samples. The order of the cells was defined by the amount of protein that was obtained from the secretome, from relatively high (left) to low amounts (right). As can be seen, there was no apparent influence of the protein preparation yield. (B) A box plot representation is shown of all signal intensities of the secretome samples normalized to the pool reference.*

10.4.2. Cancer cell secretome characterization and comparison

The secretome of the cancer cell lines and fibroblasts were profiled with antibody microarrays and analyzed by Chipster software package. Comparing the cancer cell lines secretome to the fibroblasts resulted in 112 differentially abundant proteins which were similarly expressed at least in 14 cancer cell lines (online suppl. Table. 2 [180]). Functional data analysis was performed with the IPA software which revealed that most of the proteins are involved in functional categories of cell death and survival, inflammatory response, decreased apoptosis and cell death as well as increase in organismal death and cancer (Table 7). “This result indicates a potential role of secreted proteins as anti-apoptotic factors that could be involved in the control of the maintenance and survival of pancreatic tumor cells and reflects the bad

prognosis associated with the tumor. In addition, the secretome profiles predict an influence of PDAC tumor cells on regulating immune cells and their quantity within the tumor, suggesting that tumor cells could control the trafficking of immune cells, such as phagocytes, monocytes and neutrophils, into the tumor microenvironment" [180]. However, in order to verify the predicted role of pancreatic cancer cell secretome by IPA analysis, macrophages polarization was evaluated under the effect of PDAC secretome. Remarkably, the PDAC secretome promotes macrophages polarization towards the anti-inflammatory M2 type (Figure 15 & Figure 16). "Moreover, there was not a big difference between the secretome of established and primary pancreatic cancer cell lines. That means, the origin of tumor, tumor location and the grade did not make a noticeable change in the secretome data. However, this is inconsistent with the proteomic data of the same cell lines where a significant variation has been seen between them [185]. Besides, some of the proteins that were regulated in the tumor cell secretome had been reported to be present in body fluids, such as saliva, cerebrospinal fluid, tears, blood or urine" [180].

Table 7. List of the most frequently predicted functions associated with the secretome of pancreatic cancer cell lines. *The prediction z-score was calculated within IPA software. The complete list can be found as supplemental information online (Suppl. Tab. 3). [180]*

Function annotation	Predicted activation state	Prediction (z-score)	p-Value	Proteins	Number of proteins
Cell death of pancreatic cancer cell lines	Decreased	-2.568	4.59 E-07	ALB, CXCL8, DDIT3, FN1, MTOR, RPS19, SPP1, TGFB1	8
Apoptosis of pancreatic cancer cell lines	Decreased	-2.365	2.27 E-06	ALB, CXCL8, DDIT3, FN1, MTOR, RPS19, TGFB1	7
Quantity of phagocytes	Increased	+2.049	3.53 E-12	BCL2A1, CNN2, CXCL8, DCN, FABP1, FASTK, FPR1, GJA1, ID1, IL10, IL1A, IL2, S100A8, SELE, SELL, SPP1, TGFB1, TGFBR2, TIA1, VCAM1	20
Quantity of neutrophils	Increased	+2.156	1.23 E-10	CNN2, DCN, FASTK, FPR1, GJA1, ID1, IL10, IL1A, S100A8, SELE, SELL, TGFB1, TIA1, VCAM1, AKR1C3, APC, ATP6AP1,	14
Organismal death	Increased	+2.174	1.49 E-15	BCL2A1, BGN, CTTN, CXCL8, DAB2, DCN, DDX17, EIF2AK4, EPHB3, FN1, FOS, GAS1, GJA1, GPM6B, HNRNPC, HSP90B1, ID1, IL10, IL2, IMPDH2, KLF4, LAMTOR1, MAPK3, MLH1, MME, MMP2, MTOR, NCOR2, NUSAP1, PAX2, POU2F1, PVRL1, RPS19, RPSA, S100A8, SELE, SERPINB5, SLC19A1, SPINT2, SPP1, TCEA1, TGFB1, TGFBR2, TIA1, TIE1, TJP2, TOP2A, TPT1, UBC, VCAM1, ZBTB17	54
Quantity of monocytes	Increased	+2.256	1.85 E-08	CNN2, CXCL8, GJA1, ID1, IL10, IL1A, SELE, SELL, VCAM1	9

10.4.3. Comparison of secretome to the related intracellular proteome

Intracellular proteome of the same PDAC cell lines have been studied previously with the same antibody microarrays [185] however, to know the regulation of different proteins, a comparison was necessary. “Comparing the profiles, the majority of changes in abundance were unique to either the intracellular proteome or the secretome. Only 17 proteins were similarly regulated between the two sample types (Figure 30). This represents 15% (17/112) of the secretome-specific and 13%

(17/132) of the intracellular proteome variations, or some 2% (17/735) of all studied proteins. Most of the 17 proteins are actually associated with extracellular functions, according to gene ontology (GO) terms, or are sheded components of the plasma membrane. All exhibited a substantially larger abundance variation in the secretome than intracellularly. For the large majority of proteins, however, the expression patterns were different in secretome and intracellular proteome. For example, most cytokines were found up-regulated in the secretome and down-regulated intracellularly, while the opposite was observed for nuclear proteins like RPS19, NCL and BRPF3" [180].

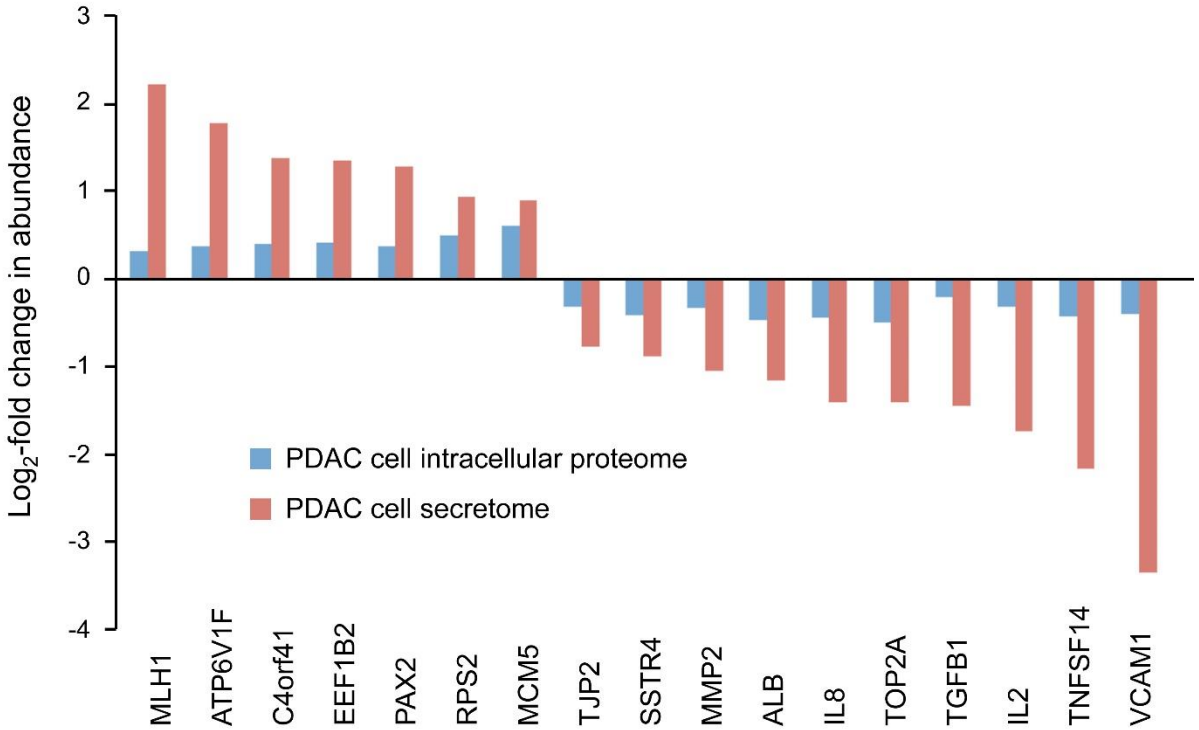

Figure 30. Proteins that are commonly regulated in secretome and intracellular proteome of the tumor cells. *The proteins are listed, which exhibited similar regulation in both secretome and proteome analyses of the established pancreatic cancer cell lines in comparison to non-tumor cells. The bar sizes indicate the relative degree of regulation*.

10.4.4. Protein variations in patient serum samples

"To investigate the impact of secretome data on the quality of a patient diagnosis based on serum protein data, serum samples from patients were studied. Two independent sample groups, a training and test set, were used in this analysis. The training set consisted of sera from 47 PDAC patients, 18 people with chronic pancreatitis (CP) and 27 age and sex-matched healthy individuals. The test set was composed of 25, 25 and 22 serum samples, respectively. The characteristics of the

patients and donors are summarized in Table 8. Two distinct antibody microarrays were used for the analysis as it is described in the method. However, several antibodies of the smaller microarray were missing on the larger array as supplies had run out and could not be replaced" [180].

Table 8. Characteristics of healthy donors and patients from whom serum samples were collected.

Healthy donors	
Age: range (average)	Sample set 1: 39-71 (52) Sample set 2: 35-74 (55)
Gender: male/female	Sample set 1: 0.60 Sample set 2: 0.62
CP patients	
Age: range (average)	Sample set 1: 25-76 (44) Sample set 2: 24-78 (51)
Gender: male/female	Sample set 1: 0.70 Sample set 2: 0.85
PDAC patients	
Age: range (average)	Sample set 1: 39-74 (58) Sample set 2: 38-81 (61)
Gender: male/female	Sample set 1: 0.66 Sample set 2: 0.67
Tumour localisation	**% of cases**
Pancreas head	55
Pancreas body	14
Pancreas tail	3
Papilla vateri	10
Multiple	18
Grading	**% of cases**
G2	48
G3	34
unknown	18
R classification	**% of cases**
R0	55
R1	38
R2	3

"Looking at the individual diagnostic accuracy of the 189 proteins that were found to be differentially abundant in serum of PDAC patients and healthy donors (online suppl. Tabs. 5 and 6 [180]), they differed in their ability to discriminate between the two groups as indicated by their individual AUC values. In the training set, rather good accuracy values could be determined for some of the proteins (Figure 31 A). When controlling these performances in the test set, however, none exhibited an overall accuracy that would be sufficient individually (Figure 31 B)" [180].

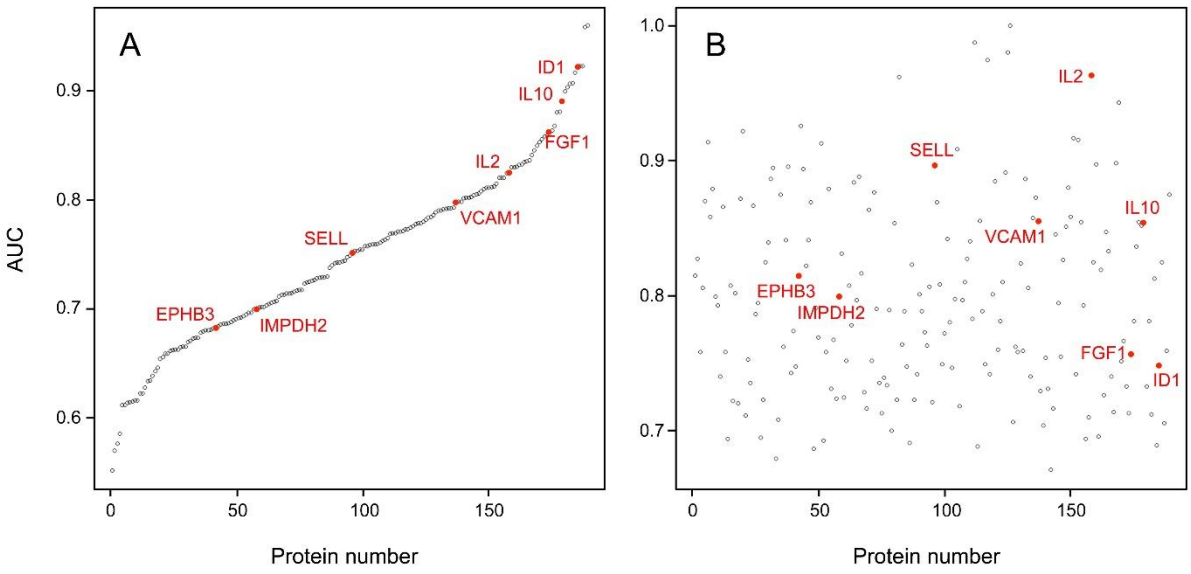

***Figure 31. AUC values of the 189 individual serum markers**. Analysis by Receiver Operating Characteristic (ROC) curves was performed for all identified serum protein markers individually. Panel A shows the result calculated from the training set; the respective AUC values are shown, ranging from 55.2% to 96.0%. In panel B, the AUC values are shown as calculated for the individual marker molecules in the test set. For presentation, the order of the markers along the x-axis was kept as in panel A, highlighting the limited degree of reproducibility for individual markers.*

"Out of the 112 proteins found to vary in the secretome of tumor cells, only 8 proteins were similarly regulated in serum samples of PDAC patients, but not exhibiting different abundance in CP sera (Figure 32). In all cases, the variation was substantially bigger in the secretome than in the serum. Since it is likely that a tumor's secretome gets diluted and in part obscured by the proteins that are secreted by cells in other organs and tissues, such a difference is expected. The expression of most proteins was either unchanged in one or both sample types or varied even inversely in secretome and serum" [180].

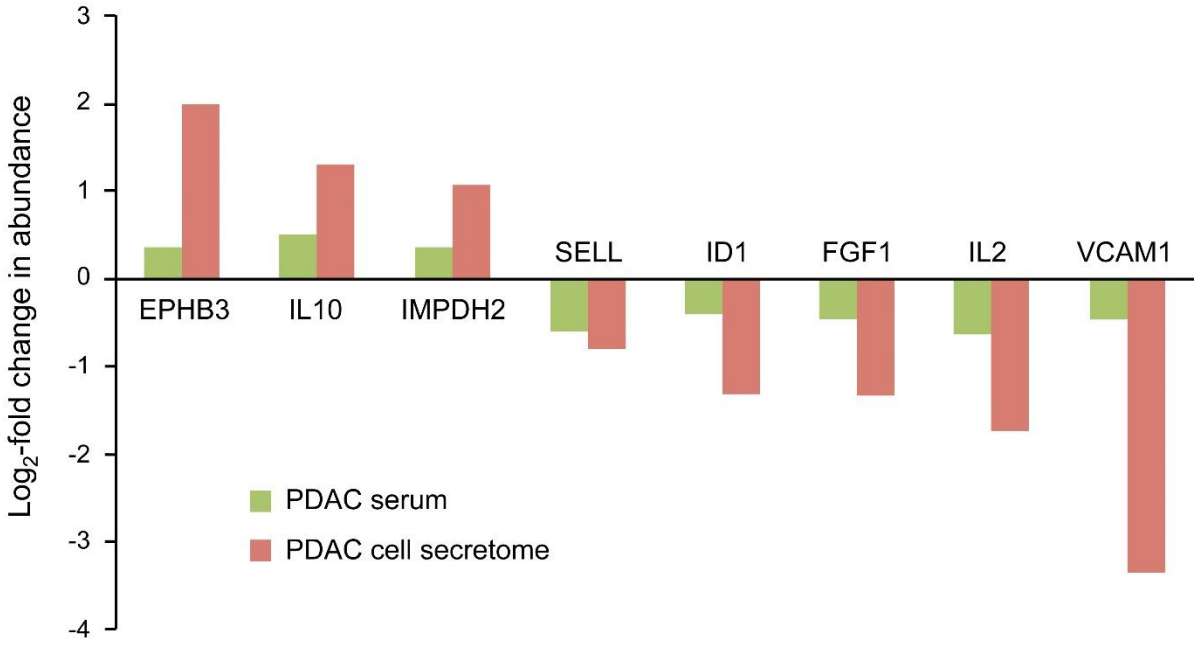

Figure 32. Proteins that were similarly regulated in both tumor cell secretome and PDAC patient sera. *Out of the 112 differentially expressed proteins in the tumor cell secretome compared to the non-tumorous cells, only 8 were similarly regulated in the serum. The red and green bars indicate the degree of regulation in secretome and PDAC serum, respectively.*

10.4.5. Serum-based diagnostics

"The 8 proteins that similarly varied in abundance in PDAC sera and in tumor cell secretome – EPHB3, FGF1, ID1, IL2, IL10, IMPDH2, SELL, VCAM1 – did not exhibit a superior performance as markers individually (Figure 31). When applied as a signature for PDAC diagnosis, however, a Receiver Operating Characteristic (ROC) curve analysis yielded an accuracy – expressed as area under the curve (AUC) value – of 95.1% for distinguishing PDAC from healthy (Figure 33 A). For comparison, the best performing panel of 8 marker molecules, which were differentially abundant in sera but not in the secretome, was selected based on the training set. Applied to the test set, they produced an AUC value of 84.2% (Figure 33 B). Even applying more than 8 of the proteins that showed variation in serum abundance only, no better distinction of sera from cancer and healthy patients could be achieved. This documents that the information content of the signature based on molecules that varied in both secretome and serum is significantly higher than that derived from serum-only markers" [180].

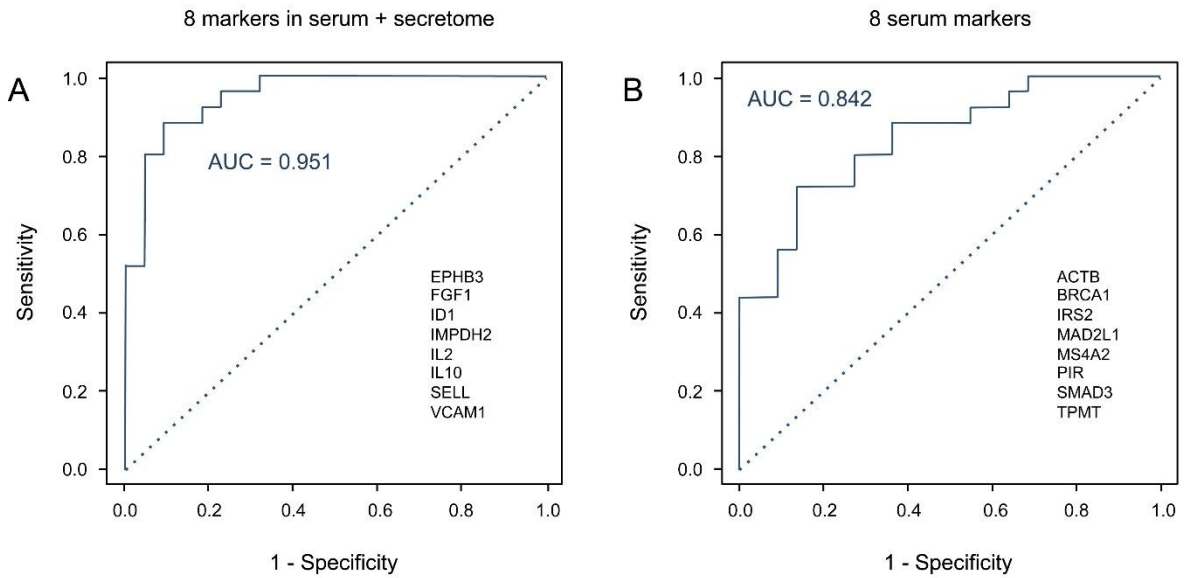

***Figure 33. Diagnostic potential of the protein signatures in serum**. (A) A Receiver Operating Characteristic (ROC) curves was calculated for the signature of 8 proteins that exhibited shared expression changes in the analyses of PDAC serum and secretome, yielding an AUC value of 95.1%. The protein names are shown. (B) In comparison, the ROC curve is presented for the best performing panel of 8 proteins that differed in abundance in the serum only; AUC is 84.2%. The relevant proteins are listed.*

"The 8 markers shared between PDAC cell secretome and PDAC patient sera were not able to separate PDAC from CP sera, however. In this context, they performed basically identical to the best serum-only marker signature with AUC values of 71.2% and 72.2%, respectively (Figure 34). For discriminating PDAC from CP sera, the best 8 common proteins regulated similarly between PDAC and CP yielded AUC values of 72.2% (Figure 34 B) whereas the most informative signature was made up of 25 proteins, yielding in a ROC analysis an AUC value of 97.1% (Figure 35)" [180].

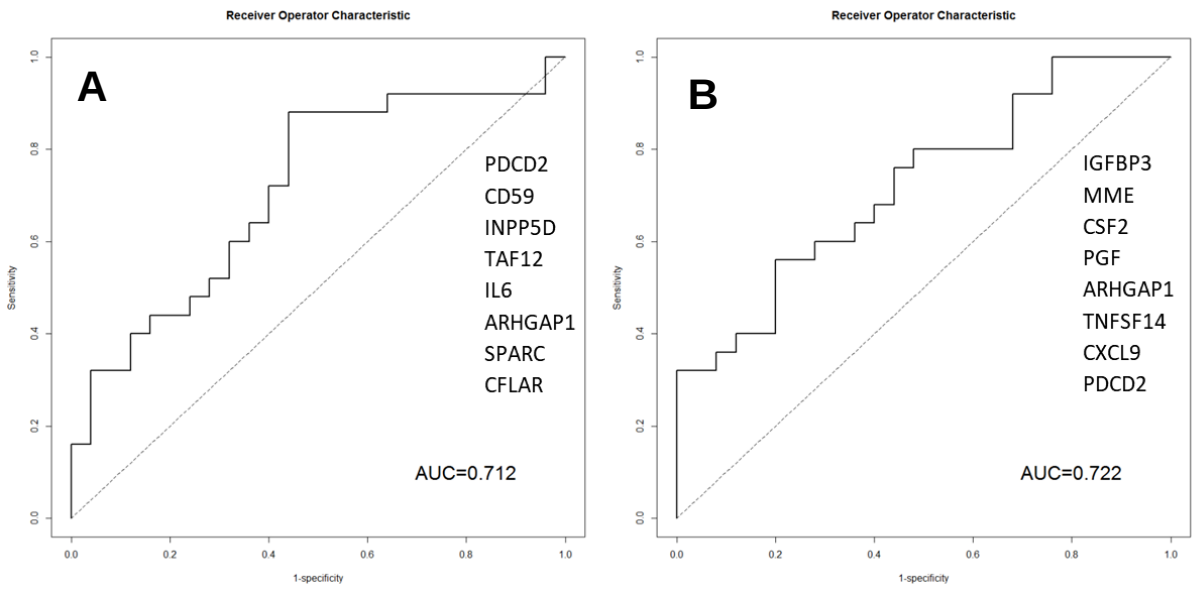

***Figure 34. Diagnostic potential of PDAC and CP serum markers only**. (A) Receiver Operating Characteristic (ROC) curves was calculated for the best 8 proteins of PDAC alone discriminating PDAC from healthy that yielded an AUC value of 71.2%. (B) Common regulated proteins between PDAC and CP sera with the similar expression yielded an AUC value of 72.2%. The relevant proteins are listed in the right side.*

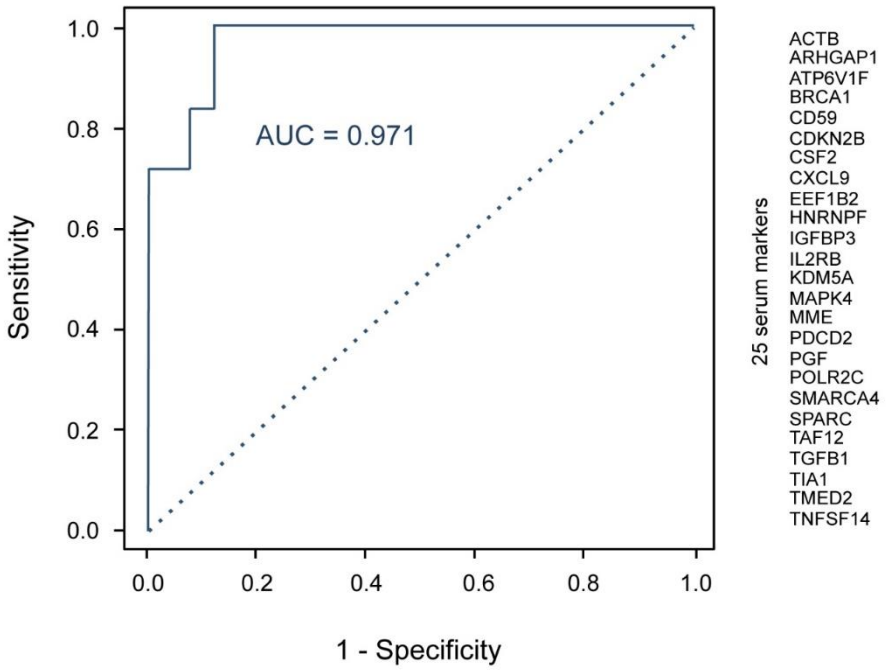

***Figure 35. Discrimination of sera from PDAC and CP patients.** A ROC curve was calculated for the best performing serum proteins that distinguish PDAC from CP sera. AUC is 97.1%. The names of the 25 proteins are listed at the right margin.*

10.4.6. Validation by ELISA

“Complex antibody microarrays like the ones used here are unlikely to be utilized in clinical routine. An analysis would produce information that is not required for diagnosis. Also, in terms of robustness, other methods are superior and already established in a clinical setting. Therefore, we confirmed our results not just by applying a scheme of independent training and test samples but used commercial ELISA kits for IL2, ID1, and IL10 in addition. The antibodies of the three ELISA kits were different from the molecules on the microarray used to define the diagnostic signature. IL2, ID1, and IL10 were selected at random from the eight proteins that define the signature. An analysis of all eight was not possible, since the amount of serum was limiting. While a protein amount equivalent to about two microliters of serum is sufficient for a microarray analysis that studies as many antigens as there are antibodies on the microarray, the protein content of 50 µl to 150 µl serum was required for each individual ELISA. In total, we analyzed 25 and 21 sera from PDAC and healthy control samples, respectively. In agreement with the microarray data, both ID1 and IL2 were found significantly lower in PDAC sera as compared to healthy control samples and IL10 was present at a significantly higher level (all three with $p < 0.0001$) (Figure 36)” [180].

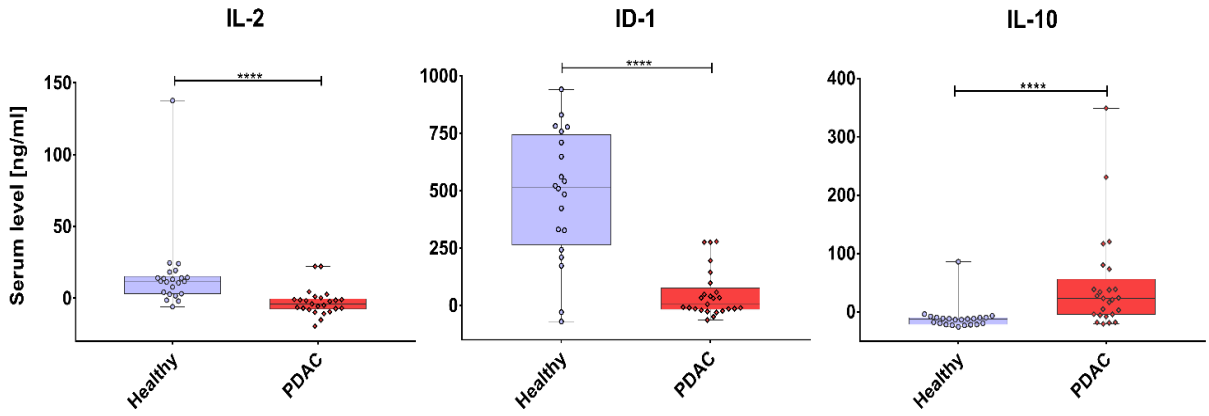

Figure 36. ELISA validation of identified marker proteins. *The protein content was analyzed of 25 and 21 sera, respectively, isolated from PDAC patients and healthy blood donors. Proteins IL2, ID1, and IL10 were studied with commercially available assays. Data were analyzed by GraphPad Prism and all markers showed a highly significant degree of variation of abundance. ****P-value<0.0001*

11. Discussion

11.1. PSC activation, validation and secretome characterization

11.1.1. Activation of PSC with TNF-α

Under the pathological conditions such as pancreatic cancer, the activation of PSCs is one of the earliest cellular events that occurs by the different factors such as oxidative stress [201], pressure [80], high glucose [202] and proinflammatory factors [181]. PSCs even stay activated in vivo after chemoradiation [193]. Activated PSCs highly express alpha-smooth muscle actin (α-SMA) and release extracellular matrix (ECM) proteins such as collagen [71], metalloproteinases [77] and fibronectin [192]. In the present study, the activation of PSCs by TNF-α is confirmed by the increase in α-SMA and fibronectin expression. In normal tissues, activated PSCs undergo cell apoptosis soon after healing is complete [203] while, during fibrotic diseases, PSCs remain activated and highly proliferative leading to the expansion of the ECM and induce stromal reaction [71]. The persistent activation of PSCs is involved in the development of tumor and metastasis as well as it contributes to inflammatory cytokine signaling [71, 94]. Therefore, identifying the secreted proteins of the activated PSCs could lead to a better understanding of the functional molecules in the tumor microenvironment.

11.1.2. Characterization and validation of PSC secretome

The analysis of PSCs secretome using antibody microarrays demonstrated that in the secretome of activated PSCs most of the proteins are secreted or are part of the plasma membrane. VEGF, ICAM-1, MMP-10, 11,12 and 14 are highly upregulated, which are important in the tumor microenvironment. VEGF, for example, promotes angiogenesis and activates various signal transduction pathways which subsequently leads to the secretion of matrix metalloproteinases (MMPs) [204]. MMPs then facilitate the degradation of the ECM leading to the tumor invasion [205] in addition, MMP10 is increasing macrophage migration and invasion [206]. Moreover, expression of ICAM-1 by activated PSCs mediate the transmigration of leukocytes to the site of tissue injury [207]. Our results are in agreement with the findings of Wehr et al. who profiled the secretome of PSCs but without activation [208] nevertheless, the study plan, experimental design and analysis technique are different. The number of proteins identified in their study is higher due to the limited number of antibodies on the arrays we used. Still, FN-1, MSN, SERPINE, IGFBP1, for example, are

similarly upregulated whereas ANXA2 and CLUSTERIN are in contrast downregulated in our study. There are some important proteins which were not identified in their study such as IL-2, IL-4, IL-6 and MMPs-10, 11, 12 and 14. Despite these variations due to the stimulation of the PSCs with TNF-α, we validated the secretome of PSCs using western blot and ELISA.

The western blot analysis and ELISA confirmed that activated PSCs secreted higher amount of IL-6, IL-4, IL-1β, FGF-1, SERPINE, FN-1 and collagen compared to the non-activated PSCs. These proteins participate in the cell signaling and promote PSC activation, fibrosis, cancer cell proliferation, immunosuppression and angiogenesis [126]. IL-6, for example, is a bioactive multifunctional cytokine which promotes the accumulation of myeloid derived suppressor cells (MDSC) and increased the migration of pancreatic cancer cells via STAT-3 pathway [170, 171]. Our validated results agreed with the previous studies which have proven that IL-6 is secreted by PSCs [88] and is considered as the main regulator of immunosuppression in autoimmune diseases and cancer [139]. In the secretome of activated PSCs, both fibronectin and collagens are also highly upregulated. Recent studies indicated that PSCs are the main producer of ECM proteins in PDAC microenvironment [209]. Such ECM proteins can have different functions; fibronectin is known to induce macrophages migration [210] whereas, increased collagen secretion is attributed to a rapid differentiation of monocytes to macrophages [211]. Moreover, the ECM proteins play critical roles in the tumor-stromal interactions in pancreatic cancer and form a barrier to chemotherapy [72].

11.1.3. The IPA analysis of the PSC's secretome

Notably, the diseases or functions annotation by IPA analysis for the secreted proteins designated most of the secreted proteins are predicted to participate in the immune response of cells, antigen presenting cells activation, cell apoptosis, cellular growth and proliferation and transmigration of cells. Also, the downstream analysis showed that, the regulated proteins in the secretome of activated PSCs are particularly involved in macrophage activation, movement, migration and induction. It has already been shown that IL-1β, TNF-α and IL-6, which are upregulated in the secretome of activated PSCs, enhance the expression of GM-CSF which in turn stimulates immune cells response against pathogens [212]. However, GM-CSF may induce monocytes and macrophages to secrete mediators such as IL-10 and prostaglandin E2 (PGE-2) which are negatively affecting T-cells function [213, 214].

Therefore, as discussed above, the secreted proteins by PSCs are actively involved in the stromal cross-talks in the PDAC microenvironment. It is also highly possible that these proteins are secreted in vivo and contribute to the initiation and progress of PDAC.

11.1.4. Increased ROS and PDAC proliferation by PSCs

Our results have shown that intracellular ROS are increased in the TNF-α-activated PSCs which is in accordance with the previous finding [194]. TNF-α is a known cell apoptosis or survival inducer [215] through inducing reactive oxygen species (ROS) production [194] thus, ROS could be considered as a marker for the activation of PSCs by TNF-α. Intracellular ROS can be measured using H2DCFDA (2′,7′-dichlorodihydrofluorescein diacetate) which is non-fluorescent. The acetate group is cleaved by the intracellular esterases which is then converted to a highly fluorescent dye [216]. High ROS level is also expected when activated PSCs secret an elevated level of platelet-derived growth factor (PDGF) which activates the nicotinamide adenine dinucleotide phosphate (NADPH) oxidase enzymes [217]. Of note, increased ROS synthesis by the oxidative enzymes leads to the persistent activation of PSC [218]. It has been reported that ROS with the secreted growth factors and cytokines by activated PSCs participate in transforming chronic pancreatitis (CP) into cancer [219]. Nevertheless, ROS is a double-edged sword in physiological and pathological processes, for example, ROS at low concentrations could act as a signaling molecule in tumorigenesis but at high concentrations it is toxic and could exert apoptosis in cancer cells [220].

In the light of the important role of the PSCs in PDAC development and tumor size [83], we investigated the impact of PSCs secretome on the pancreatic cancer cells proliferation. Interestingly, our results show that the secretome of activated PSCs has significantly increased PDAC cell proliferation. It could be attributed to the differential regulation of different molecules associated to the cell proliferation. The analysis of PSC's secretome using antibody microarrays shows several upregulated proteins which are associated to the increase in cell proliferation. Proteins such as, fibronectin [221], insulin-like growth factor 2 (IGF-2) [222], IL-4 [223], VEGF-C [224] and MMP-14 [225] have previously been attributed to the increased proliferation of different cancer cells. However, there are also proteins which are involved in intrinsic and extrinsic apoptosis pathways, such as Bax, Bak [226], cytochrome C [227], caspase 8 [226] and IL-15 [228]. These proteins are downregulated in the secretome

of activated PSCs. Given these points, the increased cell proliferation can mainly be explained by the differential regulation of the mentioned markers in the PSCs secretome.

One of the highly upregulated proteins in the secretome of activated PSCs is IL-6. Our results demonstrated that IL-6 has no significant effect on the proliferation of Panc-1 cells. This is possibly due to the multifunctional influence of IL-6 which has been shown to inhibit the proliferation of breast cancer cell [229] while on the contrary, IL-6 increased satellite cells and glioma cells proliferation through inducing syndecan-binding protein and activation of JAK2/STAT3 signaling pathway [230, 231]. The IPA analysis of the activated PSCs secretome demonstrated that, apoptosis, necrosis and cell death are predicted to decrease whereas, in contrast, cell proliferation, survival, migration and invasion are increased. It has also been noted that, IL-6 induced the expression of VEGF on CFPAC-1 cells [232]. Also, higher serum level of IL-6 is considered as an independent risk factor and contributed to PDAC progression [233]. Hence, IL-6 may indirectly contribute to the cell proliferation via inducing growth factors and activating the relevant signaling pathways.

11.2. Impact of PSCs secretome on monocyte differentiation and macrophages polarization

11.2.1. Monocyte differentiation to macrophages

The pancreatic tumor microenvironment is very complex where different cells, mainly PSCs and macrophages coexist with the tumor cells. To explain the cross-talk between PSCs and macrophages in pancreatic cancer, highly purified monocytes were isolated and treated with the secretome of PSCs. Monocytes are direct precursors of macrophages which polarize afterwards into classically activated (M1) or alternatively activated (M2) macrophages [234]. Monocyte's differentiation into macrophages is accompanied by phenotypical changes however with some differences between M1 and M2 types in different environments [235].

In our study, M1 positive macrophages are more elongated cells whereas M2 macrophages have round-shaped structure but cells treated with the PSC's secretome contain both cell types. Thus, no conclusion can be drawn based on the cell morphology because alteration in macrophages' morphology is associated with

the changes in extracellular matrix [236]. Also, cell morphology is not merely associated with the expression of macrophage markers [237]. Therefore, the expression of HLA-DR marker [238] was analyzed on the treated macrophages. Interestingly, macrophages treated with the PSC secretome has expressed higher HLA-DR than the cells treated only with the priming factors M-CSF and GM-CSF. It is not well known yet, how HLA-DR is stimulated on macrophages, but studies suggest that IL-4, TGF-β, Prostglandin-E2 and IFNγ may increase HLA-DR on macrophages [237]. Also, HLA-DR expression is interleukin dependent, particularly IL-2, IL-4 and IL-12 [239]. Accordingly, increase of HLA-DR expression could be attributed to the elevated level of interleukins such as IL-2 and IL-4 in the secretome of PSCs.

11.2.2. Macrophage polarization

There are no established markers to define differences and similarities between M1 and M2 macrophages, however, a few markers were considered to distinguish M1 from M2 phenotype [110]. Polarization of macrophages is therefore categorized by the expression of special surface markers and regulation of certain cyto-chemokines.

Expression of cell surface markers

We have demonstrated that M2 markers, CD163 and CD206, were highly expressed on the macrophages which were treated with the secretome of activated PSC and PDAC (Figure 15). This acts in accordance with what has been reported in PDAC tissues where CD163-positive macrophages were found primarily in the tumor stroma [240]. This finding indicates the role of the secreted signals by the tumor and stromal cells on macrophages. CD163 is induced by the anti-inflammatory signals such as IL-6 and IL-10 [241] and it is attributed to the pro-tumoral activation of macrophages in sarcoma [242]. Notably, IL-6 and IL-10 are highly upregulated in the secretome of activated PSCs and PDAC cell lines respectively. Above all, several studies have shown that, high numbers of CD163-positive macrophages are associated with advanced cancer stages, bad prognosis and reduced survival rate [243, 244]. Still, it is believed that CD163 is not restricted to M2 macrophages only, therefore it is not a reliable M2 marker when used alone [245]. Accordingly, we also measured the expression of mannose receptor (CD206) which is a type-I transmembrane glycoprotein and is a recognized M2 specific marker in human and mouse [246]. In normal tissues, CD206-positive macrophages involved in the resolution of inflammation whereas, in pathological conditions, they promote fibrosis [247]. In

tumors, mucins were shown to bind to CD206 and exert immunosuppressive properties of TAMs [248]. Of note, it is reported that TNF-α and IL-1β, which are secreted by the activated PSCs, induce the overexpression of mucin [249] hence they promote immunosuppression.

In contrast, the expression of the M1-marker CD86 is reduced upon treatment with the secretome of the activated PSCs in comparison to the macrophages which were treated with the secretome of non-activated PSCs. This is in accordance with the fact that CD86 is required to bind to CD28 on the surface of T-cells to initiate an effective immune response and modulate the diseases [250]. CD86 is identical to CD80 and is stimulated by IFN-γ [251]. It is highly unlikely that macrophages gained M1 or M2 phenotypes affected by the serum-free medium. Tarique et al. has demonstrated that polarized macrophages will revert back to the uncommitted M0 state when incubated in a cytokine-free medium for 12 days [252]. They have also reported that, macrophages could be switched from M1 to M2 and vice versa, when induced by the alternative polarizing stimulus. Accordingly, secreted proteins into the tumor microenvironment by the activated PSCs and tumor cells may switched and increased the number of CD163+ and CD206+ M2 macrophages, leading to the immunosuppression.

RNA level of Cytokine and chemokines

In addition to the cell surface markers, macrophage polarization was checked at the level of RNA by qRT-PCR based on the expression of specific cytokine and chemokines. Markers such as IL-1β and TNF-α, as M1 markers [110] or mannose receptor (CD206) and CCL17 as M2 markers [128] were analyzed in the treated macrophages. CD206 was checked again at the RNA level to validate the FACS data. Remarkably, the secretome of activated PSCs has significantly increased CD206 and CCL-17 on macrophages whereas, in opposite IL-1β and TNF-α are significantly reduced. The results clearly show the potent anti-inflammatory role of activated PSCs to modify macrophage's response in the tumor microenvironment. The secretion of CCL17 by TAMs recruits T-regulatory cells (Treg) to the tumor, which in turn, they secret TGF-β, arginase and IL-10 to promote M2 polarization of macrophages with reduced antigen presenting ability and NO production [253, 254]. The proinflammatory cytokines IL-1β and TNF-α which are increased under the effect of non-activated PSCs secretome, are involved in tumor metastasis and invasiveness by promoting the expression of matrix metalloproteinases [255, 256]. Thus, based on

the present data, secretome of PSCs show promising effects on the activation state of macrophages in the tumor development.

Arginase expression and NO production in the treated macrophages

To distinguish between the two activation states of macrophages, metabolism of L-arginine is thought to be a distinctive means [122]. Arginase-1 (Arg-1) is a key feature of M2 macrophages which contributes in wound healing and fibrosis by catalyzing arginine to urea and ornithine [122, 123]. Macrophage's arginase activity and expression has significantly increased when treated with the conditioned medium of activated PSCs. Our results are consistent with the previous studies which showed that co-culture of fibroblasts and pancreatic cancer cells with monocytes, polarized monocytes to the M2 phenotype which highly expressed Arg-1 [257]. It was also shown that, Arg-1 is induced by exogenous Th2 cytokines such as IL-4 and IL-13 through STAT-6 activation [125]. In contrast, recent studies suggested recombinant human arginase as therapeutic agent in treatment of non-Hodgkin's lymphoma [258], acute lymphoblastic leukemia [259], triple negative breast cancer [260] and glioblastoma [261] through blocking autophagy. Of note, autophagy is required for the activation of PSCs [262] hence, blocking the activation mechanism of PSCs could improve cancer treatment.

On the other hand, L-arginine could be metabolized to nitric oxide (NO) and citrulline by induced nitric oxide synthase (iNOS), an enzyme which is highly expressed by M1 macrophage [195]. As an indicator of iNOS enzyme, NO was measured in the conditioned media of the treated macrophages with the different PSCs secretome. Remarkably, the CM of activated PSCs have significantly suppressed NO production in macrophages. It could be suggested that, the increased expression of arginase in macrophages by the activated PSCs depleted arginine leading to the reduction of NO production by iNOS. In tumors, depending on its concentration, NO has both pro- and anti-tumor effects [116] for example, high NO production is the main weapon of macrophages against pathogens and tumors. It has been shown that NO inhibits T-cell function by nitrating CD8 molecules and various proteins involved in T-cell receptor signaling [263]. Our results are supported by the findings of Cho et al. who found that, mesenchymal stem cells induce arginase activity in the adjacent macrophages but reduce iNOS [264]. They suggest that, macrophages shift from M1 to M2 phenotype by the immune modulating characteristic of MSC. The same

mechanism however could be true for the role of activated PSCs secretome in switching macrophages to the M2 type.

ROS synthesis in macrophages after treatment with the CM of PSCs

Macrophages produce ROS that is needed for the uptake and clearance of apoptotic cells. However, maintaining high level of ROS may cause macrophage apoptosis during infection [265] and inhibit PDAC apoptosis [266]. In fact, ROS are attributed to the M2 polarization of macrophages [267] and the activation of PSCs [268]. Interestingly, the secretome of activated PSCs significantly decreased ROS synthesis in macrophages. This finding contradicts the results of Zhang et al. [196] who found that, monocytes treated with the CM of fibroblasts synthesize high amount of ROS which polarized macrophages towards the M2 type. Nevertheless, because activated PSCs induced Arg-1 activity and decreased NO production in the macrophages, therefore, it is highly expected that ROS is also decreasing. Thus, all the experiments indicate that the secretome of activated PSCs induce M2 polarization of macrophages.

Role of PSC-educated macrophages in PDAC cell proliferation

We have earlier shown that, the secretome of activated PSCs induced macrophages towards the pro-tumor M2 type. It has been shown that CAF-induced M2 macrophages increased pancreatic cancer cell proliferation, migration and invasion [196]. Therefore, it is expected that the CM of the activated PSC-induced macrophages increase pancreatic cancer cell proliferation. The results agree with the findings of other studies as they demonstrated that M2 macrophages increase ovarian cancer cell proliferation via secreting EGFR and MMP-9 [198]. Taking into consideration, induced macrophages with the CM of non-activated PSCs didn’t inhibit cell proliferation although they highly expressed the M1 markers. This is however contradicting the findings of Engstrom et al. who demonstrated that CM of M1 macrophages inhibit colon cancer cells [269]. Our data could suggest that non-activated PSCs may induce M1 phenotype that have different characteristics and weaker anti-tumor activity.

11.2.3. Impact of IL-6 on macrophages pre and post-polarization

As discussed above, the secretome of PSCs could be considered as the potent macrophage stimulants. Still, because of the high number of differentially regulated proteins in the secretome of PSCs and their quantity, it might be experimentally difficult to evaluate the role of each single molecule on macrophage polarization. The functional effect of some of the identified proteins have already been investigated on macrophage polarization. Molecules such as VEGF [270], TGF-β [271], IL-4 [272], are involved in macrophages M2 polarization. Whereas IFN-γ with LPS [273] and TNF-α [274] polarize macrophages towards M1 type. The M1 and M2 stimuli and the signals which influence their functional phenotypes are well reviewed [110, 275].

IL-6 is one of the main pro-inflammatory factors which was upregulated in the activated PSCs secretome and has been studied in macrophages. Chomarat et al. reported that, IL-6 is switching the differentiation of monocytes from dendritic cells to macrophages, considering IL-6 as an essential factor in the molecular control of antigen presenting cells development [199]. It is also known that, IL-6 determines macrophage's M2 polarization through IL-1β inhibition and regulation of excessive NO release [276]. Still, to our knowledge, the influence of IL-6 on macrophages before and after polarization is not studied.

Accordingly, on one hand, the macrophages were treated with the standard stimuli, IFN-γ / LPS and IL-4 with and without IL-6 to polarize to M1 and M2 macrophages, respectively. On the other hand, the previously polarized macrophages were then incubated with recombinant IL-6 followed by analyzing macrophage markers in each condition. Surprisingly, IL-6 shows different impacts on the expression of M1 and M2 markers and the results were contradictory to each other. When IL-6 was used with the standard stimuli (pre-polarization), it didn't affect M1 surface marker CD80, but in contrary, IL-6 decreased the expression of M2 surface markers, CD206 (Figure 23). In fact, this finding is consistent with the role of IL-6 where it is known that IL-6 stimulates a range of signaling pathways to elicit inflammatory responses and eradicate pathogens [277]. But influence of IL-6 on the polarized macrophages was opposite to the pre-polarization results. When polarized macrophages were treated with IL-6, the expression of M2 marker CD206 was elevated on M1 and M2 types. Whereas, the M1 surface marker, CD80 was adversely affected by incubation with IL-6 and was decreased on both macrophage phenotypes. These results interestingly suggest that, persistent release of inflammatory cytokines, such as IL-6, establishes

a tumor microenvironment which promotes switching macrophages from pro-inflammatory to the anti-inflammatory type. However, the exact molecular pathway is not elucidated, but it has been proven that IL-6 increases the expression of IL-4 receptor on macrophages which then induces M2 polarization after binding to IL-4 [140]. It has also been shown that, continuous action of IL-6 in macrophages exerts the anti-inflammatory effects of IL-10 [278].These results may highlight the role of macrophages in the relationship between chronic pancreatitis and pancreatic cancer development [279]. Taken together, these results suggest that secretion of IL-6 by activated PSCs and immune cells at different stages of inflammation, may play different roles in macrophage polarization and as a result affecting immune response and tumor growth.

11.2.4. Effect of IL-6 on arginase expression and NO synthesis

The secretome of activated PSCs has increased arginase and reduced NO production. However, here we assess the impact of IL-6 on arginase and NO production which is one of the highly upregulated proteins in the activated PSCs secretome. The results show that arginase activity is increased by IL-6 but it is not significant in comparison to the non-treated macrophages whereas, IL-6 shows no significant impact on NO production. It has already been shown that IL-4/13 induce arginase activity and downregulate the production of NO in macrophages [280]. Nonetheless, when IL-6 was used with IL-4/13, arginase activity has significantly increased suggesting that, IL-6 increases the expression of IL-4rα on macrophages [281]. Therefore, it can be concluded that, role of IL-6 is situation dependent and it may also act as anti-inflammatory factor. IL-6 may exert its impact on arginase activity and NO synthesis but through enhancing the role of other molecules in the secretome of PSCs such as IL-4.

11.2.5. Characterization of macrophages secretome and proteome

To investigate the influence of PSCs secretome on the secretome and proteome profile of macrophages, THP-1 human monocytic cell line was used. Our results show that, the secretome samples of THP-1 macrophages are clearly clustered into two separate groups upon treatment with the secretome of PSCs. This additionally supports the obtained results by showing that, the secretome of PSCs had different impacts on the macrophage’s secreted molecules. Furthermore, the IPA analysis revealed that macrophages, which were treated with the CM of activated PSCs,

secret molecules which increase cell movement, cell to cell signaling and inflammatory response (Figure 26). These findings are agreed with the previous studies which reported that tumor associated macrophages (TAM) are producing high amount of CCL20 which recruits regulatory T-cells (Treg) and induce the recruitment of macrophage [282, 283]. The recruited macrophages will be exposed to the stromal cells and se findings explain the role of macrophages in cell to cell interaction, which in our study, is increased by the activated PSCs.

The proteome analysis by IPA predicted the increase of transactivation, fibrosis and tumor invasion which are the hallmarks of pancreatic cancer. The IPA analysis predicted that the secretome of activated PSCs decrease the phagocytic function of macrophages. Even though macrophages are the main phagocytic cells, however, in the late stage of cancer, M2 macrophages are less phagocytic because of the downregulation of EGF receptor [284]. The finding suggested that IL-4 can transactivate EGF-R through releasing heparin binding EGF (HB-EGF) to mediate inhibitory feedback to M2 macrophages. Hence, increased IL-4 secretion by the activated PSCs could be attributed with the decreased phagocytosis. This highlights why the high number of immunosuppressive M2 macrophages is associated to the poor prognosis of PDAC and its short survival rate [128]. Therefore, it can be assumed that the activation of PSCs is the critical cellular transformation occurred in the tumor microenvironment that promotes immunosuppression through regulating macrophages polarization and inhibiting antigen presenting cells.

11.3. Application of cancer cell secretome in PDAC diagnosis

We have demonstrated the critical role of PSCs secretome in the cellular communications between PSCs and macrophages which could somehow explain the anti-inflammatory impact of activated PSCs on TAMs in pancreatic tumor microenvironment. Cell secretome has long been investigated in the cell to cell communication [165] and in biomarkers identification [285]. However, the application of identified biomarkers in cancer diagnosis is not well studied. Therefore, we aimed to define possible biomarkers in the pancreatic cancer cells secretome which may lead to a better accuracy of PDAC diagnosis. It is proposed that cancer cell line secretome and proximal body fluids are preferred sources for biomarker discovery [286]. “Blood-based diagnosis could improve the outcome of therapy, even for a disease as deadly as PDAC. Applied to people, who are at risk of developing pancreatic cancer – for instance, patients who have undergone tumor resection,

familial cases, and individuals with specific genetic syndromes or predisposing diseases, such as chronic pancreatitis or diabetes – an improvement in diagnostic accuracy could have significant consequences on life expectancy and quality. Analyses of peripheral blood are predestined to such an end; studies with microRNA, circulating DNA and exosomes or proteins have been reported [31, 32, 287-290]." [180].

11.3.1. The array quality and cell secretome analysis

To improve the accuracy of protein-based diagnosis, we studied the secretome of tumor cells which represent the pathological condition as secretome specifically reflects the actual changes of diseased cells. In the analysis, a large panel of antibodies was applied. The antibodies cover target proteins that are associated to cancer according to KEGG and GO term annotation and their power for diagnosis of other tumors had been demonstrated [291, 292] also, they have previously been used in the analysis of the intracellular proteome of 24 pancreatic tumor cell lines [185]. Moreover, cell secretome has previously been studied, however using different techniques. "An earlier, mass spectrometry-based analysis of conditioned media of six tumor cells had reported 63 most differentially abundant molecules [293]. No overlap was found between them and the 112 molecules that we identified. This is not too surprising given the many differences between the studies. The criteria for selecting differentially abundant proteins were different; sample preparation was also very different. In addition, only about 15% of all detected proteins overlapped between the two studies. The reasons for this are the facts that the microarray analysis was biased by the availability of antibodies, but that its detection sensitivity is substantially higher. Therefore, the results are likely to be complementary." [180].

11.3.2. Cancer cell secretome characterization

"The fact that there was very little correlation of protein abundance in secretome and the related intracellular proteomes suggests that the secreted proteins are regulated independent of the intracellular protein expression. Similar data, although focusing on the protein content of exosomes released from colorectal cancer cells showed also a nearly inverse protein abundance in exosomes and intracellularly [294]. In view of these results, a transfer of tumor markers that were identified in tissues for an identification of disease in serum does not seem promising. The functional annotations of the 112 proteins that were found to differ in the secretome of tumor

and non-tumor cells indicated a potential role of secreted proteins as anti-apoptotic factors" [180]. Also, the analysis suggested an influence on immune cells which is consistent with the experimental finding as the secretome promotes macrophages polarization relatively higher towards the pro-tumor types. The macrophage phenotype which is attributed to the immunosuppression in PDAC due to the activation of STAT-3 in M2 macrophages and by secreting immunosuppressive cytokines IL-6 and IL-10 which are also associated to the poor survival of PDAC patients [295, 296]. Markedly, IL-10 is significantly upregulated in the pancreatic cancer cell lines secretome and PDAC serum. It is likely that several properties of PDAC are mediated by the interaction via secretory factors of the various cell types in the tumor microenvironment, of which tumor cells are only a part.

11.3.3. Comparison of cell secretome to the related intracellular proteome

The comparison of the secretome of PDAC cell lines with the relevant cellular proteome shows unique protein signatures with only 15% resemblance in their regulation most of which are attributed to the extracellular functions. "Surprisingly, the secretome analysis did not reveal any apparent correlation of secretome composition with the tumor cells' original location – primary tumor, metastatic tumors or ascites – or the degree of differentiation, while the intracellular proteome had shown significant differences [185]. This suggests that it is unlikely to detect informative variations of this type in serum either, assuming that the serum acts as a combined representation of the various cell secretome. However, other cells of the respective microenvironment of primary tumors, metastatic tumor or ascites may well secrete protein signatures, which differ in their composition, and may permit serum-based diagnosis" [180].

11.3.4. Protein variations in patient serum samples

"The 8 proteins that exhibited similar abundance differences in the serum and secretome profiles belong to the proteins that are most strongly regulated in terms of their abundance level in tumor secretome. One could speculate that they are therefore the ones most likely to remain detectable after becoming part of the serum. Other proteins may lose their discriminative power as they get diluted and obscured too much to remain informative. While for understanding tumor biology the identification of even subtle variations could be as important as that of large changes in expression, it could be advantageous for serum diagnostics to concentrate on

proteins, which in secretome analyses are present at high concentrations and exhibit large differences in expression. The value of comparing secretome analyses and serum studies for the definition of reliable biomarkers is demonstrated by the results obtained for protein GRPR, for example, which was implicated as a marker molecule [297]. In view of the contradictory results of the secretome and serum analysis, with GRPR being up-regulated in tumor cell secretome while down-regulated in PDAC patient serum, the reliability of the marker could be questioned. It cannot be excluded that it is a bona fide marker of high predictive value nevertheless and that the serum abundance reflects the overall release of the protein from other cell types in or around a tumor. However, as long as this is not evaluated in more detail, one should act carefully with utilizing GRPR as a marker in liquid biopsy" [180].

11.3.5. Serum-based diagnostics and validation

The diagnosis based on the sera yielded a signature of just eight proteins, which permitted the identification of PDAC patients with an accuracy of 95.1%. Some of the proteins, such as IL10, ID1 and IL2, had been implicated as possible biomarkers of pancreatic cancer before [298-300]. "However, the result sheds new light on the process by which marker molecules should be selected for a useful diagnostic signature. Compared to the other 181 serum markers, the eight molecules shared between secretome and serum do not show any particular discriminative performance individually. In combination, however, they beat any panel of eight markers made only from serum proteins by quite a margin. Actually, even adding up more serum markers could not yield a signature with a better diagnostic performance. In the comparison of PDAC and CP sera, the eight proteins were again not different from other markers individually. But also, as a signature, they were not superior to other panels. The reason for this could be the fact that they were identified in a secretome analysis, in which tumor and normal cells were compared to each other. This suggests that adding to a signature the apparently best individual markers may not yield the best possible signature. Instead, considering biological and functional data, such as variation in the secretion from different cell types, could contribute valuable information for selecting useful markers" [180].

12. Conclusions

Understanding the stromal cells and cancer cells networking in the tumor microenvironment have become a hotspot in pancreatic cancer research. However, the alteration of PSCs activity and the interaction between PSCs and macrophages remain largely unclear. The present study demonstrates that TNF-α activates PSCs through increasing the expression of α-SMA and FN and augments the secretome profile of PSCs. We demonstrated that activated PSCs increase the proliferation of pancreatic cancer cells, which was confirmed by analyzing the secretome content of the activated PSCs that contained proteins related to cancer cell proliferation such as VEGF-C, FN-1, MMP14 and IGF-2. This supports that, the secretome of activated PSCs are an important means of intercellular communication and have a considerable impact on PDAC development [301].

in PDAC M2-polarized tumor associated macrophages (TAMs) were identified as the most prominent immune cell subpopulation which are associated with the poor prognosis and therefore were considered a good target for cancer therapy [128, 302]. The present study demonstrates how activated PSCs enhance the immunosuppression through the polarization of macrophages towards the pro-tumor phenotype. We have shown that, the secretome of activated PSCs induced the expression of CD163 and CD206 surface markers as well as increased arginase activity and inhibited NO and ROS production. Analyzing the downstream effect of activated PSCs revealed their immunosuppressive effects by secreting CCL17 and impairing the production of pro-inflammatory cytokines IL-1β and TNF-α in macrophages. Interestingly, IL-6 enhances and sustains the polarization of M2 markers and could be attributed to the transformation of macrophages to the M2 type in chronic pancreatitis. Still, future studies are required to dissect the PSC-macrophage interaction and to unlock the barriers to therapies in pancreatic cancer.

Identifying the origin of the secreted proteins and the characterization of their functional effects are key elements for understanding the dynamic changes in the tumor microenvironment during tumorigenesis. We, therefore, analyzed the common markers between the secretome of pancreatic cancer cells and serum of PDAC patients to identify suitable biomarkers for PDAC diagnosis. The identified markers EPHB3, FGF1,

ID1, IL2, IL10, IMPDH2, SELL, VCAM1, were analyzed in two different sample batches and they increased the accuracy of PDAC diagnosis compared to the patient's serum samples only. However, the data shown here are an initial step of identifying suitable biomarkers of high accuracy and highlight the fact that cell secretome can be enormously helpful in this identification process.

It can be concluded that, PSCs secrete massive amount of proteins into the tumor microenvironment which are mainly involved in stromal cell communications, such interactions may further establish favorable environment for tumor cells, increase anti-inflammatory effects and tumor growth. However, because of the heterogeneity of PDAC microenvironment and sensitivity of macrophages to the stimuli in the tumor microenvironment, more investigation is necessary to understand the stromal cells interactions and identify better targets for therapy.

13. References

1. Bynigeri, R.R., et al., *Pancreatic stellate cell: Pandora's box for pancreatic disease biology.* World J Gastroenterol, 2017. **23**(3): p. 382-405.
2. Ryan, D.P., T.S. Hong, and N. Bardeesy, *Pancreatic adenocarcinoma.* N Engl J Med, 2014. **371**(11): p. 1039-49.
3. Ferlay, J., et al., *Cancer incidence and mortality worldwide: sources, methods and major patterns in GLOBOCAN 2012.* Int J Cancer, 2015. **136**(5): p. E359-86.
4. Siegel, R.L., K.D. Miller, and A. Jemal, *Cancer statistics, 2018.* CA Cancer J Clin, 2018. **68**(1): p. 7-30.
5. Ilic, M. and I. Ilic, *Epidemiology of pancreatic cancer.* World J Gastroenterol, 2016. **22**(44): p. 9694-9705.
6. Kleeff, J., et al., *Pancreatic cancer.* Nat Rev Dis Primers, 2016. **2**: p. 16022.
7. Rahib, L., et al., *Projecting cancer incidence and deaths to 2030: the unexpected burden of thyroid, liver, and pancreas cancers in the United States.* Cancer Res, 2014. **74**(11): p. 2913-21.
8. Poruk, K.E., et al., *Screening for pancreatic cancer: why, how, and who?* Ann Surg, 2013. **257**(1): p. 17-26.
9. Yachida, S. and C.A. Iacobuzio-Donahue, *The pathology and genetics of metastatic pancreatic cancer.* Arch Pathol Lab Med, 2009. **133**(3): p. 413-22.
10. Goggins, M., R.H. Hruban, and S.E. Kern, *BRCA2 is inactivated late in the development of pancreatic intraepithelial neoplasia: evidence and implications.* Am J Pathol, 2000. **156**(5): p. 1767-71.
11. Jones, S., et al., *Core signaling pathways in human pancreatic cancers revealed by global genomic analyses.* Science, 2008. **321**(5897): p. 1801-6.
12. Raimondi, S., P. Maisonneuve, and A.B. Lowenfels, *Epidemiology of pancreatic cancer: an overview.* Nat Rev Gastroenterol Hepatol, 2009. **6**(12): p. 699-708.
13. Bosetti, C., et al., *Cigarette smoking and pancreatic cancer: an analysis from the International Pancreatic Cancer Case-Control Consortium (Panc4).* Ann Oncol, 2012. **23**(7): p. 1880-8.
14. Maisonneuve, P. and A.B. Lowenfels, *Risk factors for pancreatic cancer: a summary review of meta-analytical studies.* Int J Epidemiol, 2015. **44**(1): p. 186-98.
15. Bracci, P.M., *Obesity and pancreatic cancer: overview of epidemiologic evidence and biologic mechanisms.* Mol Carcinog, 2012. **51**(1): p. 53-63.
16. Zheng, Z., et al., *Risk Factors for Pancreatic Cancer in China: A Multicenter Case-Control Study.* J Epidemiol, 2016. **26**(2): p. 64-70.
17. Bosetti, C., et al., *Diabetes, antidiabetic medications, and pancreatic cancer risk: an analysis from the International Pancreatic Cancer Case-Control Consortium.* Ann Oncol, 2014. **25**(10): p. 2065-72.
18. Barone, E., et al., *Environmental risk factors for pancreatic cancer: an update.* Arch Toxicol, 2016. **90**(11): p. 2617-2642.
19. Landi, S., *Genetic predisposition and environmental risk factors to pancreatic cancer: A review of the literature.* Mutat Res, 2009. **681**(2-3): p. 299-307.
20. Oberstein, P.E. and K.P. Olive, *Pancreatic cancer: why is it so hard to treat?* Therap Adv Gastroenterol, 2013. **6**(4): p. 321-37.
21. Ballehaninna, U.K. and R.S. Chamberlain, *Biomarkers for pancreatic cancer: promising new markers and options beyond CA 19-9.* Tumour Biol, 2013. **34**(6): p. 3279-92.
22. Pan, S., T.A. Brentnall, and R. Chen, *Proteomics analysis of bodily fluids in pancreatic cancer.* Proteomics, 2015. **15**(15): p. 2705-15.
23. Alexakis, N., et al., *High serum CA 19-9 but not tumor size should select patients for staging laparoscopy in radiological resectable pancreas head and peri-ampullary cancer.* Eur J Surg Oncol, 2015. **41**(2): p. 265-9.

24. Ballehaninna, U.K. and R.S. Chamberlain, *The clinical utility of serum CA 19-9 in the diagnosis, prognosis and management of pancreatic adenocarcinoma: An evidence based appraisal.* J Gastrointest Oncol, 2012. **3**(2): p. 105-19.
25. Baine, M.J., et al., *Differential gene expression analysis of peripheral blood mononuclear cells reveals novel test for early detection of pancreatic cancer.* Cancer Biomark, 2011. **11**(1): p. 1-14.
26. He, M., et al., *A genome wide association study of genetic loci that influence tumour biomarkers cancer antigen 19-9, carcinoembryonic antigen and alpha fetoprotein and their associations with cancer risk.* Gut, 2014. **63**(1): p. 143-51.
27. Tsutsumi, K., et al., *Monitoring of CA19-9 and SPan-1 can facilitate the earlier confirmation of progressing pancreatic cancer during chemotherapy.* Pancreatology, 2012. **12**(5): p. 409-16.
28. Tholey, R.M., et al., *MUC1 Promoter-Driven DTA as a Targeted Therapeutic Strategy against Pancreatic Cancer.* Mol Cancer Res, 2015. **13**(3): p. 439-48.
29. Han, S., et al., *The role of PAM4 in the management of pancreatic cancer: diagnosis, radioimmunodetection, and radioimmunotherapy.* J Immunol Res, 2014. **2014**: p. 268479.
30. Loosen, S.H., et al., *Current and future biomarkers for pancreatic adenocarcinoma.* Tumour Biol, 2017. **39**(6): p. 1010428317692231.
31. Melo, S.A., et al., *Glypican-1 identifies cancer exosomes and detects early pancreatic cancer.* Nature, 2015. **523**(7559): p. 177-82.
32. Wingren, C., et al., *Identification of serum biomarker signatures associated with pancreatic cancer.* Cancer Res, 2012. **72**(10): p. 2481-90.
33. Omenn, G.S., et al., *Overview of the HUPO Plasma Proteome Project: results from the pilot phase with 35 collaborating laboratories and multiple analytical groups, generating a core dataset of 3020 proteins and a publicly-available database.* Proteomics, 2005. **5**(13): p. 3226-45.
34. Anderson, N.L. and N.G. Anderson, *The human plasma proteome: history, character, and diagnostic prospects.* Mol Cell Proteomics, 2002. **1**(11): p. 845-67.
35. Brembeck, F.H., et al., *The mutant K-ras oncogene causes pancreatic periductal lymphocytic infiltration and gastric mucous neck cell hyperplasia in transgenic mice.* Cancer Res, 2003. **63**(9): p. 2005-9.
36. Morris, J.P.t., S.C. Wang, and M. Hebrok, *KRAS, Hedgehog, Wnt and the twisted developmental biology of pancreatic ductal adenocarcinoma.* Nat Rev Cancer, 2010. **10**(10): p. 683-95.
37. Liu, J., et al., *TGF-beta1 promotes acinar to ductal metaplasia of human pancreatic acinar cells.* Sci Rep, 2016. **6**: p. 30904.
38. Rooman, I. and F.X. Real, *Pancreatic ductal adenocarcinoma and acinar cells: a matter of differentiation and development?* Gut, 2012. **61**(3): p. 449-58.
39. Guerra, C., et al., *Chronic pancreatitis is essential for induction of pancreatic ductal adenocarcinoma by K-Ras oncogenes in adult mice.* Cancer Cell, 2007. **11**(3): p. 291-302.
40. Kopp, J.L., et al., *Identification of Sox9-dependent acinar-to-ductal reprogramming as the principal mechanism for initiation of pancreatic ductal adenocarcinoma.* Cancer Cell, 2012. **22**(6): p. 737-50.
41. Collins, M.A., et al., *MAPK signaling is required for dedifferentiation of acinar cells and development of pancreatic intraepithelial neoplasia in mice.* Gastroenterology, 2014. **146**(3): p. 822-834 e7.
42. Shen, R., et al., *The biological features of PanIN initiated from oncogenic Kras mutation in genetically engineered mouse models.* Cancer Lett, 2013. **339**(1): p. 135-43.
43. Biankin, A.V., et al., *Pancreatic cancer genomes reveal aberrations in axon guidance pathway genes.* Nature, 2012. **491**(7424): p. 399-405.
44. Pelosi, E., G. Castelli, and U. Testa, *Pancreatic Cancer: Molecular Characterization, Clonal Evolution and Cancer Stem Cells.* Biomedicines, 2017. **5**(4).
45. Edge, S.B. and C.C. Compton, *The American Joint Committee on Cancer: the 7th edition of the AJCC cancer staging manual and the future of TNM.* Ann Surg Oncol, 2010. **17**(6): p. 1471-4.

46. Hanahan, D. and L.M. Coussens, *Accessories to the crime: functions of cells recruited to the tumor microenvironment.* Cancer Cell, 2012. **21**(3): p. 309-22.
47. Hainaut, P. and A. Plymoth, *Targeting the hallmarks of cancer: towards a rational approach to next-generation cancer therapy.* Curr Opin Oncol, 2013. **25**(1): p. 50-1.
48. Hanahan, D. and R.A. Weinberg, *Hallmarks of cancer: the next generation.* Cell, 2011. **144**(5): p. 646-74.
49. Li, H., X. Fan, and J. Houghton, *Tumor microenvironment: the role of the tumor stroma in cancer.* J Cell Biochem, 2007. **101**(4): p. 805-15.
50. Neesse, A., et al., *Stromal biology and therapy in pancreatic cancer: a changing paradigm.* Gut, 2015. **64**(9): p. 1476-84.
51. Whatcott, C.J., et al., *Desmoplasia in Primary Tumors and Metastatic Lesions of Pancreatic Cancer.* Clin Cancer Res, 2015. **21**(15): p. 3561-8.
52. Jacobetz, M.A., et al., *Hyaluronan impairs vascular function and drug delivery in a mouse model of pancreatic cancer.* Gut, 2013. **62**(1): p. 112-20.
53. Yuen, A. and B. Diaz, *The impact of hypoxia in pancreatic cancer invasion and metastasis.* Hypoxia (Auckl), 2014. **2**: p. 91-106.
54. Sousa, C.M., et al., *Pancreatic stellate cells support tumour metabolism through autophagic alanine secretion.* Nature, 2016. **536**(7617): p. 479-83.
55. Qian, L.W., et al., *Co-cultivation of pancreatic cancer cells with orthotopic tumor-derived fibroblasts: fibroblasts stimulate tumor cell invasion via HGF secretion whereas cancer cells exert a minor regulative effect on fibroblasts HGF production.* Cancer Lett, 2003. **190**(1): p. 105-12.
56. Zhu, Y., et al., *Tissue-Resident Macrophages in Pancreatic Ductal Adenocarcinoma Originate from Embryonic Hematopoiesis and Promote Tumor Progression.* Immunity, 2017. **47**(2): p. 323-338 e6.
57. Carr, R.M. and M.E. Fernandez-Zapico, *Pancreatic cancer microenvironment, to target or not to target?* EMBO Mol Med, 2016. **8**(2): p. 80-2.
58. Lu, P., V.M. Weaver, and Z. Werb, *The extracellular matrix: a dynamic niche in cancer progression.* J Cell Biol, 2012. **196**(4): p. 395-406.
59. Gjorevski, N. and C.M. Nelson, *Bidirectional extracellular matrix signaling during tissue morphogenesis.* Cytokine Growth Factor Rev, 2009. **20**(5-6): p. 459-65.
60. Erkan, M., et al., *Periostin creates a tumor-supportive microenvironment in the pancreas by sustaining fibrogenic stellate cell activity.* Gastroenterology, 2007. **132**(4): p. 1447-64.
61. Erkan, M., et al., *The activated stroma index is a novel and independent prognostic marker in pancreatic ductal adenocarcinoma.* Clin Gastroenterol Hepatol, 2008. **6**(10): p. 1155-61.
62. Horimoto, Y., et al., *Emerging roles of the tumor-associated stroma in promoting tumor metastasis.* Cell Adh Migr, 2012. **6**(3): p. 193-202.
63. von Ahrens, D., et al., *The role of stromal cancer-associated fibroblasts in pancreatic cancer.* J Hematol Oncol, 2017. **10**(1): p. 76.
64. Ozawa, F., et al., *Growth factors and their receptors in pancreatic cancer.* Teratog Carcinog Mutagen, 2001. **21**(1): p. 27-44.
65. Frantz, C., K.M. Stewart, and V.M. Weaver, *The extracellular matrix at a glance.* J Cell Sci, 2010. **123**(Pt 24): p. 4195-200.
66. Cox, T.R. and J.T. Erler, *Remodeling and homeostasis of the extracellular matrix: implications for fibrotic diseases and cancer.* Dis Model Mech, 2011. **4**(2): p. 165-78.
67. Rice, A.J., et al., *Matrix stiffness induces epithelial-mesenchymal transition and promotes chemoresistance in pancreatic cancer cells.* Oncogenesis, 2017. **6**(7): p. e352.
68. Lee, H.O., et al., *FAP-overexpressing fibroblasts produce an extracellular matrix that enhances invasive velocity and directionality of pancreatic cancer cells.* BMC Cancer, 2011. **11**: p. 245.
69. Lunardi, S., R.J. Muschel, and T.B. Brunner, *The stromal compartments in pancreatic cancer: are there any therapeutic targets?* Cancer Lett, 2014. **343**(2): p. 147-55.

70. Koninger, J., et al., *Pancreatic tumor cells influence the composition of the extracellular matrix.* Biochem Biophys Res Commun, 2004. **322**(3): p. 943-9.
71. Apte, M.V., et al., *Desmoplastic reaction in pancreatic cancer: role of pancreatic stellate cells.* Pancreas, 2004. **29**(3): p. 179-87.
72. Miyamoto, H., et al., *Tumor-stroma interaction of human pancreatic cancer: acquired resistance to anticancer drugs and proliferation regulation is dependent on extracellular matrix proteins.* Pancreas, 2004. **28**(1): p. 38-44.
73. Nielsen, M.F., M.B. Mortensen, and S. Detlefsen, *Key players in pancreatic cancer-stroma interaction: Cancer-associated fibroblasts, endothelial and inflammatory cells.* World J Gastroenterol, 2016. **22**(9): p. 2678-700.
74. Apte, M.V., R.C. Pirola, and J.S. Wilson, *Pancreatic stellate cells: a starring role in normal and diseased pancreas.* Front Physiol, 2012. **3**: p. 344.
75. Omary, M.B., et al., *The pancreatic stellate cell: a star on the rise in pancreatic diseases.* J Clin Invest, 2007. **117**(1): p. 50-9.
76. Means, A.L., *Pancreatic stellate cells: small cells with a big role in tissue homeostasis.* Lab Invest, 2013. **93**(1): p. 4-7.
77. Phillips, P.A., et al., *Rat pancreatic stellate cells secrete matrix metalloproteinases: implications for extracellular matrix turnover.* Gut, 2003. **52**(2): p. 275-82.
78. Bachem, M.G., et al., *Pancreatic carcinoma cells induce fibrosis by stimulating proliferation and matrix synthesis of stellate cells.* Gastroenterology, 2005. **128**(4): p. 907-21.
79. Apte, M.V., et al., *Does alcohol directly stimulate pancreatic fibrogenesis? Studies with rat pancreatic stellate cells.* Gastroenterology, 2000. **118**(4): p. 780-94.
80. Asaumi, H., et al., *Externally applied pressure activates pancreatic stellate cells through the generation of intracellular reactive oxygen species.* Am J Physiol Gastrointest Liver Physiol, 2007. **293**(5): p. G972-8.
81. Kloppel, G., S. Detlefsen, and B. Feyerabend, *Fibrosis of the pancreas: the initial tissue damage and the resulting pattern.* Virchows Arch, 2004. **445**(1): p. 1-8.
82. Wilson, J.S., R.C. Pirola, and M.V. Apte, *Stars and stripes in pancreatic cancer: role of stellate cells and stroma in cancer progression.* Front Physiol, 2014. **5**: p. 52.
83. Vonlaufen, A., et al., *Pancreatic stellate cells: partners in crime with pancreatic cancer cells.* Cancer Res, 2008. **68**(7): p. 2085-93.
84. Shinozaki, S., et al., *Indian hedgehog promotes the migration of rat activated pancreatic stellate cells by increasing membrane type-1 matrix metalloproteinase on the plasma membrane.* J Cell Physiol, 2008. **216**(1): p. 38-46.
85. Ikenaga, N., et al., *CD10+ pancreatic stellate cells enhance the progression of pancreatic cancer.* Gastroenterology, 2010. **139**(3): p. 1041-51, 1051 e1-8.
86. Jiang, H.B., M. Xu, and X.P. Wang, *Pancreatic stellate cells promote proliferation and invasiveness of human pancreatic cancer cells via galectin-3.* World J Gastroenterol, 2008. **14**(13): p. 2023-8.
87. Vaquero, E.C., et al., *Extracellular matrix proteins protect pancreatic cancer cells from death via mitochondrial and nonmitochondrial pathways.* Gastroenterology, 2003. **125**(4): p. 1188-202.
88. Nagathihalli, N.S., et al., *Pancreatic stellate cell secreted IL-6 stimulates STAT3 dependent invasiveness of pancreatic intraepithelial neoplasia and cancer cells.* Oncotarget, 2016. **7**(40): p. 65982-65992.
89. Fujita, H., et al., *Tumor-stromal interactions with direct cell contacts enhance proliferation of human pancreatic carcinoma cells.* Cancer Sci, 2009. **100**(12): p. 2309-17.
90. Haqq, J., et al., *Pancreatic stellate cells and pancreas cancer: current perspectives and future strategies.* Eur J Cancer, 2014. **50**(15): p. 2570-82.
91. Mahadevan, D. and D.D. Von Hoff, *Tumor-stroma interactions in pancreatic ductal adenocarcinoma.* Mol Cancer Ther, 2007. **6**(4): p. 1186-97.

92. Tjomsland, V., et al., *Functional heterogeneity in tumor-derived human pancreatic stellate cells: Differential expression of HGF and implications for mitogenic signaling and migration in pancreatic cancer cells.* Oncotarget, 2017. **8**(42): p. 71672-71684.
93. Xu, Y., et al., *Wnt2 protein plays a role in the progression of pancreatic cancer promoted by pancreatic stellate cells.* Med Oncol, 2015. **32**(4): p. 97.
94. Xu, Z., et al., *Role of pancreatic stellate cells in pancreatic cancer metastasis.* Am J Pathol, 2010. **177**(5): p. 2585-96.
95. Onishi, H., et al., *Hedgehog inhibitor decreases chemosensitivity to 5-fluorouracil and gemcitabine under hypoxic conditions in pancreatic cancer.* Cancer Sci, 2012. **103**(7): p. 1272-9.
96. Cheng, Z.X., et al., *Effects of the HIF-1alpha and NF-kappaB loop on epithelial-mesenchymal transition and chemoresistance induced by hypoxia in pancreatic cancer cells.* Oncol Rep, 2014. **31**(4): p. 1891-8.
97. He, X., et al., *Hypoxia regulates ABCG2 activity through the activivation of ERK1/2/HIF-1alpha and contributes to chemoresistance in pancreatic cancer cells.* Cancer Biol Ther, 2016. **17**(2): p. 188-98.
98. Rebours, V., et al., *Hypoxia pathways and cellular stress activate pancreatic stellate cells: development of an organotypic culture model of thick slices of normal human pancreas.* PLoS One, 2013. **8**(9): p. e76229.
99. Masamune, A., et al., *Hypoxia stimulates pancreatic stellate cells to induce fibrosis and angiogenesis in pancreatic cancer.* Am J Physiol Gastrointest Liver Physiol, 2008. **295**(4): p. G709-17.
100. Masamune, A. and T. Shimosegawa, *Pancreatic stellate cells--multi-functional cells in the pancreas.* Pancreatology, 2013. **13**(2): p. 102-5.
101. Hwang, R.F., et al., *Cancer-associated stromal fibroblasts promote pancreatic tumor progression.* Cancer Res, 2008. **68**(3): p. 918-26.
102. Hesler, R.A., et al., *TGF-beta-induced stromal CYR61 promotes resistance to gemcitabine in pancreatic ductal adenocarcinoma through downregulation of the nucleoside transporters hENT1 and hCNT3.* Carcinogenesis, 2016. **37**(11): p. 1041-1051.
103. Damhofer, H., et al., *Assessment of the stromal contribution to Sonic Hedgehog-dependent pancreatic adenocarcinoma.* Mol Oncol, 2013. **7**(6): p. 1031-42.
104. Muerkoster, S., et al., *Tumor stroma interactions induce chemoresistance in pancreatic ductal carcinoma cells involving increased secretion and paracrine effects of nitric oxide and interleukin-1beta.* Cancer Res, 2004. **64**(4): p. 1331-7.
105. Wynn, T.A., A. Chawla, and J.W. Pollard, *Macrophage biology in development, homeostasis and disease.* Nature, 2013. **496**(7446): p. 445-55.
106. Lavin, Y., et al., *Regulation of macrophage development and function in peripheral tissues.* Nat Rev Immunol, 2015. **15**(12): p. 731-44.
107. Karp, C.L. and P.J. Murray, *Non-canonical alternatives: what a macrophage is 4.* J Exp Med, 2012. **209**(3): p. 427-31.
108. Murray, P.J. and T.A. Wynn, *Protective and pathogenic functions of macrophage subsets.* Nat Rev Immunol, 2011. **11**(11): p. 723-37.
109. Chanmee, T., et al., *Tumor-associated macrophages as major players in the tumor microenvironment.* Cancers (Basel), 2014. **6**(3): p. 1670-90.
110. Martinez, F.O. and S. Gordon, *The M1 and M2 paradigm of macrophage activation: time for reassessment.* F1000Prime Rep, 2014. **6**: p. 13.
111. Mantovani, A., et al., *The chemokine system in diverse forms of macrophage activation and polarization.* Trends Immunol, 2004. **25**(12): p. 677-86.
112. Biswas, S.K., A. Sica, and C.E. Lewis, *Plasticity of macrophage function during tumor progression: regulation by distinct molecular mechanisms.* J Immunol, 2008. **180**(4): p. 2011-7.

113. Kigerl, K.A., et al., *Identification of two distinct macrophage subsets with divergent effects causing either neurotoxicity or regeneration in the injured mouse spinal cord.* J Neurosci, 2009. **29**(43): p. 13435-44.
114. Rey-Giraud, F., M. Hafner, and C.H. Ries, *In vitro generation of monocyte-derived macrophages under serum-free conditions improves their tumor promoting functions.* PLoS One, 2012. **7**(8): p. e42656.
115. Rahat, M.A. and B. Hemmerlein, *Macrophage-tumor cell interactions regulate the function of nitric oxide.* Front Physiol, 2013. **4**: p. 144.
116. Lechner, M., P. Lirk, and J. Rieder, *Inducible nitric oxide synthase (iNOS) in tumor biology: the two sides of the same coin.* Semin Cancer Biol, 2005. **15**(4): p. 277-89.
117. Van Dyken, S.J. and R.M. Locksley, *Interleukin-4- and interleukin-13-mediated alternatively activated macrophages: roles in homeostasis and disease.* Annu Rev Immunol, 2013. **31**: p. 317-43.
118. Gordon, S. and F.O. Martinez, *Alternative activation of macrophages: mechanism and functions.* Immunity, 2010. **32**(5): p. 593-604.
119. Stein, M., et al., *Interleukin 4 potently enhances murine macrophage mannose receptor activity: a marker of alternative immunologic macrophage activation.* J Exp Med, 1992. **176**(1): p. 287-92.
120. Katakura, T., et al., *CCL17 and IL-10 as effectors that enable alternatively activated macrophages to inhibit the generation of classically activated macrophages.* J Immunol, 2004. **172**(3): p. 1407-13.
121. Lee, C.G., et al., *Interleukin-13 induces tissue fibrosis by selectively stimulating and activating transforming growth factor beta(1).* J Exp Med, 2001. **194**(6): p. 809-21.
122. Gordon, S., *Alternative activation of macrophages.* Nat Rev Immunol, 2003. **3**(1): p. 23-35.
123. Yang, Z. and X.F. Ming, *Functions of arginase isoforms in macrophage inflammatory responses: impact on cardiovascular diseases and metabolic disorders.* Front Immunol, 2014. **5**: p. 533.
124. Morris, S.M., Jr., *Arginine metabolism: boundaries of our knowledge.* J Nutr, 2007. **137**(6 Suppl 2): p. 1602S-1609S.
125. Pauleau, A.L., et al., *Enhancer-mediated control of macrophage-specific arginase I expression.* J Immunol, 2004. **172**(12): p. 7565-73.
126. Wu, Q., et al., *Functions of pancreatic stellate cell-derived soluble factors in the microenvironment of pancreatic ductal carcinoma.* Oncotarget, 2017. **8**(60): p. 102721-102738.
127. Kurahara, H., et al., *Significance of M2-polarized tumor-associated macrophage in pancreatic cancer.* J Surg Res, 2011. **167**(2): p. e211-9.
128. Hu, H., et al., *The M2 phenotype of tumor-associated macrophages in the stroma confers a poor prognosis in pancreatic cancer.* Tumour Biol, 2016. **37**(7): p. 8657-64.
129. Habtezion, A., M. Edderkaoui, and S.J. Pandol, *Macrophages and pancreatic ductal adenocarcinoma.* Cancer Lett, 2016. **381**(1): p. 211-6.
130. Biswas, S.K. and A. Mantovani, *Macrophage plasticity and interaction with lymphocyte subsets: cancer as a paradigm.* Nat Immunol, 2010. **11**(10): p. 889-96.
131. Balkwill, F., K.A. Charles, and A. Mantovani, *Smoldering and polarized inflammation in the initiation and promotion of malignant disease.* Cancer Cell, 2005. **7**(3): p. 211-7.
132. Roca, H., et al., *CCL2 and interleukin-6 promote survival of human CD11b+ peripheral blood mononuclear cells and induce M2-type macrophage polarization.* J Biol Chem, 2009. **284**(49): p. 34342-54.
133. Kuang, D.M., et al., *Tumor-derived hyaluronan induces formation of immunosuppressive macrophages through transient early activation of monocytes.* Blood, 2007. **110**(2): p. 587-95.
134. Casazza, A., et al., *Impeding macrophage entry into hypoxic tumor areas by Sema3A/Nrp1 signaling blockade inhibits angiogenesis and restores antitumor immunity.* Cancer Cell, 2013. **24**(6): p. 695-709.

135. Grivennikov, S.I., F.R. Greten, and M. Karin, *Immunity, inflammation, and cancer.* Cell, 2010. **140**(6): p. 883-99.
136. Lewis, J.S., et al., *Expression of vascular endothelial growth factor by macrophages is up-regulated in poorly vascularized areas of breast carcinomas.* J Pathol, 2000. **192**(2): p. 150-8.
137. Linde, N., et al., *Vascular endothelial growth factor-induced skin carcinogenesis depends on recruitment and alternative activation of macrophages.* J Pathol, 2012. **227**(1): p. 17-28.
138. Jinushi, M., et al., *Tumor-associated macrophages regulate tumorigenicity and anticancer drug responses of cancer stem/initiating cells.* Proc Natl Acad Sci U S A, 2011. **108**(30): p. 12425-30.
139. Yao, X., et al., *Targeting interleukin-6 in inflammatory autoimmune diseases and cancers.* Pharmacol Ther, 2014. **141**(2): p. 125-39.
140. Mauer, J., et al., *Signaling by IL-6 promotes alternative activation of macrophages to limit endotoxemia and obesity-associated resistance to insulin.* Nat Immunol, 2014. **15**(5): p. 423-30.
141. Sheldon, K.E., et al., *Shaping the murine macrophage phenotype: IL-4 and cyclic AMP synergistically activate the arginase I promoter.* J Immunol, 2013. **191**(5): p. 2290-8.
142. Noy, R. and J.W. Pollard, *Tumor-associated macrophages: from mechanisms to therapy.* Immunity, 2014. **41**(1): p. 49-61.
143. Kanno, H., et al., *Expression of CD163 prevents apoptosis through the production of granulocyte colony-stimulating factor in meningioma.* Neuro Oncol, 2013. **15**(7): p. 853-64.
144. Bharadwaj, U., et al., *Elevated interleukin-6 and G-CSF in human pancreatic cancer cell conditioned medium suppress dendritic cell differentiation and activation.* Cancer Res, 2007. **67**(11): p. 5479-88.
145. Delitto, D., S.M. Wallet, and S.J. Hughes, *Targeting tumor tolerance: A new hope for pancreatic cancer therapy?* Pharmacol Ther, 2016. **166**: p. 9-29.
146. Mayers, J.R., et al., *Tissue of origin dictates branched-chain amino acid metabolism in mutant Kras-driven cancers.* Science, 2016. **353**(6304): p. 1161-5.
147. Kikuta, K., et al., *Pancreatic stellate cells promote epithelial-mesenchymal transition in pancreatic cancer cells.* Biochem Biophys Res Commun, 2010. **403**(3-4): p. 380-4.
148. Zhan, H.X., et al., *Crosstalk between stromal cells and cancer cells in pancreatic cancer: New insights into stromal biology.* Cancer Lett, 2017. **392**: p. 83-93.
149. Esposito, I., et al., *Inflammatory cells contribute to the generation of an angiogenic phenotype in pancreatic ductal adenocarcinoma.* J Clin Pathol, 2004. **57**(6): p. 630-6.
150. Kitamura, T., et al., *CCL2-induced chemokine cascade promotes breast cancer metastasis by enhancing retention of metastasis-associated macrophages.* J Exp Med, 2015. **212**(7): p. 1043-59.
151. Bayne, L.J., et al., *Tumor-derived granulocyte-macrophage colony-stimulating factor regulates myeloid inflammation and T cell immunity in pancreatic cancer.* Cancer Cell, 2012. **21**(6): p. 822-35.
152. Belgiovine, C., et al., *Tumor-associated macrophages and anti-tumor therapies: complex links.* Cell Mol Life Sci, 2016. **73**(13): p. 2411-24.
153. Affara, N.I., et al., *B cells regulate macrophage phenotype and response to chemotherapy in squamous carcinomas.* Cancer Cell, 2014. **25**(6): p. 809-821.
154. Shi, C., et al., *Fibrogenesis in pancreatic cancer is a dynamic process regulated by macrophage-stellate cell interaction.* Lab Invest, 2014. **94**(4): p. 409-21.
155. Nielsen, S.R., et al., *Corrigendum: Macrophage-secreted granulin supports pancreatic cancer metastasis by inducing liver fibrosis.* Nat Cell Biol, 2016. **18**(7): p. 822.
156. Tjalsma, H., et al., *Signal peptide-dependent protein transport in Bacillus subtilis: a genome-based survey of the secretome.* Microbiol Mol Biol Rev, 2000. **64**(3): p. 515-47.
157. Agrawal, G.K., et al., *Plant secretome: unlocking secrets of the secreted proteins.* Proteomics, 2010. **10**(4): p. 799-827.
158. Viotti, C., *ER to Golgi-Dependent Protein Secretion: The Conventional Pathway.* Methods Mol Biol, 2016. **1459**: p. 3-29.

159. Rabouille, C., *Pathways of Unconventional Protein Secretion.* Trends Cell Biol, 2017. **27**(3): p. 230-240.
160. Clamp, M., et al., *Distinguishing protein-coding and noncoding genes in the human genome.* Proc Natl Acad Sci U S A, 2007. **104**(49): p. 19428-33.
161. Skalnikova, H., et al., *Mapping of the secretome of primary isolates of mammalian cells, stem cells and derived cell lines.* Proteomics, 2011. **11**(4): p. 691-708.
162. Thery, C., L. Zitvogel, and S. Amigorena, *Exosomes: composition, biogenesis and function.* Nat Rev Immunol, 2002. **2**(8): p. 569-79.
163. Muralidharan-Chari, V., et al., *Microvesicles: mediators of extracellular communication during cancer progression.* J Cell Sci, 2010. **123**(Pt 10): p. 1603-11.
164. Wang, M. and R.J. Kaufman, *Protein misfolding in the endoplasmic reticulum as a conduit to human disease.* Nature, 2016. **529**(7586): p. 326-35.
165. Zullo, J., et al., *The cell secretome, a mediator of cell-to-cell communication.* Prostaglandins Other Lipid Mediat, 2015. **120**: p. 17-20.
166. Anderson, N.S., et al., *Bcl-2 expression is altered with ovarian tumor progression: an immunohistochemical evaluation.* Journal of Ovarian Research, 2009. **2**(1).
167. Makridakis, M. and A. Vlahou, *Secretome proteomics for discovery of cancer biomarkers.* J Proteomics, 2010. **73**(12): p. 2291-305.
168. Eckstein, N., et al., *Epidermal growth factor receptor pathway analysis identifies amphiregulin as a key factor for cisplatin resistance of human breast cancer cells.* J Biol Chem, 2008. **283**(2): p. 739-50.
169. Lonardo, E., et al., *Pancreatic stellate cells form a niche for cancer stem cells and promote their self-renewal and invasiveness.* Cell Cycle, 2012. **11**(7): p. 1282-90.
170. Hamada, S., et al., *IL-6/STAT3 Plays a Regulatory Role in the Interaction Between Pancreatic Stellate Cells and Cancer Cells.* Dig Dis Sci, 2016. **61**(6): p. 1561-71.
171. Wu, Y.S., et al., *Paracrine IL-6 signaling mediates the effects of pancreatic stellate cells on epithelial-mesenchymal transition via Stat3/Nrf2 pathway in pancreatic cancer cells.* Biochim Biophys Acta, 2017. **1861**(2): p. 296-306.
172. Brown, K.J., et al., *Advances in the proteomic investigation of the cell secretome.* Expert Rev Proteomics, 2012. **9**(3): p. 337-45.
173. Stastna, M. and J.E. Van Eyk, *Secreted proteins as a fundamental source for biomarker discovery.* Proteomics, 2012. **12**(4-5): p. 722-35.
174. Paltridge, J.L., L. Belle, and Y. Khew-Goodall, *The secretome in cancer progression.* Biochim Biophys Acta, 2013.
175. Takata, T., et al., *Characterization of proteins secreted by pancreatic cancer cells with anticancer drug treatment in vitro.* Oncol Rep, 2012. **28**(6): p. 1968-76.
176. Sarkissian, G., et al., *Identification of pro-MMP-7 as a serum marker for renal cell carcinoma by use of proteomic analysis.* Clin Chem, 2008. **54**(3): p. 574-81.
177. Wu, C.C., et al., *Cancer cell-secreted proteomes as a basis for searching potential tumor markers: nasopharyngeal carcinoma as a model.* Proteomics, 2005. **5**(12): p. 3173-82.
178. Wu, C.C., et al., *Identification of collapsin response mediator protein-2 as a potential marker of colorectal carcinoma by comparative analysis of cancer cell secretomes.* Proteomics, 2008. **8**(2): p. 316-32.
179. Xiao, T., et al., *An approach to studying lung cancer-related proteins in human blood.* Mol Cell Proteomics, 2005. **4**(10): p. 1480-6.
180. Mustafa, S., et al., *Comparison of the tumor cell secretome and patient sera for an accurate serum-based diagnosis of pancreatic ductal adenocarcinoma.* Oncotarget, 2017. **8**(7): p. 11963-11976.
181. Marzoq, A.J., et al., *Proteome variations in pancreatic stellate cells upon stimulation with proinflammatory factors.* J Biol Chem, 2013. **288**(45): p. 32517-27.

182. Chanput, W., J.J. Mes, and H.J. Wichers, *THP-1 cell line: an in vitro cell model for immune modulation approach.* Int Immunopharmacol, 2014. **23**(1): p. 37-45.
183. Alhamdani, M.S., C. Schroder, and J.D. Hoheisel, *Analysis conditions for proteomic profiling of mammalian tissue and cell extracts with antibody microarrays.* Proteomics, 2010. **10**(17): p. 3203-7.
184. Alhamdani, M.S., et al., *Single-step procedure for the isolation of proteins at near-native conditions from mammalian tissue for proteomic analysis on antibody microarrays.* J Proteome Res, 2010. **9**(2): p. 963-71.
185. Alhamdani, M.S., et al., *Immunoassay-based proteome profiling of 24 pancreatic cancer cell lines.* J Proteomics, 2012. **75**(12): p. 3747-59.
186. Yi, M.H., et al., *CD200R/Foxp3-mediated signalling regulates microglial activation.* Sci Rep, 2016. **6**: p. 34901.
187. Li, Z., et al., *Differences in iNOS and arginase expression and activity in the macrophages of rats are responsible for the resistance against T. gondii infection.* PLoS One, 2012. **7**(4): p. e35834.
188. Ritchie, M.E., et al., *A comparison of background correction methods for two-colour microarrays.* Bioinformatics, 2007. **23**(20): p. 2700-7.
189. Smyth, G.K., *Linear models and empirical bayes methods for assessing differential expression in microarray experiments.* Stat Appl Genet Mol Biol, 2004. **3**: p. Article3.
190. Fellenberg, K., et al., *Correspondence analysis applied to microarray data.* Proc Natl Acad Sci U S A, 2001. **98**(19): p. 10781-6.
191. Huang, T.M. and V. Kecman, *Gene extraction for cancer diagnosis by support vector machines--an improvement.* Artif Intell Med, 2005. **35**(1-2): p. 185-94.
192. Jesnowski, R., et al., *Immortalization of pancreatic stellate cells as an in vitro model of pancreatic fibrosis: deactivation is induced by matrigel and N-acetylcysteine.* Lab Invest, 2005. **85**(10): p. 1276-91.
193. Cabrera, M.C., et al., *Human Pancreatic Cancer-Associated Stellate Cells Remain Activated after in vivo Chemoradiation.* Front Oncol, 2014. **4**: p. 102.
194. Kim, J.J., et al., *TNF-alpha-induced ROS production triggering apoptosis is directly linked to Romo1 and Bcl-X(L).* Cell Death Differ, 2010. **17**(9): p. 1420-34.
195. Murray, P.J., et al., *Macrophage activation and polarization: nomenclature and experimental guidelines.* Immunity, 2014. **41**(1): p. 14-20.
196. Zhang, A., et al., *Cancer-associated fibroblasts promote M2 polarization of macrophages in pancreatic ductal adenocarcinoma.* Cancer Med, 2017. **6**(2): p. 463-470.
197. Lindsten, T., et al., *Effect of macrophages on breast cancer cell proliferation, and on expression of hormone receptors, uPAR and HER-2.* Int J Oncol, 2017. **51**(1): p. 104-114.
198. Carroll, M.J., et al., *M2 macrophages induce ovarian cancer cell proliferation via a heparin binding epidermal growth factor/matrix metalloproteinase 9 intercellular feedback loop.* Oncotarget, 2016. **7**(52): p. 86608-86620.
199. Chomarat, P., et al., *IL-6 switches the differentiation of monocytes from dendritic cells to macrophages.* Nat Immunol, 2000. **1**(6): p. 510-4.
200. Karnevi, E., R. Andersson, and A.H. Rosendahl, *Tumour-educated macrophages display a mixed polarisation and enhance pancreatic cancer cell invasion.* Immunol Cell Biol, 2014. **92**(6): p. 543-52.
201. Wilson, J.S. and M.V. Apte, *Role of alcohol metabolism in alcoholic pancreatitis.* Pancreas, 2003. **27**(4): p. 311-5.
202. Kiss, K., et al., *Chronic hyperglycemia induces trans-differentiation of human pancreatic stellate cells and enhances the malignant molecular communication with human pancreatic cancer cells.* PLoS One, 2015. **10**(5): p. e0128059.
203. Hinz, B., *Formation and function of the myofibroblast during tissue repair.* J Invest Dermatol, 2007. **127**(3): p. 526-37.

204. Tang, Y., et al., *Extracellular matrix metalloproteinase inducer stimulates tumor angiogenesis by elevating vascular endothelial cell growth factor and matrix metalloproteinases.* Cancer Res, 2005. **65**(8): p. 3193-9.
205. Gialeli, C., A.D. Theocharis, and N.K. Karamanos, *Roles of matrix metalloproteinases in cancer progression and their pharmacological targeting.* FEBS J, 2011. **278**(1): p. 16-27.
206. Rohani, M.G., et al., *MMP-10 Regulates Collagenolytic Activity of Alternatively Activated Resident Macrophages.* J Invest Dermatol, 2015. **135**(10): p. 2377-2384.
207. Masamune, A., et al., *Activated rat pancreatic stellate cells express intercellular adhesion molecule-1 (ICAM-1) in vitro.* Pancreas, 2002. **25**(1): p. 78-85.
208. Wehr, A.Y., et al., *Analysis of the human pancreatic stellate cell secreted proteome.* Pancreas, 2011. **40**(4): p. 557-66.
209. Pandol, S., et al., *Desmoplasia of pancreatic ductal adenocarcinoma.* Clin Gastroenterol Hepatol, 2009. **7**(11 Suppl): p. S44-7.
210. Digiacomo, G., et al., *Fibronectin induces macrophage migration through a SFK-FAK/CSF-1R pathway.* Cell Adh Migr, 2017. **11**(4): p. 327-337.
211. Jacob, S.S. and P.R. Sudhakaran, *Monocyte-macrophage differentiation in three dimensional collagen lattice.* Biochim Biophys Acta, 2001. **1540**(1): p. 50-8.
212. Lukens, J.R., et al., *Inflammasome-derived IL-1beta regulates the production of GM-CSF by CD4(+) T cells and gammadelta T cells.* J Immunol, 2012. **188**(7): p. 3107-15.
213. Young, A., et al., *Cutting edge: suppression of GM-CSF expression in murine and human T cells by IL-27.* J Immunol, 2012. **189**(5): p. 2079-83.
214. Heystek, H.C., et al., *Granulocyte-macrophage colony-stimulating factor (GM-CSF) has opposing effects on the capacity of monocytes versus monocyte-derived dendritic cells to stimulate the antigen-specific proliferation of a human T cell clone.* Clin Exp Immunol, 2000. **120**(3): p. 440-7.
215. Wajant, H., K. Pfizenmaier, and P. Scheurich, *Tumor necrosis factor signaling.* Cell Death Differ, 2003. **10**(1): p. 45-65.
216. Rastogi, R.P., et al., *Detection of reactive oxygen species (ROS) by the oxidant-sensing probe 2',7'-dichlorodihydrofluorescein diacetate in the cyanobacterium Anabaena variabilis PCC 7937.* Biochem Biophys Res Commun, 2010. **397**(3): p. 603-7.
217. Hu, R., et al., *Ethanol augments PDGF-induced NADPH oxidase activity and proliferation in rat pancreatic stellate cells.* Pancreatology, 2007. **7**(4): p. 332-40.
218. Masamune, A., et al., *NADPH oxidase plays a crucial role in the activation of pancreatic stellate cells.* Am J Physiol Gastrointest Liver Physiol, 2008. **294**(1): p. G99-G108.
219. Algul, H., et al., *Mechanisms of disease: chronic inflammation and cancer in the pancreas--a potential role for pancreatic stellate cells?* Nat Clin Pract Gastroenterol Hepatol, 2007. **4**(8): p. 454-62.
220. de Sa Junior, P.L., et al., *The Roles of ROS in Cancer Heterogeneity and Therapy.* Oxid Med Cell Longev, 2017. **2017**: p. 2467940.
221. Kuwada, S.K. and X. Li, *Integrin alpha5/beta1 mediates fibronectin-dependent epithelial cell proliferation through epidermal growth factor receptor activation.* Mol Biol Cell, 2000. **11**(7): p. 2485-96.
222. Ji, Y., et al., *Silencing IGF-II impairs C-myc and N-ras expressions of SMMC-7721 cells via suppressing FAK/PI3K/Akt signaling pathway.* Cytokine, 2017. **90**: p. 44-53.
223. Prokopchuk, O., et al., *Interleukin-4 enhances proliferation of human pancreatic cancer cells: evidence for autocrine and paracrine actions.* Br J Cancer, 2005. **92**(5): p. 921-8.
224. Dias, S., et al., *Vascular endothelial growth factor (VEGF)-C signaling through FLT-4 (VEGFR-3) mediates leukemic cell proliferation, survival, and resistance to chemotherapy.* Blood, 2002. **99**(6): p. 2179-84.
225. Xu, M. and Y.Z. Wang, *miR133a suppresses cell proliferation, migration and invasion in human lung cancer by targeting MMP14.* Oncol Rep, 2013. **30**(3): p. 1398-404.

226. Westphal, D., et al., *Molecular biology of Bax and Bak activation and action.* Biochim Biophys Acta, 2011. **1813**(4): p. 521-31.
227. Goldstein, J.C., et al., *Cytochrome c is released in a single step during apoptosis.* Cell Death Differ, 2005. **12**(5): p. 453-62.
228. Van Audenaerde, J.R.M., et al., *Interleukin-15 stimulates natural killer cell-mediated killing of both human pancreatic cancer and stellate cells.* Oncotarget, 2017. **8**(34): p. 56968-56979.
229. Badache, A. and N.E. Hynes, *Interleukin 6 inhibits proliferation and, in cooperation with an epidermal growth factor receptor autocrine loop, increases migration of T47D breast cancer cells.* Cancer Res, 2001. **61**(1): p. 383-91.
230. Kurosaka, M. and S. Machida, *Interleukin-6-induced satellite cell proliferation is regulated by induction of the JAK2/STAT3 signalling pathway through cyclin D1 targeting.* Cell Prolif, 2013. **46**(4): p. 365-73.
231. Cao, F., et al., *IL-6 increases SDCBP expression, cell proliferation, and cell invasion by activating JAK2/STAT3 in human glioma cells.* Am J Transl Res, 2017. **9**(10): p. 4617-4626.
232. Masui, T., et al., *Expression of IL-6 receptor in pancreatic cancer: involvement in VEGF induction.* Anticancer Res, 2002. **22**(6C): p. 4093-100.
233. Kim, H.W., et al., *Serum interleukin-6 is associated with pancreatic ductal adenocarcinoma progression pattern.* Medicine (Baltimore), 2017. **96**(5): p. e5926.
234. Irvine, K.M., et al., *Colony-stimulating factor-1 (CSF-1) delivers a proatherogenic signal to human macrophages.* J Leukoc Biol, 2009. **85**(2): p. 278-88.
235. Stout, R.D., et al., *Macrophages sequentially change their functional phenotype in response to changes in microenvironmental influences.* J Immunol, 2005. **175**(1): p. 342-9.
236. McWhorter, F.Y., et al., *Modulation of macrophage phenotype by cell shape.* Proc Natl Acad Sci U S A, 2013. **110**(43): p. 17253-8.
237. Porcheray, F., et al., *Macrophage activation switching: an asset for the resolution of inflammation.* Clin Exp Immunol, 2005. **142**(3): p. 481-9.
238. Arnold, C.E., et al., *The activation status of human macrophages presenting antigen determines the efficiency of Th17 responses.* Immunobiology, 2015. **220**(1): p. 10-9.
239. Salgado, F.J., et al., *Interleukin-dependent modulation of HLA-DR expression on CD4and CD8 activated T cells.* Immunol Cell Biol, 2002. **80**(2): p. 138-47.
240. Hu, J.M., et al., *CD163 as a marker of M2 macrophage, contribute to predicte aggressiveness and prognosis of Kazakh esophageal squamous cell carcinoma.* Oncotarget, 2017. **8**(13): p. 21526-21538.
241. Buechler, C., et al., *Regulation of scavenger receptor CD163 expression in human monocytes and macrophages by pro- and antiinflammatory stimuli.* J Leukoc Biol, 2000. **67**(1): p. 97-103.
242. Shiraishi, D., et al., *CD163 is required for protumoral activation of macrophages in human and murine sarcoma.* Cancer Res, 2018.
243. Tiainen, S., et al., *High numbers of macrophages, especially M2-like (CD163-positive), correlate with hyaluronan accumulation and poor outcome in breast cancer.* Histopathology, 2015. **66**(6): p. 873-83.
244. Shabo, I., et al., *Macrophage Infiltration in Tumor Stroma is Related to Tumor Cell Expression of CD163 in Colorectal Cancer.* Cancer Microenviron, 2014. **7**(1-2): p. 61-9.
245. Barros, M.H., et al., *Macrophage polarisation: an immunohistochemical approach for identifying M1 and M2 macrophages.* PLoS One, 2013. **8**(11): p. e80908.
246. Shaul, M.E., et al., *Dynamic, M2-like remodeling phenotypes of CD11c+ adipose tissue macrophages during high-fat diet--induced obesity in mice.* Diabetes, 2010. **59**(5): p. 1171-81.
247. Bellon, T., et al., *Alternative activation of macrophages in human peritoneum: implications for peritoneal fibrosis.* Nephrol Dial Transplant, 2011. **26**(9): p. 2995-3005.

248. Allavena, P., et al., *Engagement of the mannose receptor by tumoral mucins activates an immune suppressive phenotype in human tumor-associated macrophages.* Clin Dev Immunol, 2010. **2010**: p. 547179.
249. Koo, J.S., et al., *Overexpression of mucin genes induced by interleukin-1 beta, tumor necrosis factor-alpha, lipopolysaccharide, and neutrophil elastase is inhibited by a retinoic acid receptor alpha antagonist.* Exp Lung Res, 2002. **28**(4): p. 315-32.
250. Gardner, D., L.E. Jeffery, and D.M. Sansom, *Understanding the CD28/CTLA-4 (CD152) pathway and its implications for costimulatory blockade.* Am J Transplant, 2014. **14**(9): p. 1985-91.
251. Orlikowsky, T.W., et al., *Expression and regulation of B7 family molecules on macrophages (MPhi) in preterm and term neonatal cord blood and peripheral blood of adults.* Cytometry B Clin Cytom, 2003. **53**(1): p. 40-7.
252. Tarique, A.A., et al., *Phenotypic, functional, and plasticity features of classical and alternatively activated human macrophages.* Am J Respir Cell Mol Biol, 2015. **53**(5): p. 676-88.
253. Balkwill, F., *Cancer and the chemokine network.* Nat Rev Cancer, 2004. **4**(7): p. 540-50.
254. Liu, G., et al., *Phenotypic and functional switch of macrophages induced by regulatory CD4+CD25+ T cells in mice.* Immunol Cell Biol, 2011. **89**(1): p. 130-42.
255. Hagemann, T., et al., *Enhanced invasiveness of breast cancer cell lines upon co-cultivation with macrophages is due to TNF-alpha dependent up-regulation of matrix metalloproteases.* Carcinogenesis, 2004. **25**(8): p. 1543-9.
256. Mosaffa, F., et al., *Pro-inflammatory cytokines interleukin-1 beta, interleukin 6, and tumor necrosis factor-alpha alter the expression and function of ABCG2 in cervix and gastric cancer cells.* Mol Cell Biochem, 2012. **363**(1-2): p. 385-93.
257. Kuen, J., et al., *Pancreatic cancer cell/fibroblast co-culture induces M2 like macrophages that influence therapeutic response in a 3D model.* PLoS One, 2017. **12**(7): p. e0182039.
258. Zeng, X., et al., *Recombinant human arginase induced caspase-dependent apoptosis and autophagy in non-Hodgkin's lymphoma cells.* Cell Death Dis, 2013. **4**: p. e840.
259. De Santo, C., et al., *The arginine metabolome in acute lymphoblastic leukemia can be targeted by the pegylated-recombinant arginase I BCT-100.* Int J Cancer, 2018. **142**(7): p. 1490-1502.
260. Wang, Z., et al., *Blocking autophagy enhanced cytotoxicity induced by recombinant human arginase in triple-negative breast cancer cells.* Cell Death Dis, 2014. **5**: p. e1563.
261. Hinrichs, C.N., et al., *Arginine Deprivation Therapy: Putative Strategy to Eradicate Glioblastoma Cells by Radiosensitization.* Mol Cancer Ther, 2018. **17**(2): p. 393-406.
262. Endo, S., et al., *Autophagy Is Required for Activation of Pancreatic Stellate Cells, Associated With Pancreatic Cancer Progression and Promotes Growth of Pancreatic Tumors in Mice.* Gastroenterology, 2017. **152**(6): p. 1492-1506 e24.
263. Monu, N.R. and A.B. Frey, *Myeloid-derived suppressor cells and anti-tumor T cells: a complex relationship.* Immunol Invest, 2012. **41**(6-7): p. 595-613.
264. Cho, D.I., et al., *Mesenchymal stem cells reciprocally regulate the M1/M2 balance in mouse bone marrow-derived macrophages.* Exp Mol Med, 2014. **46**: p. e70.
265. Dey, N., et al., *Caspase-1/ASC inflammasome-mediated activation of IL-1beta-ROS-NF-kappaB pathway for control of Trypanosoma cruzi replication and survival is dispensable in NLRP3-/- macrophages.* PLoS One, 2014. **9**(11): p. e111539.
266. Lee, J.K., et al., *NADPH oxidase promotes pancreatic cancer cell survival via inhibiting JAK2 dephosphorylation by tyrosine phosphatases.* Gastroenterology, 2007. **133**(5): p. 1637-48.
267. Zhang, Y., et al., *ROS play a critical role in the differentiation of alternatively activated macrophages and the occurrence of tumor-associated macrophages.* Cell Res, 2013. **23**(7): p. 898-914.
268. Lei, J., et al., *alpha-Mangostin inhibits hypoxia-driven ROS-induced PSC activation and pancreatic cancer cell invasion.* Cancer Lett, 2014. **347**(1): p. 129-38.

269. Engstrom, A., et al., *Conditioned media from macrophages of M1, but not M2 phenotype, inhibit the proliferation of the colon cancer cell lines HT-29 and CACO-2.* Int J Oncol, 2014. **44**(2): p. 385-92.
270. Wheeler, K.C., et al., *VEGF may contribute to macrophage recruitment and M2 polarization in the decidua.* PLoS One, 2018. **13**(1): p. e0191040.
271. Zhang, F., et al., *TGF-beta induces M2-like macrophage polarization via SNAIL-mediated suppression of a pro-inflammatory phenotype.* Oncotarget, 2016. **7**(32): p. 52294-52306.
272. Luhmann, T., et al., *Interleukin-4-Clicked Surfaces Drive M2 Macrophage Polarization.* Chembiochem, 2016. **17**(22): p. 2123-2128.
273. Muller, E., et al., *Toll-Like Receptor Ligands and Interferon-gamma Synergize for Induction of Antitumor M1 Macrophages.* Front Immunol, 2017. **8**: p. 1383.
274. Lee, J.Y. and K.E. Sullivan, *Gamma interferon and lipopolysaccharide interact at the level of transcription to induce tumor necrosis factor alpha expression.* Infect Immun, 2001. **69**(5): p. 2847-52.
275. Wang, N., H. Liang, and K. Zen, *Molecular mechanisms that influence the macrophage m1-m2 polarization balance.* Front Immunol, 2014. **5**: p. 614.
276. Sanmarco, L.M., et al., *IL-6 promotes M2 macrophage polarization by modulating purinergic signaling and regulates the lethal release of nitric oxide during Trypanosoma cruzi infection.* Biochim Biophys Acta, 2017. **1863**(4): p. 857-869.
277. Kumar, H., T. Kawai, and S. Akira, *Pathogen recognition by the innate immune system.* Int Rev Immunol, 2011. **30**(1): p. 16-34.
278. Yasukawa, H., et al., *IL-6 induces an anti-inflammatory response in the absence of SOCS3 in macrophages.* Nat Immunol, 2003. **4**(6): p. 551-6.
279. Lesina, M., et al., *Stat3/Socs3 activation by IL-6 transsignaling promotes progression of pancreatic intraepithelial neoplasia and development of pancreatic cancer.* Cancer Cell, 2011. **19**(4): p. 456-69.
280. Hodgkinson, J.W., C. Fibke, and M. Belosevic, *Recombinant IL-4/13A and IL-4/13B induce arginase activity and down-regulate nitric oxide response of primary goldfish (Carassius auratus L.) macrophages.* Dev Comp Immunol, 2017. **67**: p. 377-384.
281. Braune, J., et al., *IL-6 Regulates M2 Polarization and Local Proliferation of Adipose Tissue Macrophages in Obesity.* J Immunol, 2017. **198**(7): p. 2927-2934.
282. Liu, J., et al., *Tumor-associated macrophages recruit CCR6+ regulatory T cells and promote the development of colorectal cancer via enhancing CCL20 production in mice.* PLoS One, 2011. **6**(4): p. e19495.
283. Han, Y.L., et al., *Reciprocal interaction between macrophages and T cells stimulates IFN-gamma and MCP-1 production in Ang II-induced cardiac inflammation and fibrosis.* PLoS One, 2012. **7**(5): p. e35506.
284. Zhao, G., et al., *Activation of Epidermal Growth Factor Receptor in Macrophages Mediates Feedback Inhibition of M2 Polarization and Gastrointestinal Tumor Cell Growth.* J Biol Chem, 2016. **291**(39): p. 20462-72.
285. Gronborg, M., et al., *Biomarker discovery from pancreatic cancer secretome using a differential proteomic approach.* Mol Cell Proteomics, 2006. **5**(1): p. 157-71.
286. Pavlou, M.P. and E.P. Diamandis, *The cancer cell secretome: a good source for discovering biomarkers?* J Proteomics, 2010. **73**(10): p. 1896-906.
287. Keller, A., et al., *miRNAs can be generally associated with human pathologies as exemplified for miR-144.* BMC Med, 2014. **12**: p. 224.
288. Bauer, A.S., et al., *Diagnosis of pancreatic ductal adenocarcinoma and chronic pancreatitis by measurement of microRNA abundance in blood and tissue.* PLoS One, 2012. **7**(4): p. e34151.
289. Gall, T.M., et al., *Circulating molecular markers in pancreatic cancer: ready for clinical use?* Future Oncol, 2013. **9**(2): p. 141-4.

290. Sikora, K., et al., *Evaluation of cell-free DNA as a biomarker for pancreatic malignancies.* Int J Biol Markers, 2015. **30**(1): p. e136-41.
291. Schroder, C., et al., *Dual-color proteomic profiling of complex samples with a microarray of 810 cancer-related antibodies.* Mol Cell Proteomics, 2010. **9**(6): p. 1271-80.
292. Schroder, C., et al., *Plasma protein analysis of patients with different B-cell lymphomas using high-content antibody microarrays.* Proteomics Clin Appl, 2013. **7**(11-12): p. 802-12.
293. Makawita, S., et al., *Integrated proteomic profiling of cell line conditioned media and pancreatic juice for the identification of pancreatic cancer biomarkers.* Mol Cell Proteomics, 2011. **10**(10): p. M111 008599.
294. Ragusa, M., et al., *Highly skewed distribution of miRNAs and proteins between colorectal cancer cells and their exosomes following Cetuximab treatment: biomolecular, genetic and translational implications.* Oncoscience, 2014. **1**(2): p. 132-57.
295. Farren, M.R., et al., *Systemic Immune Activity Predicts Overall Survival in Treatment-Naive Patients with Metastatic Pancreatic Cancer.* Clin Cancer Res, 2016. **22**(10): p. 2565-74.
296. Mantovani, A., et al., *Macrophage polarization: tumor-associated macrophages as a paradigm for polarized M2 mononuclear phagocytes.* Trends Immunol, 2002. **23**(11): p. 549-55.
297. Cornelio, D.B., et al., *The gastrin-releasing peptide receptor as a marker of dysplastic alterations in cervical epithelial cells.* Oncology, 2012. **82**(2): p. 90-7.
298. Chung, H.W., S. Jang, and J.B. Lim, *Clinical implications and diagnostic usefulness of correlation between soluble major histocompatibility complex class I chain-related molecule a and protumorigenic cytokines in pancreatic ductal adenocarcinoma.* Cancer, 2013. **119**(1): p. 233-44.
299. Georgiadou, D., et al., *VEGF and Id-1 in pancreatic adenocarcinoma: prognostic significance and impact on angiogenesis.* Eur J Surg Oncol, 2014. **40**(10): p. 1331-7.
300. Zhang, P., et al., *Development of serum parameters panels for the early detection of pancreatic cancer.* Int J Cancer, 2014. **134**(11): p. 2646-55.
301. Ferdek, P.E. and M.A. Jakubowska, *Biology of pancreatic stellate cells-more than just pancreatic cancer.* Pflugers Arch, 2017. **469**(9): p. 1039-1050.
302. Mantovani, A., et al., *Tumour-associated macrophages as treatment targets in oncology.* Nat Rev Clin Oncol, 2017. **14**(7): p. 399-416.